MONASH University

Investigating the function of MACPF proteins in development and growth using *Drosophila melanogaster*

Melissa Jane Saligari

BSc. (Honours), BA (Honours)

A thesis submitted for the degree of Doctor of Philosophy
at Monash University

School of Biological Sciences

Monash University

June 2018

Copyright notice

Abstract

The membrane attack complex/perforin-like (MACPF) protein superfamily is conserved across most kingdoms of life. Many MACPF proteins play important roles as pore-forming toxins in vertebrate immunity. Moreover, it is becoming clear that not all MACPF proteins are capable of forming pores. In addition, other MACPF proteins perform a variety of roles in development and neurobiology in both vertebrate and invertebrate species. These developmental MACPF proteins are generally less well understood than their immunity counterparts.

To address this, the *Drosophila* model system has been used to investigate the *in vivo* functions of a number of MACPF proteins. *Drosophila* has a sole member of the MACPF protein superfamily, Torso-like (Tsl), which is best-known for its role in terminal patterning in the developing embryo. Tsl also acts to regulate growth and developmental timing in the larval prothoracic gland (PG).

This thesis first characterised two candidate receptors that Tsl may work with in the larval PG to regulate growth and developmental timing: Pigment-dispersing factor receptor and Adipokinetic hormone receptor. Although these receptors do not appear to work with Tsl, these genes were characterised and found to be novel regulators of PG function.

Secondly, to further elucidate the importance of the MACPF domain for Tsl function, MACPF proteins from mammals and the sea urchin were expressed in *Drosophila* to determine if they could function in the same manner as Tsl. Due to the high level of functional conservation between *Drosophila* and mammals for many key signalling pathways, this method was also used to discover novel functions for MACPF proteins. The MACPF proteins tested could not function in the same manner as Tsl in embryonic terminal patterning. However, a novel function in the Notch pathway was uncovered for two ancient and related MACPF proteins: the sea urchin protein Apextrin and the mammalian protein Mpeg1.

Thirdly, two candidate regions from a genome-wide genetic suppressor screen to identify novel genes that interact with Tsl were investigated. Two genes, *Pdi* and *CG13827* (a Pex

gene), were found to have a role in terminal patterning, although a direct interaction with Tsl was unable to be established at this time.

Overall this thesis demonstrates the diverse developmental roles of MACPF proteins and highlights the effectiveness of using *Drosophila* as a model system to investigate gene function. Due to the high level of conservation of gene function between flies and humans, the study of MACPF proteins in *Drosophila* can provide significant insight into the function of MACPF proteins in new developmental roles. The possible cellular effects of MACPF proteins are discussed in relation to these novel findings.

Declaration

This thesis contains no material which has been accepted for the award of any other degree or diploma at any university or equivalent institution and that, to the best of my knowledge and belief, this thesis contains no material previously published or written by another person, except where due reference is made in the text of the thesis.

Signature:

Name: Melissa Jane Saligari

Date: Monday, 18th June 2018

Acknowledgements

Firstly, I would like to thank my supervisors Assoc. Prof. Coral Warr, Dr. Travis Johnson and Dr. Christen Mirth for all of their advice and support throughout my PhD. Coral, I can't thank you enough for all of the support, encouragement and guidance that you have given me over the years, and for helping shape me into a better researcher, educator and person. Trav, thanks so much for always being so willing to share your expertise with me, you have taught me so much about all things science, and made this journey possible. Christen, your energy and enthusiasm for my project has been inspiring, and your thought-provoking discussions on all things growth have been very valuable. Thanks also go to my former co-supervisors, Prof. James Whisstock and Dr. Anabel Herr, and my advisory panel, Assoc. Prof. Rob Bryson-Richardson, Assoc. Prof. Sureshkumar Balasubramanian and Dr. Richard Burke for all their valuable feedback and support throughout my PhD.

Secondly, to all the members of the Warr, Burke and Mirth fly labs, both past and present, for providing such a friendly and supportive environment in which to do science. In particular, I would like to thank Dr. Michelle Henstridge for always being around to answer my questions and for all her support, both technical and otherwise, throughout my PhD. To Karyn Moore, thanks for being such an exceptional research assistant and ensuring the lab runs smoothly, as well as taking on the 7am dev. timing counts (I'm so glad you're a morning person). Thanks to Lauren Forbes Beadle for her assistance on the Mpeg1/Apextrin project, and for the great chats about science and PhD life. I would also like to acknowledge that this research was supported by an Australian Government Research Training Program (RTP) Scholarship, formerly known as an Australian Postgraduate Award (APA).

Last but not least, a few personal acknowledgments. Emma, thanks so much for your unwavering support while I have been on this journey, for all of the fantastic food and wine we have shared, along with the laughs and the tears. And for the last-minute proof-reading; any errors that remain are my own. To my dad for supporting me in all of my academic endeavours; all that I have achieved would not have been possible without your love and encouragement. And finally, to my mum, you are my inspiration forever and for always.

x

Table of Contents

Table of Figures

Chapter 2: Novel growth factor receptors that function in the *Drosophila* prothoracic gland to affect growth and developmental timing

Chapter 3: Investigating the function of non-*Drosophila* MACPF proteins in *Drosophila* development

Chapter 4: Characterisation of genes that interact with the *Drosophila* MACPF protein Torso-like

Chapter 1: General introduction

1.1. The membrane attack complex/perforin (MACPF) protein superfamily

The membrane attack complex/perforin-like (MACPF) protein superfamily is conserved across most kingdoms of life, with more than 1000 members so far identified through bioinformatics approaches (Anderluh *et al.* 2014). MACPF proteins are defined based on the presence of the MACPF structural domain, but also often contain additional functional domains (Figure 1.1). Of the MACPF proteins functionally characterised to date, many have roles as pore-forming toxins in vertebrate immunity, specifically in pathogenesis or defence processes (Rosado *et al.* 2007; Rosado *et al.* 2008). For example, the malarial parasite (*Plasmodium* spp) uses two MACPF proteins to invade the midgut epithelium of its mosquito host and to transverse the liver sinusoidal membrane of humans prior to hepatocyte infection (Ishino *et al.* 2004; Kadota *et al.* 2004; Ishino *et al.* 2005). Alternatively, mammalian perforin and Complement components 6-9, which form the Membrane Attack Complex (MAC), are critical for the elimination of virally-infected (or transformed) cells and pathogens respectively. Indeed, this structural domain was initially identified and named because it was common to these human immunity pore-forming proteins (Tschopp *et al.* 1986).

MACPF proteins also perform a variety of roles in development and neurobiology in a range of vertebrate and invertebrate species (Ni and Gilbert 2017). Furthermore, sublytic levels of MAC have shown effects on signalling pathways involved in biological processes such as cell cycle, proliferation and migration (Niculescu *et al.* 1999; Fosbrink *et al.* 2006; Qiu *et al.* 2012). Whilst many of the immune/defence MACPF proteins are known to form pores, it is unclear whether pore formation is central to the function of all MACPF proteins, particularly those with developmental roles. It is certainly clear that not all are capable of pore formation on their own. For instance, Complement C6 mediates the protein-protein interactions between multiple members of the nascent MAC (Müller-Eberhard 1986; Kondos *et al.* 2010), and Complement C8α, which has the crucial role of anchoring the MAC to the target cell membrane, is capable of membrane insertion *without* pore formation (Hadders *et al.* 2007; Lovelace *et al.* 2011). However, neither of these can form pores alone. Indeed, it is perhaps more accurate to say that interaction with cell membranes is central to the biological functions performed by MACPF proteins, regardless of whether or not this involves *bone fide* pore formation (Anderluh *et al.* 2014).

Tsl – 353 aa

Perforin – 555 aa

C6 – 934 aa

C7 – 843 aa

C8α – 584 aa

C8β – 529 aa

C9 – 559 aa

BRINP1 – 761 aa

BRINP2 – 783 aa

BRINP3 – 766 aa

ASTN1 – 1302 aa

ASTN2 – 1339 aa

Mpeg1 – 720 aa

Apx – 491 aa

Figure 1.1. Domain architecture of Torso-like and the non-*Drosophila* MACPF proteins tested.

The *Drosophila* MACPF protein, Tsl, comprises an N-terminal signal peptide (SP, red) and a single MACPF domain, with no other annotated domains. Human Perforin contains a MACPF domain and a C2 domain required for calcium-dependent membrane binding (Yagi *et al.* 2015). Human Complement components C6-C9 share a similar architecture: an N-terminal signal peptide, TSP1 domain(s) and LDLa domain followed by some flanking sequence and the MACPF domain, and then another TSP1 domain. Complement C8β is an exception to this, with the signal peptide and TSP1 domain not present. Complement C9 appears to have lost the C-terminal TSP1 domain. Complement C6 and C7 have a substantial and more complex C-terminus, with additional CCP and FIMAC accessory domains. Human BRINPs 1-3 share a similar architecture: an N-terminal signal peptide and MACPF domain, followed by a relatively long and uncharacterised C-terminus, although BRINPs2-3 have an EGF domain. The presence of as yet uncharacterised domains in the C-terminal region has been suggested (James Whisstock, pers. comm.). The human neural proteins ASTN1 and ASTN2 have several additional domains besides the MACPF domain, including two putative transmembrane domains (TMD), two or three EGF-like domains, and an FN3 domain. Mpeg1 is an ancient MACPF protein found across taxa from sponges to mammals, although the sequence used here is from the mouse. Mpeg1 is comprised of an N-terminal signal peptide, a MACPF domain and a C-terminal TMD, with potential as yet uncharacterised domains within the C-terminal region (James Whisstock, pers. comm.). Apx is an ancient MACPF protein initially identified in sea urchins, comprising a N-terminal signal peptide, a MACPF domain, and a C-terminal ApeC domain. The length of each construct in amino acids (aa) is indicated.

Key: C2 = protein kinase C conserved region 2; TSP1 = Thrombospondin type I repeats; LDLa = low-density lipoprotein receptor domain class A; CCP = complement control proteins; FIMAC = factor I membrane attack complex; EGF/EGF-like = epidermal growth factor domains; FN3 = Fibronectin type III domain; ApeC = Apextrin, C-terminal domain. Modified from the SMART (Simple Modular Architecture Research Tool) web resource run by EMBL, found online at: http://smart.embl-heidelberg.de (Letunic and Bork 2017).

Nevertheless, pore-formation is a crucial aspect of MACPF function, and not surprisingly has been a central focus of MACPF research for many years. Structural studies in 2007 revealed significant homology between MACPF proteins and the bacterial cholesterol-dependent cytolysins (CDCs) indicating that together they form a combined superfamily (Rosado *et al.* 2007; 2008). The CDC proteins are pore-forming virulence factors used by Gram-positive bacteria for pathogenesis (Tweten 2005). Through extensive electron microscopy (EM) and biochemical experiments, it is clear that MACPF and CDC proteins form pores in a similar way (Rossjohn *et al.* 1997; Law *et al.* 2010; Lovelace *et al.* 2011; Lukoyanova *et al.* 2015). Soluble monomers bind to the cell membrane through direct interaction with lipids or indirectly through lipid-binding partner proteins and oligomerise to form a supramolecular ring (pre-pore) structure. Each monomer undergoes a major conformational change that transforms the two alpha-helices of the MACPF/CDC domain into membrane-spanning beta-hairpins (transmembrane helices, TMH1 and TMH2). Together these form the mature giant beta-barrel pore (Lukoyanova *et al.* 2016). The best characterised pore-forming MACPF proteins in humans, the MAC and perforin, will be discussed in more detail in the following sections.

1.1.1. Complement system and the Membrane Attack Complex

The terminal components of the complement system together form the membrane attack complex (MAC) that plays an essential role in host system defence against Gram-negative bacteria and other pathogens (Sarma and Ward 2011). The MAC was discovered over 100 years ago when Paul Ehrlich characterised the haemolytic properties of human blood and recognised that these proteins acted in a complementary manner to antibodies (Kaufmann 2008). The MAC is a multiprotein complex comprised of Complement components 5-9 (C5, C6, C7, C8α, C8β, and C9) which assemble sequentially into a pore on the target cell membrane, ultimately resulting in cell lysis and death (Figure 1.2; Peitsch and Tschopp 1991; reviewed in Bayly-Jones *et al.* 2017). Complement proteins C6 to C9 are the MACPF-domain containing subunits that constitute the functional MAC. Several other important domains such as the thrombospondin-1 (TSP1) domain, low-density lipoprotein receptor class A (LDLa) domain, and an epidermal growth Factor (EGF) domain assist with efficient pore formation (Aleshin *et al.* 2012; Dudkina *et al.* 2016; Serna *et al.* 2016).

The MAC forms a pore by the sequential and irreversible binding of C5b, C6, C7, C8 and C9 to the target cell membrane (reviewed in Bayly-Jones *et al.* 2017; Morgan *et al.* 2017). The

4
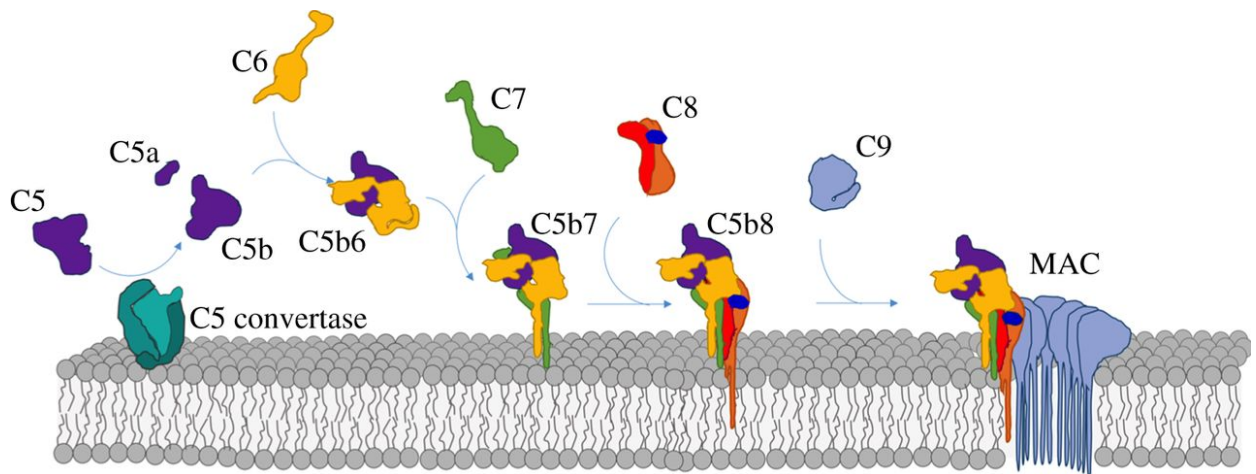
Figure 1.2. Stepwise assembly of the membrane attack complex (MAC) from soluble complement factors.

Upon complement activation, C5 (purple) is cleaved into the small C5a fragment and the larger C5b fragment by the C5 convertase (turquoise). C5b binds to C6 (yellow) to form a stable C5b6 complex. This facilitates the recruitment of C7 (green), which anchors the C5b7 complex to the membrane surface. The heterotrimeric C8 protein, comprised of C8α (orange), C8β (red) and C8γ (dark blue), is integrated into the assembly precursor to form C5b8. This marks the first membrane penetrating event of the assembly. In the final step, multiple copies of C9 (light blue) are recruited to the assembly and oligomerise to form a transmembrane pore approximately 10nm in diameter. The membrane attack complex (MAC) is formed. Figure reproduced from Bayly-Jones *et al.* (2017).

first step in MAC assembly involves the cleavage of C5 into C5a and C5b by C5 convertase, which frees C5a to perform its pro-inflammatory role, and allows C5b to bind with C6. The nascent C5b6 complex binds C7, and this highly lipophilic complex interacts with and anchors to the lipid bilayer. Membrane-binding acts to stabilise the C5b67 complex and enables the recruitment of the C8 heterotrimer (comprised of C8α, C8β and C8γ subunits), which causes a conformational change to C8 so that the TMH2 region can insert into the membrane. The C5b678 complex acts as a receptor to recruit multiple C9 monomers, which oligomerise to form a transmembrane pore, leading to target cell lysis.

Structural studies of the components of the MAC show that the beta-hairpins of C6-C8 are shorter than their C9 counterparts, meaning they are unable to fully penetrate the lipid bilayer (Serna *et al.* 2016; Sharp *et al.* 2016). These initial membrane interactions and insertions of C6-C8 may act to disrupt and reorganise the lipid bilayer to reduce the energy barrier for C9 insertion (for example, Esser *et al.* 1979; Sims and Wiedmer 1984; as discussed in Serna *et al.* 2016). Alternatively, they may confer some level of lipid selectivity to the MAC, which may bind preferentially to certain membrane microdomains (Morgan *et al.* 2017). Early biochemical and EM experiments suggested the MAC was a symmetric pore assembled from one molecule each of C6-8 and between 12 to 18 C9 monomers. In addition, C9 can form homo-oligomeric pores consisting of 22 C9 monomers (Dudkina *et al.* 2016). Together these data suggested that the mature MAC possessed a closed ring structure. However, higher resolution techniques such as cryo-EM and cryo-electron tomography, which were able to visualise MAC lesions on liposomes or lipid bilayers, have challenged this long-standing view (Serna *et al.* 2016; Sharp *et al.* 2016). These studies showed that the final C9 does not attach back to the initial C6, thereby giving the MAC an asymmetric or "split-washer" confirmation. This presumably confers some flexibility to the MAC, although the biological relevance of this is currently unknown (Morgan *et al.* 2017).

For bacterial lysis to occur, multiple MACs must assemble on the target cell membrane of the pathogen via the so-called multi-hit mechanism (Koski *et al.* 1983). Well-known for targeting of Gram-negative bacteria, the MAC has now been implicated in the elimination of Gram-positive bacteria and parasites, and possibly infected host cells too. MAC formation on the target cell is thought to cause cell death by necrosis, although there is also evidence for mitochondrial involvement (for example, Papadimitriou *et al.* 1994). In

6

addition, mouse models have shown that the MAC activates two cell death pathways, one requiring caspases and Bid, and one that is Bid-independent (Ziporen *et al.* 2009).

The importance of MAC formation for human immune system function is clear from mutational deficiencies of the MAC that result in recurrent *Neisseria meningitis* infections and an increased susceptibility to meningococcal infections (Ram *et al.* 2010). Dysregulation of the MAC can be equally damaging to human health, resulting in autoimmune disorders, and so the MAC has been investigated as a therapeutic target for such disorders (He *et al.* 2005; Lee *et al.* 2012; Fluiter *et al.* 2014).

More recently, it has become clear that the MAC is not just a lytic pore-former, but can actually initiate a range of different cellular processes (Figure 1.3). Sublytic concentrations of the MAC can trigger several signalling pathways involved in the cell cycle and cell proliferation, including the mitogen-activated protein kinase and phosphoinositide 3-kinase pathways (Rus *et al.* 1997; Niculescu *et al.* 1999; Qiu *et al.* 2012). There is also preliminary evidence of a possible interaction between G-protein-coupled receptor signalling and MAC formation, and that the MAC may trigger non-canonical pathways of NF-κB activation (reviewed in Morgan *et al.* 2017). It has also been shown that cells can recover from MAC attack by utilising endocytosis and ectocytosis to remove MAC complexes from the cell membrane (Morgan *et al.* 1986; Morgan *et al.* 1987). The crucial factor for these sublytic events is the influx of calcium ions triggered by MAC pore formation, which dramatically increases the intracellular free calcium concentration, thereby initiating various calcium-dependent signalling pathways (Morgan 2016).

1.1.2. Perforin

Perforin is a pore-forming MACPF protein that is stored in cytoplasmic secretory granules within cytotoxic T lymphocytes (CTL) and natural killer (NK) cells (Kägi *et al.* 1994). These cells play a critical role in human cellular immunity and are responsible for destroying virus-infected cells by granzyme B-induced apoptosis. In addition, these cells play an important role in immune surveillance of cancer, by killing transformed cells that have gained cancerous characteristics (Smyth *et al.* 2006; Waldhauer and Steinle 2008). As a result, individuals with partial perforin deficiency are susceptible to cancer, particularly cancers of the blood (Chia *et al.* 2009; Voskoboinik and Trapani 2013).
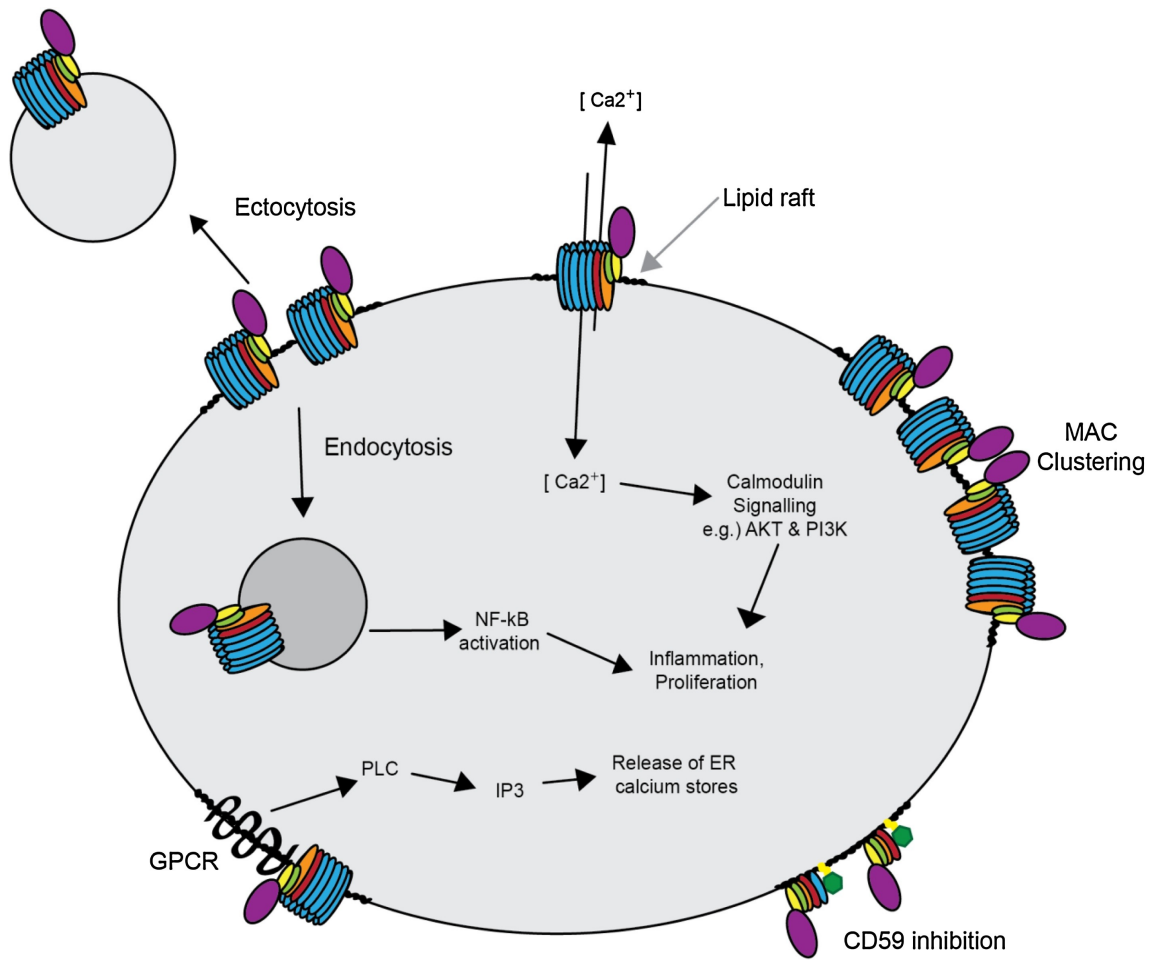
Figure 1.3. Signalling cascades associated with sublytic levels of MAC.

Sublytic concentrations of the MAC can trigger a range of different cellular effects including the membrane repair response. MAC attack triggers an influx of calcium ions to enter through the MAC pore. Changes in intracellular $[Ca^{2+}]$ impact calcium-sensing signalling systems such as calmodulin to activate downstream effectors, including the core signal hubs AKT and PI3K (Qiu *et al.* 2012). CD59 acts to inhibit MAC activity at the cell membrane. The MAC can also associate with G-proteins in the cell membrane to potentially affect the signalling capacity of the GPCR/G-protein complex (Niculescu *et al.* 1994; Niculescu and Rus 2001). This could, in turn, trigger ER calcium store release (Morgan 1989), through PLC activation and IP$_3$ production. It has also been shown that cells can recover from MAC attack by utilising endocytosis and ectocytosis to remove MAC complexes from the cell membrane (Morgan *et al.* 1986; Morgan *et al.* 1987). Once endocytosed, the MAC can cause non-canonical NF-κB activation and the inflammatory response (Jane-wit *et al.* 2015). Pore components are coloured as follows: C5 (purple), C6 (yellow), C7 (green), C8α (orange), C8β (red), and C9 (light blue). Figure reproduced from Morgan *et al.* (2017).

8

Early studies found that membrane lesions on target cells were associated with CTL-mediated cell lysis, and these lesions required the function of a protein named perforin (Dourmashkin *et al.* 1980; Podack and Dennert 1983; Blumenthal *et al.* 1984). As perforin and complement C9 shared a high level of sequence identity it was proposed that they were homologous and functioned by a similar mechanism (Tschopp *et al.* 1986; Peitsch *et al.* 1990). Recent structural studies have revealed the specific protein domains within perforin, and provided insights into how membrane disruption occurs. The MACPF domain is located at the N-terminus, with a central EGF domain, and a C-terminal lipid and Ca^{2+}-binding C2 domain also present (Figure 1.1; Law *et al.* 2010; Yagi *et al.* 2015). The C2 domain is crucially important for the membrane-binding ability of perforin. Taken together, the structural data suggest that perforin forms pores in an analogous manner to CDCs (Law *et al.* 2010; Lukoyanova *et al.* 2015; Dudkina *et al.* 2016).

Secretory granules within CTL and NK cells hold many perforin monomers in conjunction with the cytolytic proteins granulysin and granzyme proteases (Podack and Konigsberg 1984; Podack *et al.* 1985). Granzymes are a family of serine proteases that initiate caspase-dependent cell death pathways (reviewed in Cullen *et al.* 2010). Upon recognition of a target cell, it is thought that perforin and the granzymes are released from these secretory granules into the immunological synapse. Perforin monomers oligomerise to form pores in the target cell allowing the delivery of granzymes into the cytoplasm of the target cell (Tschopp *et al.* 1986; Young *et al.* 1986; Lichtenheld *et al.* 1988). Granzyme B is the main granzyme used in perforin-mediated cell death, and acts by directly cleaving BH3-interacting domain death agonist (BID), in turn initiating the caspase-mediated cell death cascade (Sutton *et al.* 2000; Sutton *et al.* 2003; Kaiserman *et al.* 2006). Perforin is required to ensure the delivery of sufficient granzyme B to initiate cell death. Indeed, perforin-deficient CTLs are unable to initiate caspase-dependent cell death, even though granzyme B is capable of autonomous entry into a target cell (Kägi *et al.* 1994; Walsh *et al.* 1994; Froelich *et al.* 1996; Shi *et al.* 1997).

Although there is broad agreement about the general aspects of perforin-mediated cell death, controversy remains about the exact mechanism of granzyme delivery to the target cell (reviewed in Stewart *et al.* 2012). The first model, called the 'endosomolysis' model, suggests that the granule contents (perforin and granzymes) accumulate in the immune synapse. Perforin then forms multiple small pores on the target cell membrane, which

triggers calcium influx and rapid endocytosis of both perforin and granzymes. Recent evidence showing that perforin can induce invaginations of membranes and the formation of vesicles at the target membrane lends support to this model (Thiery *et al.* 2010; Praper *et al.* 2011b). Perforin then forms stable pores in the endosomal membrane to trigger cytosolic release of granzymes and initiate cell death (Froelich *et al.* 1996; Browne *et al.* 1999; Thiery *et al.* 2011). However, in contradiction to this, cells exposed to perforin do not upregulate endocytosis, and blocking endocytic processes does not reduce the cytotoxic effects of perforin or granzyme B (Lopez et al. 2013).

The alternative model suggests that perforin acts by a direct or 'diffusion' mechanism, whereby perforin forms pores directly on the membrane of the target cell. Granzymes then move by diffusion into the target cell to trigger cell death. Several recent studies have shown that cationic molecules including granzyme B can be delivered directly into cells through perforin pores at the target cell membrane (Lopez *et al.* 2013; Stewart *et al.* 2014). The rapid endocytosis triggered by perforin activity could therefore be due to the membrane repair response. In addition, the formation of both incomplete (Praper *et al.* 2011a) and complete (Voskoboinik *et al.* 2015) perforin pores is more consistent with the direct delivery model (reviewed in Spicer *et al.* 2017). Finally, it is entirely possible that perforin-mediated cell lysis can be achieved by either mechanism, depending on the specific physiological conditions encountered.

Mutations in the *perforin* gene in humans cause a congenital disease called familial hemophagocytic lymphohistiocytosis (FHL) (Stepp *et al.* 1999; Janka and zur Stadt 2005). In this disease, the activity of CTL and NK cells is impaired, resulting in a failure to eliminate antigen-presenting cells. This, in turn, causes an over-proliferation of CD4+ and CD8+ T cells, and drives a systemic inflammatory response. The excessive inflammatory response and dysregulation of the immune system ultimately causes multiple organ failure and death. This condition can be cured if early treatment is sought: chemotherapy and immunosuppression are administered, followed by hematopoietic stem cell transplantation (Janka and zur Stadt 2005). Of the total FHL cases diagnosed, approximately 60% are attributable to *perforin* mutations (Voskoboinik and Trapani 2013). The remaining cases are the result of mutations in three genes, UNC13D, STX11 and STXBP2, which have important roles in exocytic processes (Feldmann *et al.* 2003; zur Stadt *et al.* 2005; Cote *et al.* 2009; zur Stadt *et al.* 2009). These latter mutations appear to cause

10

FHL by disrupting the trafficking of perforin to the immune synapse, indicating the crucial importance of trafficking for appropriate perforin function.

Overall, the immune system requires multiple strategies to combat a range of pathogens, and MACPF proteins are central to this. Complement and poly-C9 eliminate extracellular pathogens of the blood and interstitial fluid. Perforin kills intracellular viruses and cancer cells. Both form pores to facilitate the entry of other killing agents. The MAC-poly-C9 pores enable serum lysozymes to digest peptidoglycans resulting in bacterial collapse and lysis. Poly-perforin pores are required for granzyme delivery, which promotes the apoptosis of virally-infected or transformed cells. So, there are important similarities in how these immunity MACPF proteins function. In combination, these pore-forming proteins act together to protect us from microbial attack and provide surveillance against malignant cells.

1.2. Developmental MACPF proteins

In addition to the well-characterised roles of MACPF proteins in the mammalian immune system, a number of MACPF proteins have been shown to play important but poorly understood roles in development. The mammalian MACPF proteins Astrotactin 1 and 2 and Brinp1 have been implicated in neural development (Adams *et al.* 2002; Kawano *et al.* 2004). The sea urchin protein Apextrin is thought to function in early embryonic development (Haag *et al.* 1999), although more recent studies have also suggested a role in immunity (Dheilly *et al.* 2011). Of particular interest to this thesis is Torso-like, the only MACPF protein so far identified in *Drosophila melanogaster*, which is best-known for its requirement for terminal patterning in the developing embryo (Stevens *et al.* 1990; Savant-Bhonsale and Montell 1993). Whether these developmental MACPF proteins function in a similar manner to their immunity counterparts, through pore formation and membrane disruption, has not yet been established (Lukoyanova and Saibil 2008; Rosado *et al.* 2008). The better understood developmental MACPF proteins will be discussed in more detail in the following sections.

1.2.1. Mammalian MACPF proteins Astrotactin 1 and 2

Astrotactin1 and Astrotactin2 (Astn1 and Astn2) are neural-specific MACPF proteins, broadly expressed in regions of the mouse central nervous system (CNS) such as the

cerebellum, hippocampus and cortex (Zheng *et al.* 1996; Wilson *et al.* 2010). They are proposed to function in glia-guided axon pathfinding and neural development. These proteins share 48% amino acid identity and have a common domain structure (Wilson *et al.* 2010). Astn1 was initially identified when it bound to antibodies that blocked neuron-glial mediated cell migration (Edmondson *et al.* 1988). Further studies provided evidence that these proteins could act as adhesion molecules in glial-mediated post-mitotic neuronal precursor cell migration in the CNS (Stitt *et al.* 1991; Adams *et al.* 2002). Mouse knockouts of Astn1 have smaller cerebella, slowed neuronal migration and abnormally developed neural cells (Adams *et al.* 2002). This results in poorer balance and coordination compared with wild-type mice.

Astn2 is thought to regulate the intracellular trafficking of Astn1 and thus the levels of Astn1 that are present in the plasma membrane during glial-guided neuronal migration (Wilson *et al.* 2010). Biochemical and flow cytometry experiments show that Astn2 forms a complex with Astn1 and modulates the levels of Astn1 in the neuronal plasma membrane (Wilson *et al.* 2010). *In vivo* localisation experiments using differently tagged version of Astn1 and Astn2 showed co-localisation with the endosomal marker clathrin specifically along the leading edge of the migrating granule neurons. Astn1 is recycled via clathrin-mediated endocytosis, which is thought to guide the migrating neuron along the glial fibre (Figure 1.4; Wilson *et al.* 2010). How specifically the MACPF domain functions in this process is yet to be determined in functional studies (Stitt *et al.* 1991; Solecki 2012).

Genome wide association studies provide further evidence of a role for Astn proteins in neural development. The Astn loci show associations with several neurodevelopmental disorders such as schizophrenia, autism and attention deficit hyperactivity disorder (Vrijenhoek *et al.* 2008; Glessner *et al.* 2009; Lionel *et al.* 2014; Freitag *et al.* 2016). Astn proteins have also been implicated in neurological disorders such as alcohol addiction and Alzheimer's disease through similar association studies (Heinzen *et al.* 2010; Hill *et al.* 2012; Wang *et al.* 2015). Functional studies have yet to confirm any causal link with these diseases.

There is still much to be discovered about the function of these MACPF-containing neural proteins, however a recent structural study of Astn2 has moved us one step closer. Unlike the cytolytic MACPF proteins C9 and perforin which unfurl two alpha-helices to form the

12
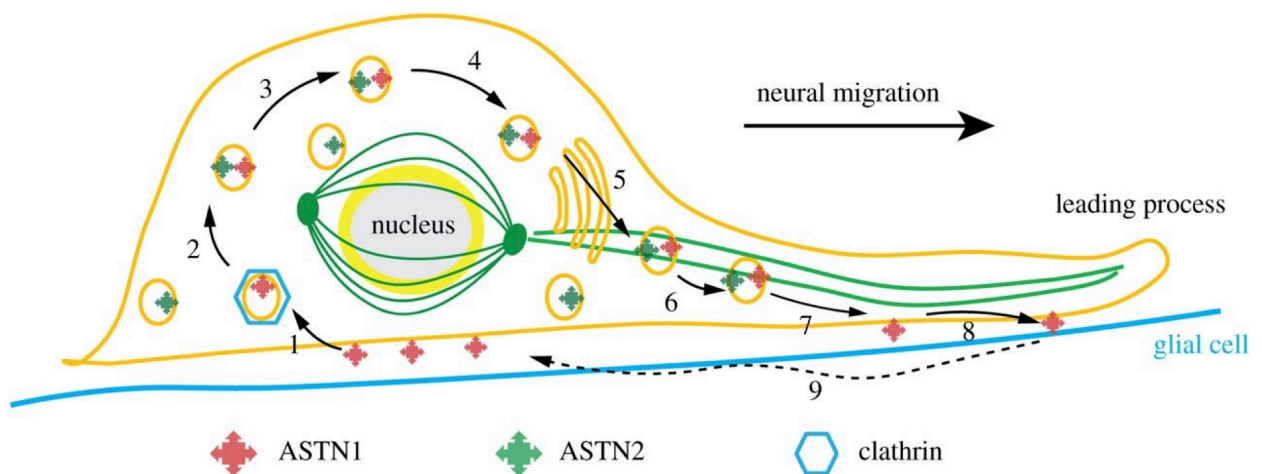
Figure 1.4. Astrotactins are required for neural migration in mammals.

ASTN1-mediated adhesions undergo endocytosis into clathrin-coated vesicles in an ASTN2-dependent manner (1); and then the vesicles containing both ASTNs cycle through the early and recycling endosomes (2–4) and migrate along the microtubules (5–7) to re-deposit ASTN1 towards the leading process (7) to form a new adhesion (8) which will be recycled again (9) in step with the migrating cell. ASTN1 and ASTN2 are depicted throughout the schematic with red and green star-like symbols respectively. The glial cell membrane is indicated by a blue line underneath the neuron cell (yellow) and the microtubules are in green. Figure reproduced from Ni and Gilbert (2017).

membrane-spanning beta-strands, the corresponding sequences in Astn2 are neither long enough nor amphipathic enough to perform this role (Law *et al.* 2010; and Dudkina *et al.* 2016; compared with Ni *et al.* 2016). Thus, Astn2 more closely parallels Complement proteins C6-C8, which are also unable to fully span the membrane (Serna *et al.* 2016; Sharp *et al.* 2016). This suggests that the MACPF domain of Astn2 may not form pores. Without a structure, it remains unknown whether Astn1 behaves like Astn2 or more like its cytolytic relatives, perforin and C9.

1.2.2. Mammalian MACPF proteins BRINP1, 2 and 3

Three MACPF proteins called **B**one Morphogenetic Protein/**R**etinoic Acid **I**nducible **N**eural-specific **P**roteins (BRINP1, BRINP2, and BRINP3) are widely expressed in neural tissue in both the central and peripheral nervous systems of mammals (Kawano *et al.* 2004; Terashima *et al.* 2010). The BRINP proteins are extremely well conserved between rodents and humans: sharing more than 95% amino acid identity (Kawano *et al.* 2004).

Generally, the mechanism of action of the BRINP proteins is less well understood than the astrotactins, and there is no evidence to indicate that BRINPs are involved in neuronal migration like their Astn counterparts (reviewed in Berkowicz *et al.* 2017). Alternatively, BRINPs are thought to be involved in neurogenesis and neuronal maturation (Kawano *et al.* 2004; Terashima *et al.* 2010; Kobayashi *et al.* 2014). Recently published knockout mouse models of all three *Brinp* genes have provided valuable insight into their *in vivo* function. The knockout of each of these genes resulted in behaviours reminiscent of human neurodevelopmental disorders (reviewed in Berkowicz *et al.* 2017), suggesting that the BRINP proteins have an important role in neural development.

In addition, all three BRINP proteins have been implicated as tumour suppressors in a variety of cancers through the identification of mutations and epigenetic changes in human tumour specimens, and the observation that changes in BRINPs expression can spontaneously generate tumourigenicity in long-term cell cultures (Wright *et al.* 2004; Burns *et al.* 2005; Shorts-Cary *et al.* 2007). The overexpression of BRINP3 in pituitary gonadotrope cells promoted proliferation, migration and invasion even in growth-restricted environments (Shorts-Cary *et al.* 2007). Overexpression experiments with all three BRINPs have shown that they suppress cell cycle progression at the G_1/S transition in multiple non-neuronal cell types (Nishiyama *et al.* 2001; Kawano *et al.* 2004; Terashima

14

et al. 2010). It is thought that BRINPs act as neuroprotective factors by suppressing cell cycle progression in cooperation with other cell cycle regulators, as well as playing a role in synaptic plasticity and neural regeneration (Motomiya *et al.* 2007). If and how the MACPF domain is required in this role is still unknown.

One study in cell lines has revealed an additional cell-killing function for BRINP1. Transiently transfecting human bladder tumour cells with an eGFP-tagged BRINP1 protein killed the cells independently of apoptosis (Wright *et al.* 2004), consistent with the lytic function of MACPF proteins. However, pore formation by BRINP proteins has not yet been shown. How this finding relates to the neurodevelopmental and neurological roles of BRINP proteins discussed previously remains to be determined.

1.2.3. The sea urchin MACPF protein Apextrin

The MACPF protein Apextrin (Apx) was originally identified in secretory vesicles in sea urchin (*Heliocidaris erythrogramma*) embryos (Haag and Raff 1998). A significant pool of maternal Apx protein is present in unfertilised eggs, and is gradually secreted following fertilisation (Haag *et al.* 1999). This occurs as part of the exocytosis of cortical granules that make up the multi-layered extracellular matrix surrounding the blastula. Apx is so named because it becomes localised to the **ap**ical **ex**tracellular ma**tri**x during the period when the cells acquire apical-basal columnar polarity. It has been suggested that Apx acts in apical cell adhesion to strengthen the ectoderm of the large *H. erythrogramma* embryos against the extrinsic and intrinsic forces experienced during development (Haag *et al.* 1999). The ingressing mesenchyme cells rapidly endocytose Apx upon their internalisation at metamorphosis.

Apx and Apextrin-like proteins (ALPs) have now been identified in multiple species of marine invertebrates including hydra, coral, oyster, amphioxus, sea anemone, and mussel. Whole-mount *in situ* hybridisation studies suggest that ALPs are involved in embryonic development in both hydra and coral (Miller *et al.* 2007). Other studies in these species suggest that Apx may have an immune function, as differential expression of these ALP genes is seen in response to infection or damage. For example, *Apx* was significantly upregulated following bacterial challenge in sea urchins (Huang *et al.* 2007; Dheilly *et al.* 2011) and in the American oyster, *Crassostrea virginica* (McDowell *et al.* 2014). In the Pacific oyster, *Apx* expression was upregulated in the digestive gland after hypoxic

exposure (David *et al.* 2005). However, in other marine invertebrates such as the coral species *Acropora millepora*, a decrease in *Apx* expression was observed as a result of damage or disease (van de Water *et al.* 2015).

Furthermore, two of these proteins, ALP1 and ALP2, in the fish-like *Amphixous* species have recently been characterised (Huang *et al.* 2014). These proteins contain a novel microbial pattern recognition domain in the C-terminus which has been designated Apextrin C-terminal domain. ALP1 works as an extracellular effector for bacterial agglutination to help clear bacteria from the gut lumen, whilst ALP2 acts intracellularly to mediate bacterial recognition and NF-κB activation (Huang *et al.* 2014). Of particular interest is that ALPs seem to defend almost exclusively against Gram-positive bacteria, as opposed to mammalian immunity MACPF proteins that protect against infection by Gram-negative bacteria. Whether this represents the standard function for Apx and ALPs in immunity remains unknown. Further functional studies are also needed to ascertain the functional mechanism of Apx in development.

1.3. The *Drosophila* MACPF protein Torso-like

Another MACPF protein, which is of particular interest to our lab, is Torso-like (Tsl), the only MACPF protein so far identified in *Drosophila* (Rosado *et al.* 2008). Tsl is unique amongst MACPF proteins so far studied, in possessing a single MACPF domain without any other apparent functional domains. This is atypical of MACPF proteins, which generally utilise various N- or C-terminal domains both to interact with other binding partners for oligomeric complex formation and for initial membrane interaction. For example, Complement C6 interacts with its protein-binding partner C5 through its Complement Control Protein (CCP) and Factor I Membrane Attack Complex (FIMAC) domains (Figure 1.1; DiScipio *et al.* 1999; Aleshin *et al.* 2012) and perforin interacts with target cell membranes through its C-terminal C2 domain (Figure 1.1; Voskoboinik *et al.* 2005). In addition, certain MACPF toxins, such as the fungal cytolysin pleurotolysin, are two-component toxins that require both a MACPF protein and a lipid-binding protein to form functional pores (Tomita *et al.* 2004; Ota *et al.* 2013). Given the absence of any detectable accessory domains in Tsl, it seems likely that unidentified protein-interaction partners are required for Tsl function. The well-known role of Tsl in terminal patterning will be discussed in detail below.

1.3.1. Terminal patterning in the *Drosophila* embryo

Pioneering genetic screens in the 1980s identified many of the maternal genes that control the three major patterning systems: the antero-posterior system, the dorso-ventral system, and the terminal system (Schüpbach and Wieschaus 1986; Nüsslein-Volhard *et al.* 1987; Schüpbach and Wieschaus 1989). Terminal patterning, the patterning of the unsegmented structures at the poles of the embryo, is controlled by the localised activation of the receptor tyrosine kinase Torso (Tor) only at the poles of the embryo (Casanova and Struhl 1989). Activation of Tor initiates canonical Ras/Mitogen activated protein kinase (Ras/MAPK) signalling, which inhibits the transcriptional repressors Capicua and Groucho (Paroush *et al.* 1997; Grimm *et al.* 2012) and leads to expression of the zygotic transcription factor genes *tailless* and *huckebein* (Brönner and Jäckle 1991). These zygotic genes are needed to specify cell fate at the poles of the embryo and ensure the formation of correct terminal structures. The *tor* gene is maternally expressed by the nurse cells which deposit their contents into the oocyte, where *tor* mRNA becomes evenly distributed (Sprenger *et al.* 1989). Fertilisation of the oocyte does not alter this uniform distribution of the *tor* transcript (Sprenger *et al.* 1989). In addition, several studies provide genetic evidence that whilst Tor is present ubiquitously on the embryo plasma membrane, its activity is restricted to the two poles of the embryo (Klingler *et al.* 1988; Sprenger and Nüsslein-Volhard 1992; Savant-Bhonsale and Montell 1993). For example, Klingler *et al.* (1988) showed that mothers carrying a *tor* gain-of-function mutation (that produces a constitutively active receptor) cause the "spliced" cuticle phenotype, in which terminal regions of the embryo are expanded at the expense of central segments, ultimately causing embryonic lethality.

Large-scale mutagenesis screens performed by Nüsslein-Volhard *et al.* (1987) identified at least four maternal genes, *trunk* (*trk*), *torso-like* (*tsl*), *fs(1)Nasrat (fs(*1*)N)* and *fs(1)polehole (fs(1)ph)*, that function upstream of Tor to somehow generate localised Tor activity. An additional gene, *closca*, was recently identified, suggesting that some genes were not found in the early screens (Ventura *et al.* 2010). Females homozygous for mutations in any of these terminal class genes lay embryos with an identical phenotype, *i.e.* the absence of all terminal structures, which is consistent with genes acting in a common pathway.

Of the terminal class genes, *trk* is thought to be the ligand for the Tor receptor because of the presence of a C-terminal cysteine knot motif, which is a feature of many extracellular ligands including growth factors (Casanova *et al.* 1995). Similarly to *tor*, *trk* is maternally expressed by the nurse cells and its mRNA is deposited into the oocyte (Schüpbach and Wieschaus 1986). As such, it has long been presumed that the Trk protein is secreted ubiquitously into the perivitelline space in an inactive form, and only activated at the poles of the embryo (Sprenger and Nüsslein-Volhard 1992; Casanova and Struhl 1993; Savant-Bhonsale and Montell 1993). This, in turn, causes the localised activation of Tor, which is essential for correct terminal patterning. In support of this idea, a 108-amino acid C-terminal Trk fragment has been shown to ubiquitously activate Tor signalling, thereby bypassing the requirement of other maternal genes normally required for Tor activation (Casali and Casanova 2001). This C-terminal fragment was proposed to be the active form of the Trk ligand, produced by a series of proteolytic cleavage events, at least one of which must be spatially restricted.

1.3.2. Torso-like is the only known localised determinant of terminal patterning

Unlike the other maternal terminal class genes, *tsl* is expressed only in a limited subpopulation of somatic follicle cells at the poles of the oocyte (Stevens *et al.* 1990; Savant-Bhonsale and Montell 1993). Females homozygous for *tsl* loss-of-function mutations lay embryos missing terminal structures, as is characteristic of terminal class genes (Stevens *et al.* 1990). In addition, genetic analyses indicate that Tsl functions upstream of Tor because in the absence of Tsl, the Tor receptor is not activated (Stevens *et al.* 1990; Furriols *et al.* 1998). Moreover, localised Tor activation is dependent on the spatially-restricted maternal expression pattern of *tsl,* as unrestricted *tsl* expression from all follicle cells leads to unrestricted Tor activation, resulting in the spliced cuticle phenotype (Savant-Bhonsale and Montell 1993; Martin *et al.* 1994). This confirms that Tsl is sufficient for Tor activation and, furthermore, indicates that the other components necessary for Tor activation are ubiquitously present in the embryo (Savant-Bhonsale and Montell 1993; Martin *et al.* 1994). Thus, *tsl* is the localised determinant of terminal patterning required for the localised activation of Tor.

One complication with this model is that the Tor receptor is not activated until early embryogenesis, when the *tsl*-expressing follicle cells have long since degenerated (Schüpbach and Wieschaus 1986; Sprenger *et al.* 1993). Therefore, there must be a
18

mechanism to ensure that the localised terminal signal provided by Tsl is transferred from the egg chamber to the oocyte and on to the early embryo (Casanova and Struhl 1993). In one study of Tsl localisation using a polyclonal antibody, Tsl protein was seen to form a symmetrical gradient on the surface of devitellinised embryos, with the gradient peaking at the anterior and posterior poles (Martin *et al.* 1994). This suggested that, after its secretion by the polar follicle cells into the perivitelline space, Tsl becomes associated with the embryonic plasma membrane (Martin *et al.* 1994). However, when Stevens *et al.* (2003) attempted to repeat these findings using a different anti-Tsl antibody, they detected strong Tsl staining at the poles of the vitelline membrane following removal of the embryo contents. In this study, Tsl staining was only observed when the antibody had access to the inner surface of the eggshell through its removal from the embryo.

Genetic characterisation of two other maternal terminal class genes provided the first clue that the mechanism for transferring the terminal signal from the egg chamber to the embryo might be linked to the eggshell. A study by Jiménez *et al.* (2002) found that the localisation of Tsl protein, in a posterior crescent between the follicle cells and the oocyte at the posterior pole of stage 10 oocytes, was consistently and noticeably reduced in both *fs(1)N* and *fs(1)ph* mutant embryos. This suggested that Nasrat and Polehole are required for the efficient accumulation and/or stability of secreted Tsl (Jiménez *et al.* 2002). Further work has confirmed that extracellular Tsl co-localises with the vitelline proteins Nasrat and Polehole during oogenesis, but is later localised specifically at the embryo plasma membrane (Mineo *et al.* 2015). This two-step mechanism, whereby Tsl is initially anchored at the vitelline membrane through its interaction with Nasrat and Polehole (and Closca), but is then translocated to the oocyte plasma membrane, brings together the previous seemingly conflicting data regarding Tsl localisation (Figure 1.5, inset). A role for Tsl at the plasma membrane is also much easier to reconcile with what is known about MACPF proteins than with an eggshell localisation. Moreover, if the translocation of Tsl to the plasma membrane and *tor* translation were triggered by a common signal or event such as egg activation, this would ensure that Tsl and Tor were present together simultaneously to facilitate the timely activation of the Tor receptor (Mineo *et al.* 2015).

1.3.3. Models for Torso-like function in embryonic patterning

The prevailing model of Tsl function for many years was that Trk was secreted into the perivitelline space in an inactive form, which then required localised cleavage prior to
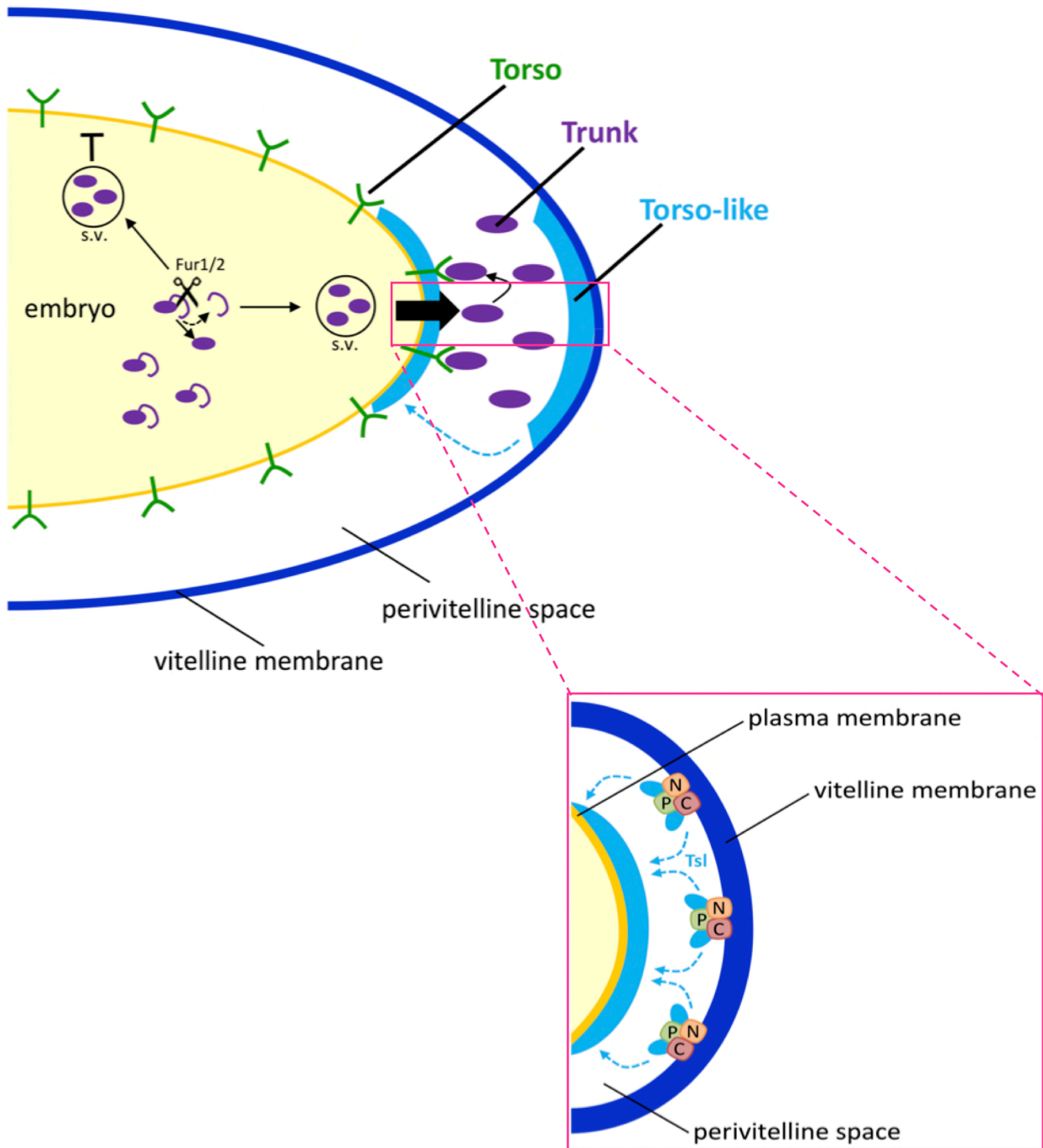
Figure 1.5. Proposed model of the terminal patterning pathway and Tsl localisation. This figure shows the posterior end of the embryo only. Torso receptor (green) is uniformly distributed along the embryo plasma membrane. The ligand pro-Trunk (purple) is cleaved within the developing embryo by Furin proteases to its mature, active form of Trunk (Trk). It is proposed that Trk is present in secretory vesicles (s.v.) at the embryonic membrane, and that membrane disruption acts to release these vesicles specifically at the terminal poles of the embryo. Once secreted into the perivitelline space, Trk binds to the Tor receptor and activates the intracellular signalling cascade. As the only known localised determinant in this system, Torso-like (Tsl, blue) is proposed to be responsible for this localised secretion event. The inset (boxed in pink) shows the currently proposed model for Tsl localisation at both the vitelline and plasma membranes. Extracellular Tsl is initially anchored at the vitelline membrane through its interaction with the structural eggshell components Nasrat (N, orange), Polehole (P, light green) and Closca (C, red). Tsl later translocates (dashed blue arrows) to the plasma membrane at the embryonic termini, where it acts to promote the extracellular accumulation of Furin-cleaved Trk. Figure based on Johnson *et al.* (2015); Mineo *et al.* (2015); and as reviewed in Johnson *et al.* (2017a).

receptor binding and Ras/MAPK activation (Casali and Casanova 2001). As the only localised member of the terminal class genes, Tsl was believed to be responsible for spatially controlling this proteolytic processing of Trk. Indeed, recent work from our lab did confirm that multiple Trk cleavage events are essential for terminal patterning *in vivo* (Henstridge *et al.* 2014). However, Trk cleavage occurred independently of Tsl, as Trk cleavage products were unaffected in a *tsl* mutant background. Whilst it is possible that the Tsl-mediated cleavage event was missed by this approach, other recent data also supports a role for Tsl other than in the localised cleavage of Trk.

A recent study showed synergy between Tsl and Trk in activating Tor in an S2 cell expression system (Amarnath *et al.* 2017). This suggests that Tsl functions after Trk secretion either by stabilising Trk/Tor binding as a co-receptor or by facilitating Tor dimerisation. This would be particularly important given that Trk is the limiting component of this pathway (Sprenger and Nüsslein-Volhard 1992). These ideas are in many ways both plausible and valid, except for the fact that two independent groups in the 1990s clearly demonstrated that Tor activation could occur where Tsl is not located (Sprenger and Nüsslein-Volhard 1992; Casanova and Struhl 1993). For example, when *tor* mRNA was injected into the central region of an oocyte otherwise devoid of *tor*, suppression of segmentation and ectopic terminal structures were observed in the central region (Sprenger and Nüsslein-Volhard 1992). As previously mentioned, the extensive localisation data on Tsl indicates that it is localised to both the inner vitelline membrane and the embryonic plasma membrane, making it highly unlikely that Tsl diffuses away from the poles. This runs counter to the suggestion that Tor activation requires the synergistic activity of Trk and Tsl (Amarnath *et al.* 2017).

However, this Tsl localisation data does not contradict a second hypothesis which proposes that Tsl is required for Trk secretion specifically at the poles of the embryo. Recent work from our lab showed that levels of a fluorescently-tagged N-terminal Trk reporter (which mimics cleaved Trk) in the perivitelline space were substantially reduced at the embryo termini in *tsl* mutants (Johnson *et al.* 2015). Additionally, this study identified two proteases responsible for Trk cleavage *in vivo* (Johnson *et al.* 2015). Two related proteases, Furin 1 and Furin 2, act in a redundant manner inside the oocyte to cleave Trk prior to its secretion. Given that Tsl accumulates at the embryonic plasma membrane (Mineo *et al.* 2015), but is not present inside the oocyte, this makes it highly

unlikely that Tsl is involved in the intracellular cleavage of Trk. Taken together, these data suggest a model whereby Tsl functions to promote the secretion of processed Trk and/or aids in Trk accumulation at the embryo poles (Figure 1.5). Support for this idea comes from evidence that some MACPF/CDC proteins can trigger defence-related secretory events in eukaryotic cells (Reddy *et al.* 2001; Idone *et al.* 2008). It is therefore possible that Tsl acts on the embryonic plasma membrane to promote localised Trk exocytosis via a pore-forming or membrane-damaging mechanism (Johnson *et al.* 2015).

1.3.4. Torso-like also has other developmental roles

Recent work from our lab and others has also shown that both Tor and Tsl have a second developmental role in the regulation of growth and developmental timing (Rewitz *et al.* 2009; Grillo *et al.* 2012; Johnson *et al.* 2013). Tsl and Tor are both expressed in the larval prothoracic gland (PG), the main endocrine organ of the fly. As well as being activated by Trk in the embryo, Tor is the receptor for prothoracicotropic hormone (PTTH), a neuropeptide responsible for initiating metamorphosis (McBrayer *et al.* 2007). Ablation of the PTTH-producing neurons or PG-specific knockdown of Tor signalling causes a developmental delay phenotype, where larvae take longer to reach pupariation, and also increases adult body size due to the prolonged feeding by larvae (Rewitz *et al.* 2009). Interestingly, PTTH and Trk belong to the same family of cysteine knot-like growth factors, and so it was proposed that Tsl might play a similar role in Tor activation in the gland as in the embryo (Grillo *et al.* 2012; Johnson *et al.* 2013).

In support of this view, both PG-specific *tsl* knockdown and *tsl* null mutants are developmentally delayed (Grillo *et al.* 2012; Johnson *et al.* 2013). Moreover, *tor* and *tsl* mutants produce a similar developmental delay. However, the developmental delay of *tor:tsl* double mutants is noticeably enhanced compared to either mutation alone, suggesting an additive rather than an epistatic relationship. Furthermore, these mutants have opposing effects on body size, with *tor* mutants being larger than wildtype, and *tsl* mutants being considerably smaller than the wildtype controls. Together these data indicate that Tsl functions independently from the PTTH/Tor pathway in the regulation of growth and developmental timing (Johnson *et al.* 2013). Given that dpERK levels are markedly reduced in the PG of *tsl* mutants, it is likely that Tsl acts with a different receptor tyrosine kinase in this tissue (Grillo *et al.* 2012). A possible candidate for this receptor is

the insulin-like receptor (InR). When insulin signalling is reduced, for example through the ubiquitous expression of a dominant-negative InR, development is delayed, and the resulting larvae and adults have reduced body size (Slack *et al.* 2011). Whether these similarities are due to a genuine genetic link or simply coincidence is yet to be established. This is particularly important given that it cannot be ruled out that the *tsl* mutant phenotypes are the result of pleiotropic effects including the disruption of Tor and MAPK signalling in the PG, as has been proposed (Grillo *et al.* 2012).

In addition to its known developmental roles in embryonic patterning and larval growth, recent work from our lab also implicates Tsl in *Drosophila* immune system development, as *tsl* null mutants show increased susceptibility to infection by Gram-positive bacteria (Forbes-Beadle *et al.* 2016). Interestingly, rather than acting as a traditional MACPF immune effector, Tsl appears to function in the development of the immune cells themselves. The PDGF- and VEGF-receptor (Pvr) plays an important role in hemocyte proliferation and survival (Brückner *et al.* 2004), and is thus a good candidate for Tsl to work with in this context (Forbes-Beadle *et al.* 2016). It is possible that Tsl acts in hemocyte development by somehow facilitating the release of the ligands for the Pvr pathway.

Finally, recent work from our lab demonstrated a second developmental role for maternal Tsl in coordinating and promoting mesoderm invagination, which is critical for correct ventral morphogenesis and gastrulation in *Drosophila* (Johnson *et al.* 2017b). In this context, Tsl regulates the extracellular activity of the secreted protein Folded Gastrulation (Fog), which signals through the G-protein coupled receptor Mesoderm-invagination signal transducer (Mist) to synchronise and coordinate the cell shape changes required for gastrulation.

Overall, through the identification of these additional roles for Tsl, it has become clear that Tsl is not just a specialised effector of the Tor signalling pathway, but has a more general role in a range of different signalling pathways and developmental contexts. In addition, recent studies on the evolution of Tsl and terminal patterning across insects indicate that Tsl was likely co-opted to the terminal patterning pathway relatively recently (Duncan *et al.* 2013; Duncan *et al.* 2014), supporting the findings that Tsl has other roles in development. By studying Tsl function in these varied developmental contexts, and

ascertaining the specific yet common nature of Tsl activity in these signalling pathways, it may be possible to gain a deeper understanding of developmental MACPF proteins, and the functional versatility of the MACPF domain.

1.4. Aims and thesis structure

Despite the progress made in recent years, there is still much to discover about how developmental MACPF proteins function at a biochemical and cellular level. In particular, do these MACPF proteins also possess lytic ability, or do they have some alternative mechanism of action? As the sole MACPF protein in *Drosophila*, Tsl provides us with a unique opportunity to explore the function of a developmental MACPF protein without the problems caused by functional redundancy often encountered in higher organisms. Whilst some of these answers are only obtainable by Tsl purification and subsequent biochemical studies, something which has so far proved intractable (Johnson *et al.* 2017a), functional studies can provide useful insights as well. In particular, the identification of other proteins that interact with Tsl and are required for Tsl activity may provide valuable clues as to how Tsl interacts with the membrane and how it interacts with Tor and/or Trk. Furthermore, as Tsl appears to act in several different developmental contexts with a variety of different signalling pathways, understanding Tsl activity in these other contexts may further elucidate the true versatility of the MACPF domain.

In this thesis, several current gaps in our knowledge are addressed to provide a better understanding of how MACPF proteins function in their developmental roles using *Drosophila* as a model. This thesis is comprised of three results chapters, each focussing on a different aspect of Tsl function in *Drosophila* development.

The first results chapter (Chapter 2) describes the use of a small RNAi screen to identify novel growth regulators that function in the PG and may interact with Tsl. Two candidate receptors were identified, and one of them was extensively characterised in the PG for a role in ecdysone biosynthesis, although it does not appear to interact with Tsl to perform this function.

In Chapter 3, the functions of various non-*Drosophila* MACPF proteins were investigated, by expressing them in *Drosophila*, primarily to determine whether they could function in

the same manner as Tsl does in terminal patterning. This provided information about the function of the MACPF domain in Tsl development. In addition, phenotypes caused by the overexpression of these MACPF proteins were used to gain insight into the biological pathways they may act in and thus into their endogenous functions.

Chapter 4 follows up on two candidate regions from a genome-wide suppressor screen performed by the Warr lab to identify novel genes required for terminal patterning. It was hoped that this work might identify protein-interaction partners required for Tsl function.

The final chapter (Chapter 5) then brings together the main findings of this research and provides a general discussion that includes suggestions for future research into developmental MACPF proteins.

Chapter 2: Novel growth factor receptors that function in the *Drosophila* prothoracic gland to affect growth and developmental timing

2.1. Introduction

A central and fundamental question of biology concerns how animals regulate growth to attain their final body size. This process is affected by both the rate of growth and the duration of the growth period. In holometabolous insects such as *Drosophila*, adult body size is determined by growth during the larval stages, as the rigid exoskeleton formed during metamorphosis prevents any subsequent increase to body size (Mirth and Riddiford 2007). Thus, by examining larval growth it is possible to understand the mechanisms that affect final body size. In *Drosophila*, the larval growth phase is divided into three stages (instars) prior to the initiation of metamorphosis. Each of these transitions requires the shedding of the old cuticle (moult) and the synthesis of a new cuticle. Both the transitions between stages and the duration of each stage are controlled by the larval neuroendocrine complex, which consists of two key components (for review see Nässel and Winther 2010; Nijhout *et al.* 2014). These are the specialised secretory neurons of the central nervous system and two paired endocrine glands – the prothoracic glands (PG) and the corpora allata (CA) (Figure 2.1). The neurosecretory cells produce various peptide hormones which are delivered to their targets through a combination of direct axonal connections and circulation via the hemolymph. The CA produce the "status quo" sesquiterpenoid juvenile hormone, and the PG produce the steroid hormone ecdysone, which together are the central effector hormones of both moulting and metamorphosis. The PG and CA, together with a third glandular tissue, the corpora cardiaca (CC), form a composite organ known as the ring gland (Figure 2.1). The CC produces a neuropeptide called adipokinetic hormone (Akh), which is secreted into the hemolymph to facilitate the release of energy-rich substrates from the fat body in response to nutritional requirements (Kim and Rulifson 2004), and is thus functionally analogous to human glucagon.

2.1.1. Growth signalling pathways in the PG

During the larval and pupal stages of development, pulses of ecdysone are produced and released from the PG in response to multiple developmental and environmental stimuli (for review see Mirth and Shingleton 2012; Danielsen *et al.* 2013; Niwa and Niwa 2014b).
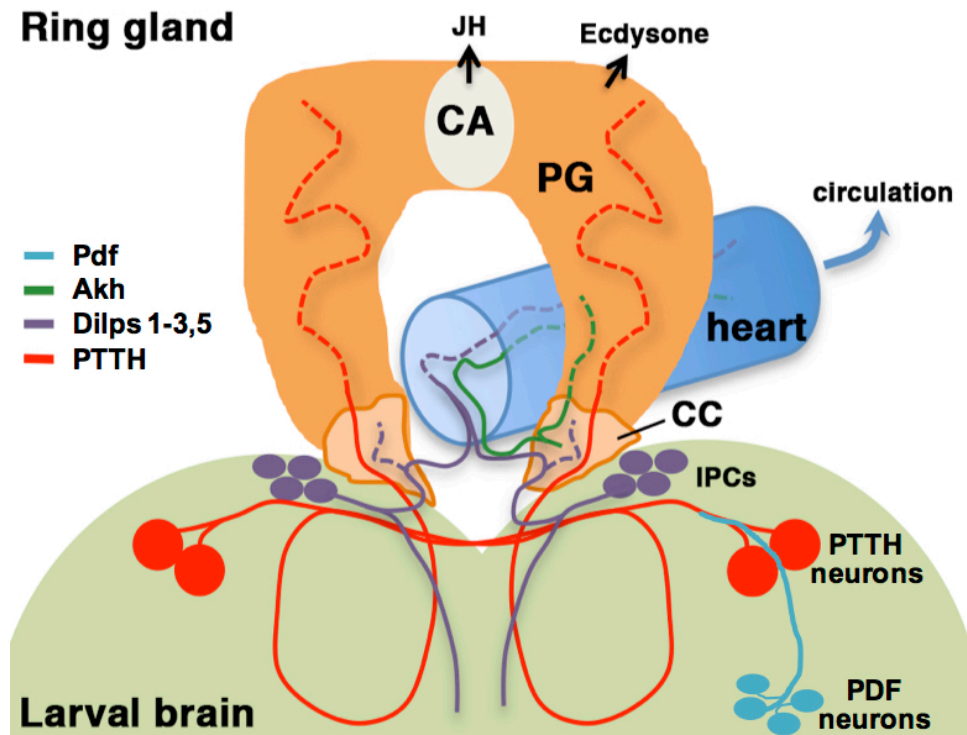
Figure 2.1. The larval neuroendocrine complex consists of the ring gland and brain.
The ring gland is comprised of three tissues: the prothoracic glands (PG), corpora allata (CA) and corpora cardiaca (CC). Prothoracicotropic hormone (PTTH) is produced by specialised neurons in the brain lobe which innervate the PG (**red**). PTTH in turn acts as the ligand for Torso in the PG to regulate developmental transitions. Circadian control of PTTH release is provided by the Pigment-dispersing factor (Pdf, **teal**) neurons in the larval brain, which directly innervate the PTTH neurons. Various other neuropeptides are produced by these tissues, such as adipokinetic hormone (Akh, **green**), and insulin-like peptides (dILPs, **purple**), which are produced by the CC and IPCs respectively.

A multitude of complex cellular signalling pathways are required to coordinate the responses to these signals (Figure 2.2). The peptide hormone prothoracicotropic hormone (PTTH) is a major factor that stimulates the ecdysteroidogenic activity of the PG, and is produced by two pairs of lateral neurons that innervate the PG (McBrayer *et al.* 2007; Figure 2.1). Prior to each larval moult, PTTH is secreted and activates the Torso receptor tyrosine kinase on the PG cells, thereby activating the canonical Ras/Mitogen-activated protein kinase (Ras/MAPK) signalling cascade to upregulate a set of ecdysone biosynthesis genes (McBrayer *et al.* 2007; Rewitz *et al.* 2009). Ablation of the PTTH-producing neurons or PG-specific knockdown of *torso* extends the larval growth period, resulting in delayed pupariation and an increase in adult body size (McBrayer *et al.* 2007; Rewitz *et al.* 2009).

In addition to the PTTH/Tor pathway, there are several other peptidergic signalling pathways that are known to regulate ecdysone biosynthesis in response to various environmental cues (Figure 2.2). The evolutionarily conserved insulin signalling pathway acts in the PG to regulate ecdysone biosynthesis in response to nutritional cues (Caldwell *et al.* 2005; Colombani *et al.* 2005; Mirth *et al.* 2005). In particular, this pathway affects larval growth rate and the timing of a specific developmental checkpoint known as critical weight, thereby controlling the time at which metamorphosis occurs (Mirth *et al.* 2005; Koyama *et al.* 2014). In *Drosophila*, a family of insulin-like peptides (dILPs) activate the insulin-like receptor (InR) (Brogiolo *et al.* 2001). A subset of these (dILPs 2, 3 and 5) are produced in the insulin-producing cells (IPCs) that innervate the CC (Figure 2.1). Ablation of these neurons results in a developmental delay and decreased body size (Ikeya *et al.* 2002; Rulifson *et al.* 2002), as does the reduction of insulin signalling in the whole fly (Chen *et al.* 1996; Böhni *et al.* 1999; Slack *et al.* 2011). Interestingly, whilst the PG-specific reduction in insulin signalling also delays development, it has an opposing effect on body size, thereby resulting in bigger adults (Colombani *et al.* 2005; Mirth *et al.* 2005; our unpublished data).

The target of rapamycin (TOR) pathway, well-known for coordinating cell growth with nutritional availability (Zhang *et al.* 2000), also stimulates the production of ecdysone in the PG (Layalle *et al.* 2008). In addition, the TGFβ/Activin pathway acts as a competence signal for the PG, being responsive both to nutritional (dILPs/InR) and developmental (PTTH/Torso) signals (Gibbens *et al.* 2011).
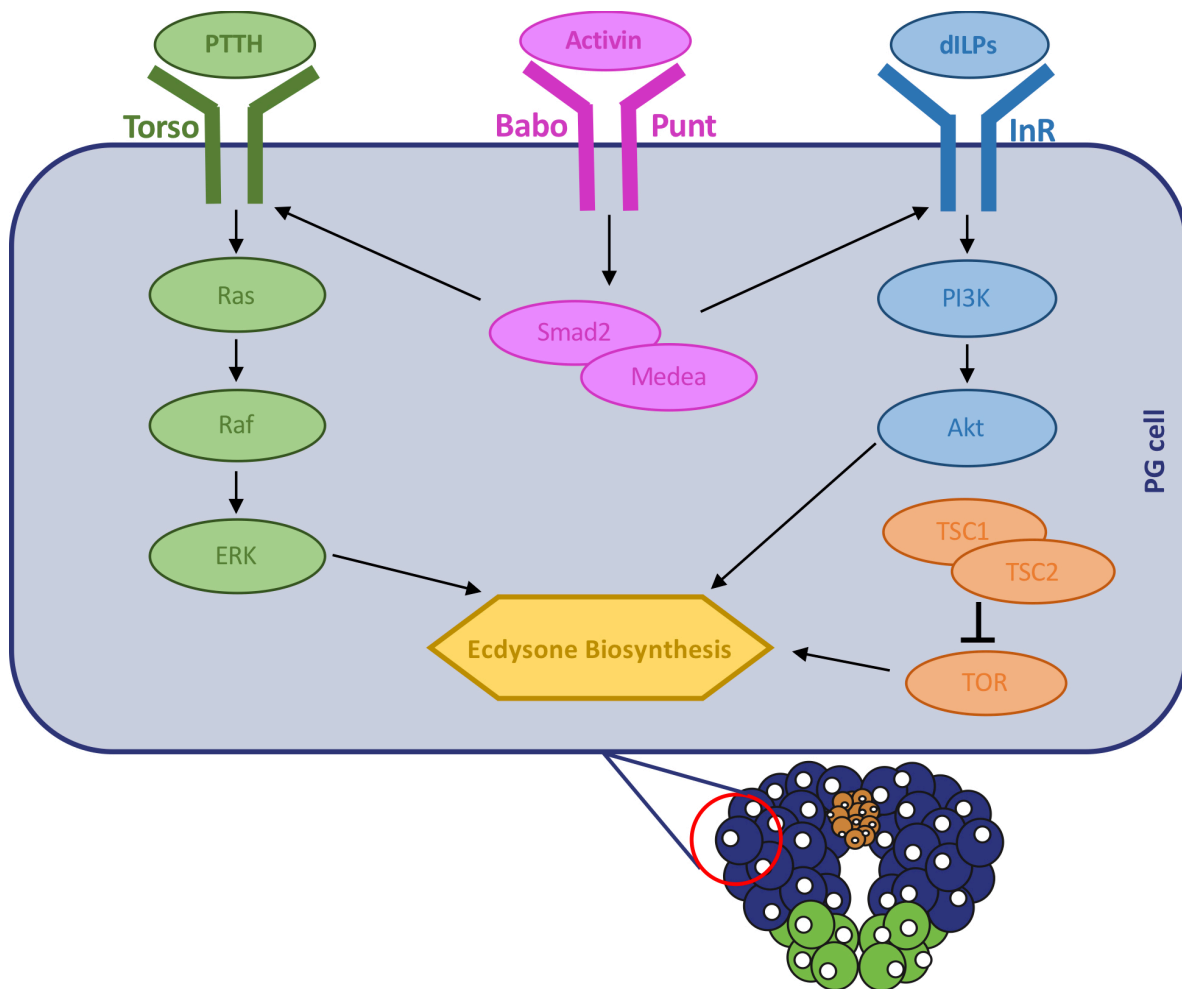
Figure 2.2. Known signalling pathways that regulate ecdysone biosynthesis.

Many environmentally responsive pathways act to regulate ecdysone biosynthesis in a combinatorial and partially redundant manner. There is likely to be extensive cross regulation between these signalling pathways. The peptide hormone PTTH is the major factor that stimulates the ecdysteroidogenic activity of the PG, where it binds to its receptor Torso, thereby activating the canonical Ras/MAPK signalling cascade (green) to upregulate a set of ecdysone biosynthesis genes. The insulin signalling pathway (blue) acts in the PG to regulate ecdysone biosynthesis in response to nutritional cues. The target of rapamycin (TOR) pathway (orange) also stimulates the production of ecdysone in the PG in response to nutritional availability. The TGFβ/Activin pathway (pink) acts as a competence signal for the PG, being responsive both to nutritional (dILPs/InR) and developmental (PTTH/Torso) signals. Moreover, there is mounting evidence from both *Drosophila* and other insect models that additional growth regulatory pathways remain to be identified that may also regulate developmental timing. Figure adapted from Yamanaka *et al.* (2013).

There is also increasing evidence from both *Drosophila* and other insect models that additional peptidergic pathways may play a role in the PG and ring gland to influence growth and developmental timing. Firstly, PTTH-neuron ablated larvae are still able to pupariate, albeit after a significant developmental delay of approximately 5 days (McBrayer *et al.* 2007). Secondly, the *ptth* null larvae only exhibit a mild developmental delay of approximately 24 hours (Shimell *et al.* 2018). In addition, when the PTTH-producing neurons are inactivated in the *ptth* null background, this developmental delay is increased by an additional day. Moreover, when the PTTH-producing neurons were activated in the *ptth* null background, this activation rescued most of the delay observed in *ptth* null animals (Shimell *et al.* 2018). Taken together, these data strongly suggest that at least one other factor is supplied by these neurons to the PG, which can activate pupariation in the absence of PTTH.

In addition, the PG and the ring gland have now been shown to be innervated by additional neurosecretory neurons other than those that secrete PTTH and the dILPs (Siegmund and Korge 2001; Niwa and Niwa 2014b). In other insects, such as the silkworm *Bombyx mori*, several prothoracicostatic factors have been shown to regulate ecdysteroidogenesis in the PG, including myosuppressin and the prothoracicostatic peptides (Yamanaka *et al.* 2010; Tanaka 2011). It is therefore likely that other as yet unknown factors and additional regulatory mechanisms work in the *Drosophila* PG to regulate ecdysteroidogenesis. As such, the complex interactions and cross-talk between these various signalling pathways and how they work combinatorially to regulate ecdysone production in response to developmental and environmental cues is only now beginning to be elucidated.

2.1.2. Tsl functions in the larval PG to regulate growth and developmental timing

Recent work from our lab and others has identified the MACPF protein Tsl as a novel regulator of growth and developmental timing in the PG (Grillo *et al.* 2012; Johnson *et al.* 2013; see Section 1.3.4). While in terminal patterning Tsl functions in Torso activation, unexpectedly Tsl acts independently of Torso to regulate growth and developmental timing (Johnson *et al.* 2013). Specifically, *tsl* and *torso* mutants have opposing effects on body size, and the developmental delay phenotype observed in *tsl:torso* double mutants is noticeably enhanced compared to either mutation alone, suggesting an additive rather than epistatic interaction between these genes (Johnson *et al.* 2013).

To identify what signalling pathway Tsl works with in growth, it was of interest to identify other neuropeptide or growth factor receptors that function in the PG to regulate growth and developmental timing. A previous Honours student in our lab (Pat Farrell) conducted a small screen in which a set of 25 candidate receptors were knocked down with RNAi in the PG using *phantom(phm)*-Gal4 (Figure 2.3). The knockdown of three receptors, *Adipokinetic hormone receptor (AkhR), platelet-derived growth factor/vascular endothelial growth factor receptor (Pvr),* and *thickveins (tkv)*, resulted in developmental arrest and larval lethality. The knockdown of *Pigment-dispersing factor receptor (PdfR),* resulted in a significant delay in the time to eclosion, as did the InR and Torso positive controls. These genes represented alternative candidate receptors that Tsl may interact with to regulate growth and developmental timing in the PG.

In a parallel study, Dr. Michelle Henstridge in our group showed that Tsl works with the insulin signalling pathway to regulate growth and developmental timing in the PG (Henstridge *et al.* 2018). For example, *tsl* null mutants closely resemble mutants with impaired insulin signalling in several key biochemical and physiological characteristics. Tsl was also found to genetically interact with the insulin signalling pathway, as larvae mutant for both *tsl* and *dilps 2, 3*, and *5*, had a similar developmental delay to *dilp 2-3^4, dilp5^3* mutants alone (Henstridge *et al.* 2018). Furthermore, *tsl* null larvae were shown to accumulate both dILP2 and dILP5 in their IPCs during larval development, and also to have increased *dilp2/5* expression, both of which are characteristic of a systemic reduction in insulin signalling (Henstridge *et al.* 2018). In addition, this same study showed that Tsl is specifically required in the PG to regulate growth and developmental timing, and is present in the larval hemolymph. Taken together, this supports a role for Tsl in regulating systemic insulin signalling, thereby affecting larval growth and developmental timing.

While the findings in the Henstridge *et al.* (2018) study decrease the likelihood that the receptors found in the RNAi screen function with Tsl, the screen identified several candidate receptors that may represent novel growth regulators not previously characterised in the *Drosophila* PG. This chapter therefore further investigates AkhR and PdfR as they have not previously been studied in the *Drosophila* PG nor been implicated in PG function.
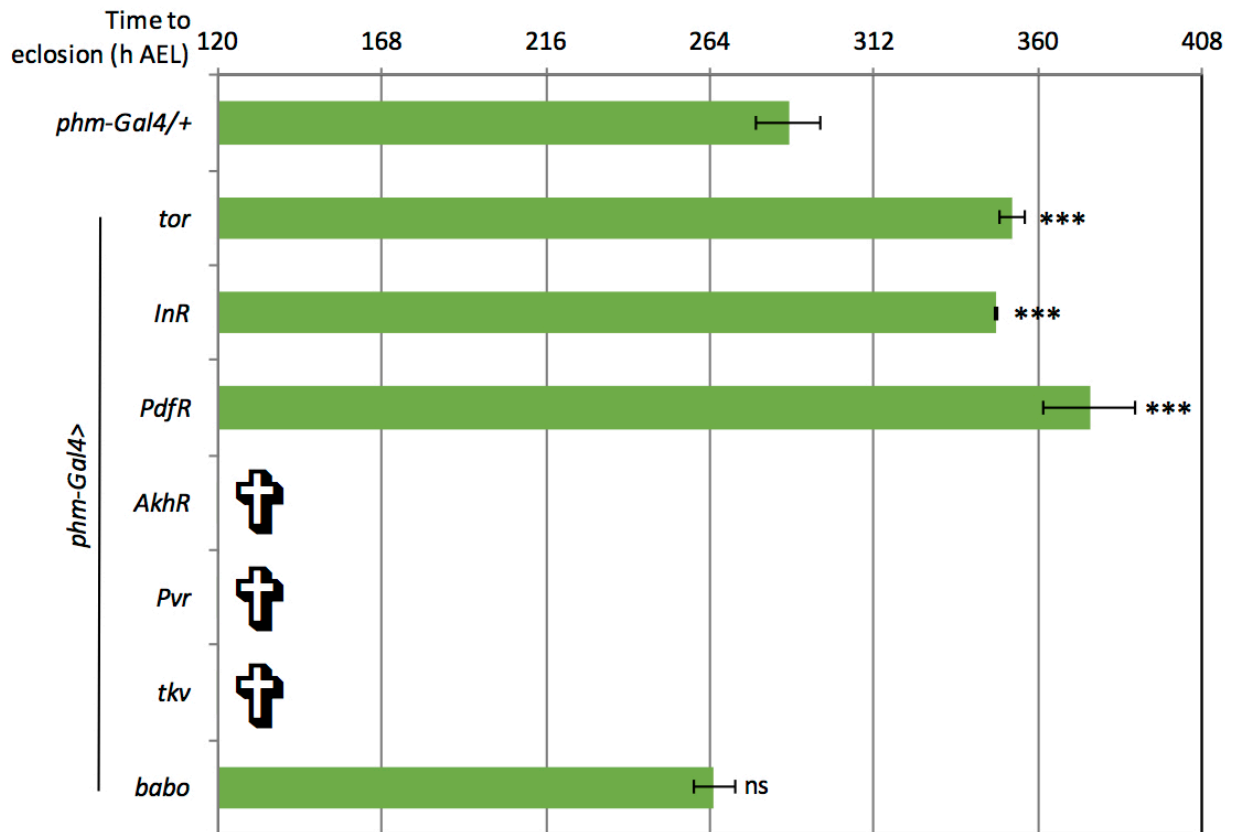
Figure 2.3. RNAi screen for neuropeptide receptor genes expressed in the PG that regulate developmental timing.

In a small screen to identify novel receptors that function in the PG to regulate developmental timing, twenty-five candidate neuropeptide receptor RNAi lines were expressed in the PG using *phm-Gal4*. Six of these gave reproducible phenotypes, with three increasing developmental time to eclosion, and three resulting in developmental arrest (lethality). The knockdown of three receptors, *Adipokinetic hormone receptor (AkhR)*, *platelet-derived growth factor/vascular endothelial growth factor receptor (Pvr)*, and *thickveins (tkv)*, resulted in developmental arrest and larval lethality. The knockdown of *Pigment-dispersing factor receptor (PdfR)*, resulted in a significant delay in the time to eclosion, in hours after egg lay (h AEL), compared to the *phm-Gal4/+* control (***$p<0.001$), as did the InR and Torso positive controls. Error bars show ±1 SEM, *n* = 2-3 biological replicates. Time to eclosion was compared between genotypes using a one-way ANOVA with multiple comparison (each genotype to control) using Sidak's correction. Data summarised from Pat Farrell's Honours thesis (2015).

2.2. Materials and Methods

2.2.1. Fly stocks and maintenance

w^{1118} (BL3605), *elav*-Gal4 (BL5146), *PdfR^{5304}* (BL33068) and UAS-*Dicer-2* (BL24650) stocks were obtained from the Bloomington *Drosophila* Stock Center. The following UAS-*RNAi* stocks were obtained from the Vienna *Drosophila* Resource Center: *AkhR* (KK109300), *InR* (GD992), *PdfR* (KK106381), *Pvr* (KK105353), *tkv* (KK105834), *torso* (KK101154). *phm*-Gal4*/CyO,GFP* was a kind gift from Leonie Quinn at the University of Melbourne (originally from Michael O'Connor). *phm*-Gal4-22, UAS-*mCD8::GFP/TM6B* was a gift from Christen Mirth, and UAS-*Dicer-2; phm*-Gal4-22, *UAS-mCD8::GFP/TM6B* was generated to improve knockdown efficiency. All stocks were maintained on standard fly media (Appendix 1) in 30mL vials at 22°C with a 12-hour alternating light/dark cycle. All crosses were performed at 25°C, unless otherwise stated.

2.2.2. Developmental timing assays

All stocks were maintained on standard fly media at 25°C. Adults were allowed to lay on apple juice agar media supplemented with yeast paste for 4 hours. Embryos were allowed to develop for 24 hours at 25°C. Upon hatching, non-GFP (on a balancer chromosome) first instar (L1) larvae were picked into vials containing standard fly media in groups of 15, with 10 replicates per genotype. Vials were maintained at 25°C in constant darkness. Time to pupariation was scored every 8 hours until all larvae had pupariated or died. One-way ANOVAs with post-hoc (Tukey) tests were used to test for statistical significance between different genotypes using GraphPad Prism v7.0a software. Graphs were generated using Microsoft Excel.

2.2.3. Adult, pupal and larval body measurements

Shortly after eclosion, adult flies from the developmental timing assay were separated by sex and frozen. Flies from each replicate vial were weighed in groups on a Mettler Toledo XP2U Ultra-microbalance [readability (d) 0.1µg]. The average weight from each replicate vial was then used to calculate an average across biological replicates. Pupae were collected as soon as the pupal case was properly hardened. They were washed briefly and dried, and then weighed as above. One-way ANOVAs with post-hoc (Tukey) tests were

used to test for statistical significance between different genotypes using GraphPad Prism v7.0a software. Graphs were generated using Microsoft Excel.

Larvae were collected every 12 hours from 90h after egg lay (h AEL) until pupariation for all genotypes. At the desired time point, larvae were collected using 20% sucrose, washed and dried and then weighed as above. The average weight from each replicate vial was then used to calculate an average across biological replicates. The raw larval weight data was analysed and graphed using GraphPad Prism v7.0a software. Additional analysis of the log_{10} transformed weight data was performed using R software (with assistance from Christen Mirth), which enabled the fitting of a linear model and statistical analysis of larval growth rate over time.

2.2.4. Ecdysone (20E) feeding assays

For ecdysone feeding experiments, 15µL of 20-Hydroxyecdysone (20E) stock solution (10 mg/mL 20E [Cayman Chemicals] in 96% EtOH) was added to 1g of pureed standard fly medium in 5mL round-bottom polypropylene tubes (Falcon). The resulting media was well mixed before being centrifuged for 1 min at 1100rpm. Control food contained 15µL 96% EtOH without any 20E. Larvae were transferred to either 20E-supplemented fly medium or control food at 96 hr after egg lay (h AEL) in groups of 10, with 10 replicate tubes per genotype. Time to pupariation and adult weight were assayed as previously stated.

2.2.5. Larval staging

Adults were allowed to lay on apple juice agar media supplemented with yeast paste for 4 hours. Newly hatched, non-GFP (on balancer chromosome) L1 larvae were picked onto standard food plates (maximum 200 larvae per 35x10mm plate). Newly moulted third instar (L3) larvae were collected every 2 hours, placed into new vials containing standard food, and allowed to feed until the appropriate time point. Egg-laying and larval rearing took place at 25°C under constant darkness.

2.2.6. PG morphology

PdfR expression was knocked down in the PG using a *phm*-Gal4 stock that also expressed UAS-*GFP::mCD8*, thus labelling all the PG cells with GFP. Appropriately aged larvae were

collected and washed with distilled H_2O to remove any affixed fly media, before being dissected with fine forceps in PBS. Larval tissues were fixed in 4% paraformaldehyde in PBS for 30 minutes while rocking. After fixation, tissue was washed several times in PTx, and then incubated in a solution of DNase-free RNase (5ng/ml) and PTx for 20 minutes at room temperature while rocking, in order to eliminate the cytoplasmic background due to RNA. Tissue was further rinsed with PTx before being incubated in H_2O with DAPI (1:3000) to stain cell nuclei. Secondary dissections were performed in PBS and tissue was mounted on poly-L-lysine-coated coverslips using VectaShield, as previously described (Mirth *et al.* 2005). Tissues were imaged using a spinning disc confocal microscope (Olympus CV1000) at 20x magnification. Once imaged, the PG outline was selected using the free-draw tool in ImageJ, and the enclosed area was measured. Unpaired student *t* tests were used to test for statistical significance between the different genotypes using GraphPad Prism v7.0a software. Graphs were generated using Microsoft Excel.

2.2.7. Ecdysteroid quantification

Ecdysteroid levels were quantified using a 20-Hydroxyecdysone enzyme immunoassay (EIA) (Cayman Chemicals). At the required time points, groups of ten staged larvae (2.2.5) were washed in distilled water, briefly dried on Kimwipes (Kimtech) before being weighed on a Mettler Toledo XP2U Ultra-microbalance [readability (d) 0.1μg], and snap-frozen on dry ice. Larvae were preserved in three-times their volume of ice-cold methanol and stored at -80°C until use. Briefly, frozen samples were homogenised by thorough grinding on ice, followed by centrifugation for 20 minutes at 4°C. The resulting supernatant was evaporated using a SpeedVac Concentrator (Thermo Scientific) for 45 minutes, and samples were re-suspended in 100μl EIA buffer. The EIA was performed according to the manufacturer's instructions (Cayman Chemicals). Absorbance was measured at 405 nm on a Synergy Mx plate reader (BioTek) using Gen5 software (BioTek). Five biological reps of ten larvae were used for each of three genotypes, across five time-points in total. Data compilation and preliminary analysis was performed using Microsoft Excel. Statistical analysis and graphing were performed in R (with assistance from Christen Mirth), where data were fit with linear models for the response of ecdysone concentration to both the linear and quadratic components of time, to genotype, and to the interaction between time and genotype.

2.2.8. Quantitative RT-PCR (qRT-PCR) for ecdysone biosynthesis genes

At the required time points, groups of ten staged larvae (2.2.5) were washed in distilled water, before being placed in Eppendorf tubes containing 100μl TRIsure reagent (Bioline) and stored at -80°C until all samples were collected. Frozen samples were homogenised by thorough grinding on ice, before an additional 400μl TRIsure reagent was added. RNA extraction was performed as per manufacturer's instructions. Following treatment with DNase (Promega), total RNA concentration was quantified and 5mg of RNA was converted into cDNA using the Tetro cDNA Synthesis Kit (Bioline) as per manufacturer's protocol. Both oligo dT and random hexamers were used in this reaction. qPCR was performed in triplicate using SensiMix SYBR Green (Bioline) on a LightCycler 480 (Roche). Primers specific for *dib*, *phm* and *rpL23* were as per Gibbens *et al.* (2011), whereas primers specific for *E74B* were as follows (F-5'-CGGAACATATGGAATCGCAGTG-3', R-5'-CATTGATTGTGGTTCCTCGCTG-3'). Melt curves for each primer pair were validated to ensure amplification of a single PCR product. Fold changes relative to *rpL23* were determined using the delta CT (ΔΔCT) method, and means and standard errors calculated from 3-6 biological replicates per genotype per time-point. One-way ANOVA was used to determine whether there were statistically significant differences in relative gene expression levels between genotypes.

2.3. Results

2.3.1. Follow-up on initial screen reduces candidate genes to just two: *AkhR* & *PdfR*

The PG-specific knockdown of four genes (*AkhR*, *PdfR*, *Pvr* and *tkv*) with RNAi gave reproducible developmental phenotypes. The screen used a set of RNAi lines from the Vienna *Drosophila* Resource Center (VDRC) called the KK lines (Dietzl *et al.* 2007). Recent work from Green *et al.* (2014) has shown that some KK RNAi lines produce non-specific dominant phenotypic effects with certain Gal4 drivers as a result of the mis-expression of the *tiptop* gene in which the target vector has been inserted erroneously (the "annotated" site). As such, it was investigated whether the RNAi lines used to identify the hits from the initial screen were affected by this problem. Each KK RNAi line was tested with the PCR diagnostic test outlined in Green *et al.* (2014), in which occupied sites produce smaller PCR products than unoccupied sites (Figure 2.4). Out of the four lines, the KK RNAi lines for both *tkv* and *Pvr* contained an occupied annotated site, but the ones for *Pdfr* and *Akhr* did not.
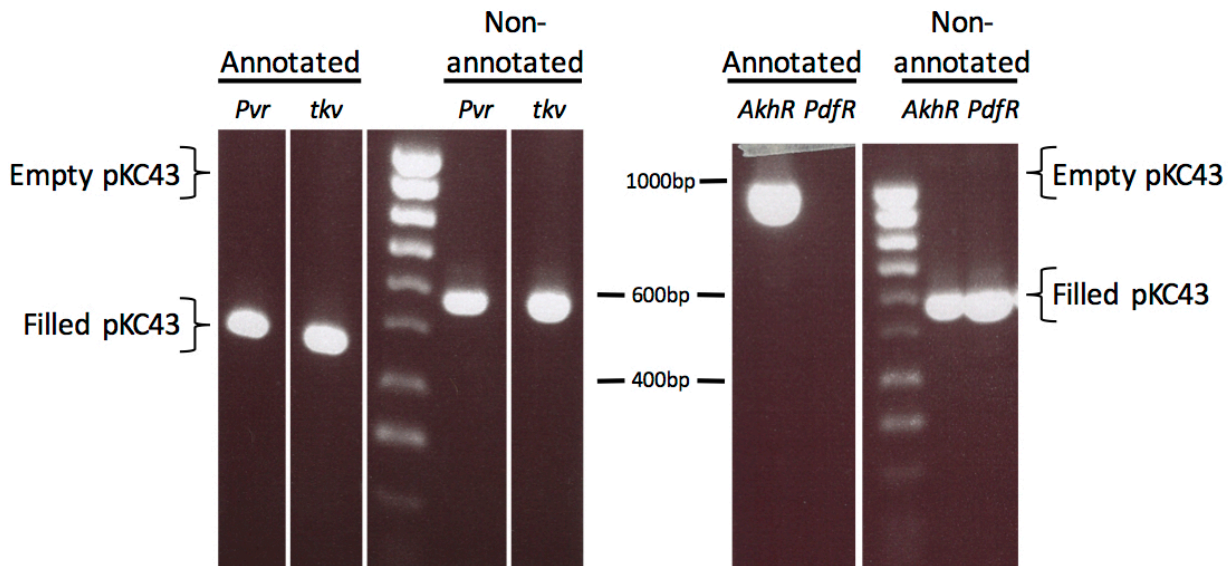
Figure 2.4. PCR-based diagnostic assay for screen KK RNAi lines.

Gel showing the results of the PCR-based diagnostic used to interrogate the pKC43 insertion sites for integration of the pKC26 vector (which carries the shRNA sequences). For the annotated insertion site, integration of pKC26 into pKC43 gave a ~450bp product, which can be seen for both the *Pvr* and *tkv* lines (left-side gels). Alternatively, the presence of pKC43 alone gave a ~1050bp product, as can be seen for the *AkhR* line (right-side gels). For the non-annotated insertion site, integration of pKC26 into pKC43 gave a ~600bp product, which can be seen for both the *Pvr* and *tkv* lines (left-side gels), and the *AkhR* and *PdfR* lines (right-side gels). Alternatively, the presence of pKC43 alone gave a ~1200bp product (not observed). In summary, the KK RNAi lines for *Pvr* and *tkv* have filled pKC43 sites at both the annotated and non-annotated sites. The KK RNAi lines for *AkhR* and *PdfR* have filled pKC43 sites at only the non-annotated site.

To confirm this result a second approach from the Green *et al.* (2014) study was also used. They showed that when KK lines with an occupied annotated site are expressed with the pan-neuronal driver *Elav*-Gal4, the resulting adults exhibit a distinctive non-inflating wing phenotype. The four KK lines were therefore expressed with *Elav*-Gal4 and the resulting F1 flies examined for a non-inflating wing phenotype. The *tkv* KK RNAi produced this phenotype when crossed to *Elav-Gal4*, suggesting that this line does contain an occupied annotated site. Pan-neuronal knockdown of *Pvr* resulted in lethality prior to eclosion, so wing formation was not able to be examined. Thus, it is possible that the delay to eclosion observed when *tkv* and *Pvr* were knocked down in the PG using the KK RNAi lines was the result of Gal4-mediated toxicity and not *tkv* or *Pvr* knockdown specifically. Given these findings, *AkhR* and *PdfR* were chosen for further investigation. They were also of interest as they both encode neuropeptide receptors.

2.3.2. PdfR is a novel regulator of developmental timing and growth in the PG

2.3.2.1 PdfR functions in the PG to control the timing of larval development

PdfR is the receptor for pigment-dispersing factor (Pdf), a neuropeptide well known as a regulator of circadian rhythm in flies. Although it is known that the Pdf neurons innervate the PTTH neurons to supply circadian input into PTTH release (Myers *et al.* 2003; McBrayer *et al.* 2007), this does not explain the delay observed in our screen (Figure 2.3), which suggests that PdfR has an additional and separate role in the PG. In further support of this hypothesis, recent investigations in the silkworm, *Bombyx mori,* have shown that *PdfR* is expressed in the PG in this species, and that the PG responds to the presence of Pdf by increasing ecdysone synthesis *ex vivo* (Iga *et al.* 2014).

To further characterise the phenotype caused by PG-specific knockdown of *PdfR*, *phm>PdfR^{RNAi}* larvae were again assayed for developmental timing, but measured to pupariation, rather than to eclosion. This provides better temporal resolution regarding when PdfR function is required in the PG, and removes the variability associated with eclosion rhythms. Reduction of *PdfR* expression in the PG of *phm>PdfR^{RNAi}* larvae was found to delay the onset of pupariation by 112h compared to both the *phm-Gal4/+* and *PdfR^{RNAi}/+* controls (*p*<0.0001, Figure 2.5A). In addition, overall adult weight was measured as a proxy for final body size, thereby indicating the effects of knockdown on overall growth. Both male and female *phm>PdfR^{RNAi}* adults were significantly heavier than both of the control genotypes (*p*<0.05, Figure 2.5B).

A Time to pupariation (h AEL)

B Males / Females
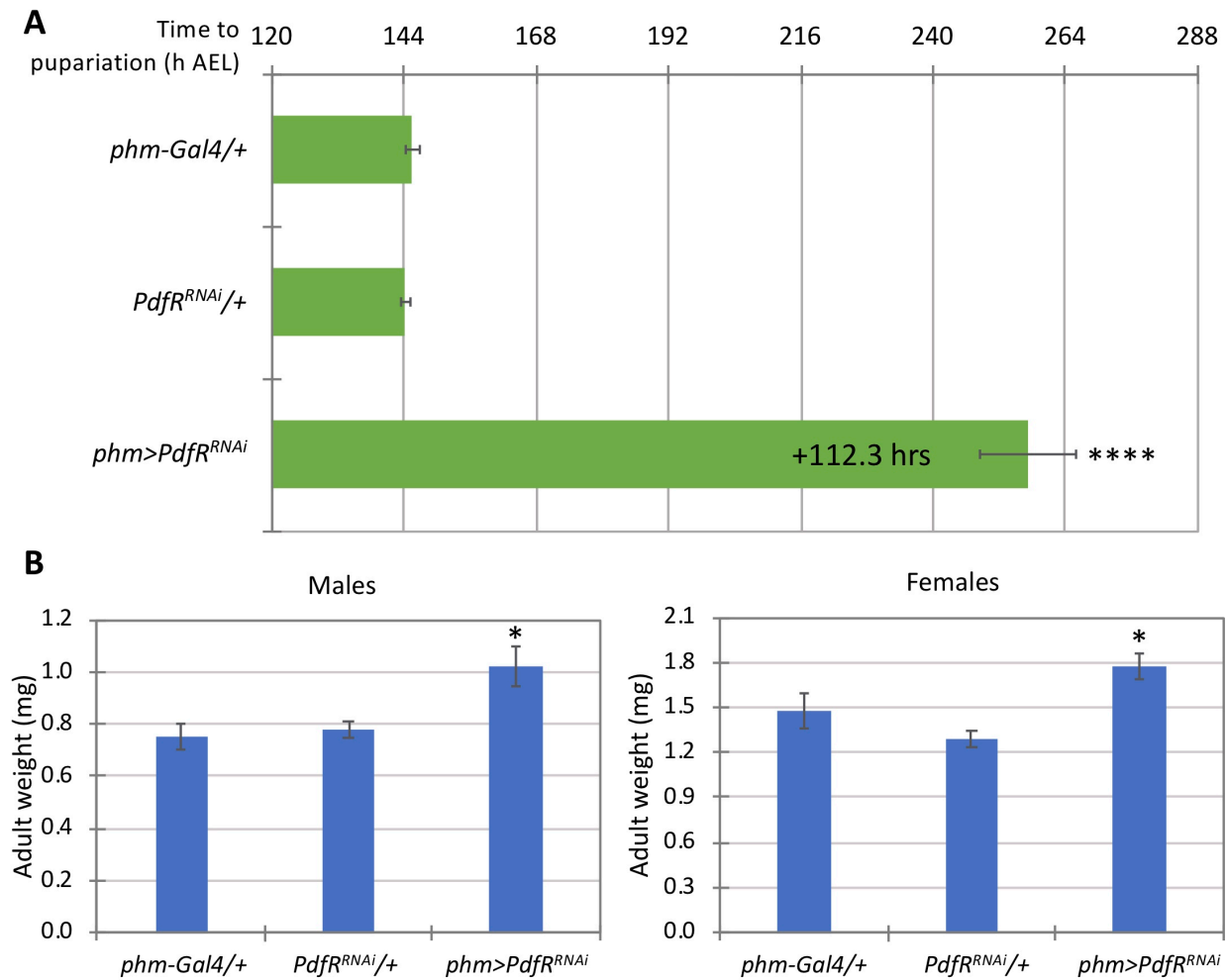
Figure 2.5. Knockdown of *PdfR* in the PG causes a severe developmental delay and increases adult body size.

(A) PG-specific *PdfR* knockdown larvae pupariate 112 hours later than both the *phm-Gal4/+* and *PdfR^RNAi^/+* controls (****$p<0.0001$). (B) The resulting males are 33% larger on average than both the control genotypes (*$p<0.05$), whereas the females were 37% larger than the RNAi controls, but not significantly different from the Gal4 controls (*$p<0.05$ and $p=0.1027$, respectively). Time measured in hours after egg lay (h AEL). Error bars represent ±1 SEM for all graphs. One-way ANOVA was performed followed by Tukey's post-hoc tests (GraphPad Prism). $n = 12$ for all means with no fewer than 100 individuals tested for each genotype, with 4 repeats of entire experiment.

While no off-targets are predicted for the RNAi line used to knockdown *Pdfr* (KK; Dietzl *et al.* 2007), it is always desirable to confirm an RNAi-generated phenotype with a second independent experiment. While an independent *PdfR* GD RNAi line was available (Dietzl *et al.* 2007), a previous study has shown that it fails to effectively knockdown *PdfR* transcripts (Agrawal *et al.* 2013). This line was therefore not able to be used to validate the RNAi phenotype. However, a null allele for *PdfR*, *PdfR^5304^* (Hyun *et al.* 2005), was available. The *PdfR^5304^* mutant was generated via P-element excision, resulting in a deletion of approximately two-thirds of the protein-coding sequence, including all seven transmembrane domains and the C-terminus required for G-protein activation (Hyun *et al.* 2005).

*PdfR^5304^* mutant larvae were found to pupariate on average 5 hours later than their heterozygous controls ($p<0.05$, Figure 2.6A). *PdfR^5304^* homozygous male adults weighed on average 12.8% more than the heterozygous controls ($p<0.01$, Figure 2.6B), although adult females were approximately the same weight. Homozygous *PdfR^5304^* mutant pupae weighed on average 11.8% more than their heterozygous counterparts ($p<0.001$, Figure 2.6C). In summary, while *PdfR^5304^* mutants were found to be developmentally delayed and have increased body size, the overall effect was less severe than with PG-specific *PdfR* RNAi. The PG-specific knockdown of *PdfR* was used in subsequent studies due to the strength of this phenotype, and our interest in genes that act within the PG to regulate ecdysone production.

2.3.2.2 PdfR is not required for PG development

While the phenotypes of developmental delay and increased body size are most likely due to an effect on PG function, it was also possible that the phenotypes observed with PG-specific knockdown of *PdfR* were due to defects in the development and morphology of the PG. To determine if this was the case, overall PG size was compared in both control and *phm>PdfR^RNAi^* larvae by dissecting PGs genetically labelled with GFP from newly wandering larvae and staining the nuclei with DAPI. The overall morphology of the *phm>PdfR^RNAi^* glands was found to be normal, with no observed changes to cell number or morphology. The apparent lack of separation between the two lobes of PGs from *phm>PdfR^RNAi^* larvae is an artefact of the dissection and mounting process, and is not indicative of defects in overall morphology (Christen Mirth, pers. comm.). Surprisingly, the average area of the gland in *phm>PdfR^RNAi^* larvae was increased by 34% compared with time-matched control

41
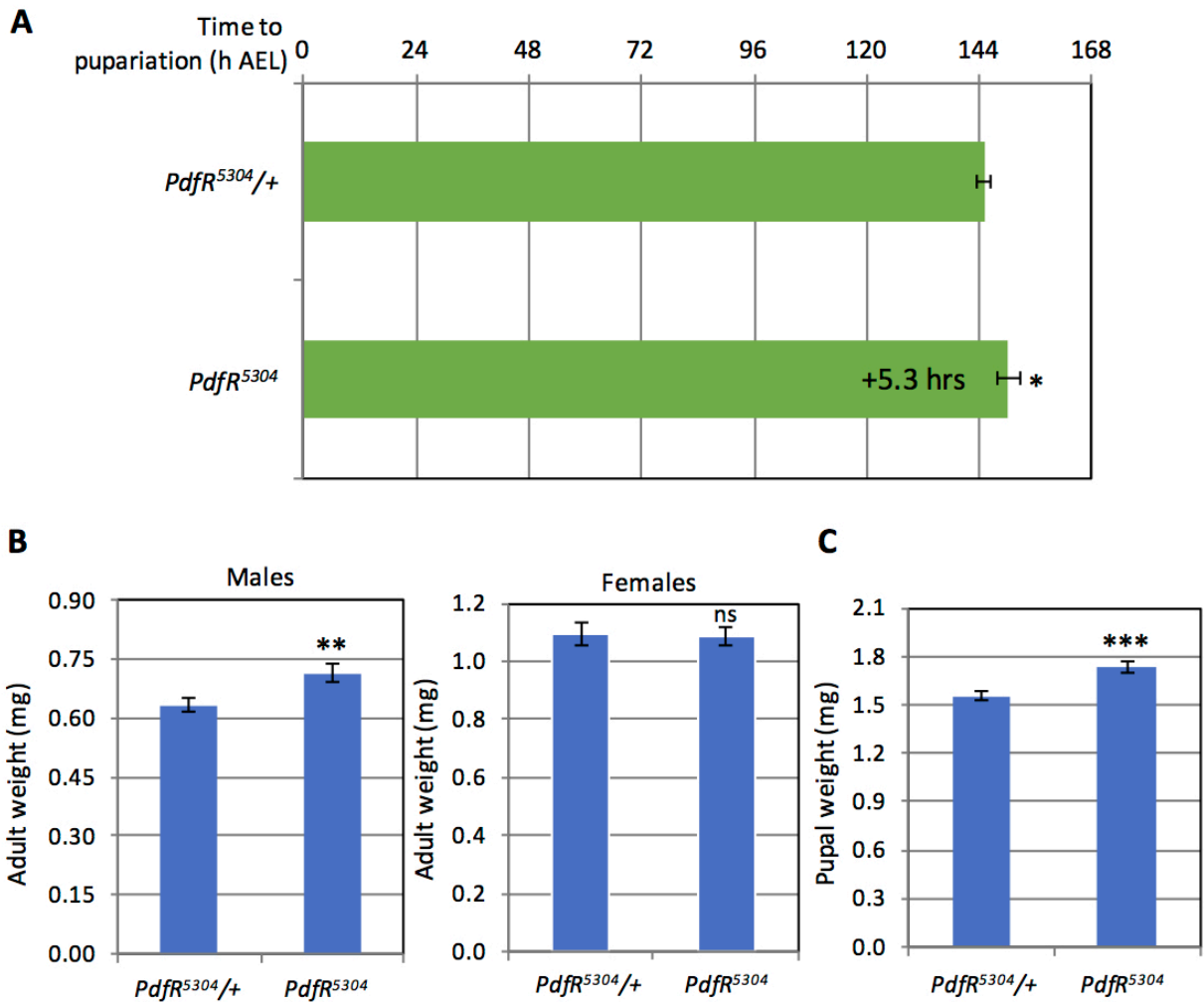
Figure 2.6. *PdfR^5304* mutants are developmentally delayed and have increased body size, but the overall effect is much milder than with PG-specific *PdfR* loss.

(A) *PdfR^5304* homozygous mutants pupariate on average 5 hours later than their heterozygous controls (**p<0.05*, *n* = 12 reps of 10). (B) *PdfR^5304* homozygous male adults weighed 12% more than heterozygous controls (***p<0.01*) although adult females were approximately the same weight (ns). No fewer than 100 adults were weighed for each genotype. (C) Homozygous *PdfR^5304* mutant pupae (mixed sex) weighed more than their heterozygous counterparts (1.5522 mg vs. 1.7371 mg, ****p<0.001*, *n* = 30-35). Error bars represent ±1 SEM for all graphs. One-tailed *t* tests performed in all cases (GraphPad Prism).

glands ($p<0.05$, n = 5-6, Figure 2.7). This may indicate a role for PdfR in the growth of the gland itself. However, it is not immediately apparent how increased gland size would result in developmentally-delayed larvae and larger adults. In fact, increased gland size might more reasonably be expected to result in an accelerated developmental time due to increased ecdysone production. It therefore seems more likely that the observed phenotypes are due to a role for PdfR in PG function.

To further interrogate the effects of PG-specific *PdfR* knockdown on larval growth, the growth rate was investigated directly by weighing larvae at regular time points throughout development from 90h AEL to pupariation. In this experiment, both sets of control larvae (*phm*-Gal4*/+* and *PdfR^{RNAi}/+*) pupariated at 138h AEL on average, whereas *phm>PdfR^{RNAi}* larvae took until 258h AEL on average. This indicates the dramatically increased duration of growth for the *phm>PdfR^{RNAi}* larvae, which spent an extra 120 hours as larvae compared with the controls (Figure 2.8A) and is consistent with the delay seen in the first experiment (Figure 2.5A). By log-transforming this data, it was possible to examine the change in growth over time, thereby generating a linear growth rate for each genotype. Between 90h and 138h AEL, both control genotypes have equivalent growth rates (*ns*, Figure 2.8B), although the *phm*-Gal4*/+* controls were heavier throughout this period (mean ±1 SEM, $p<0.05$). In comparison to both control genotypes, the *phm>PdfR^{RNAi}* larvae have a significantly reduced growth rate during this period ($p<0.001$, Figure 2.8B). Given that the *phm>PdfR^{RNAi}* larvae continued to feed for another 120h after the controls pupariated, the *phm>PdfR^{RNAi}* larvae were substantially heavier than both of the control genotypes when they pupariated ($p<0.0001$, n = 14-23, Figure 2.8C). Overall, PG-specific knockdown of *PdfR* results in an enlarged PG and decreases the larval growth rate, whilst dramatically increasing the duration of the larval growth period, ultimately leading to heavier pupae. Taken together, these data suggest that PdfR functions in the PG to regulate both the duration and the rate of growth.

2.3.2.3 Low ecdysone levels are responsible for the developmental delay phenotype of phm>PdfR^{RNAi} larvae

Given that the morphology of the PG was not affected by *PdfR* knockdown specifically in this tissue, whether ecdysone production was directly affected was investigated by feeding larvae exogenous ecdysone (20E). *PdfR* knockdown larvae were raised on 20E-supplemented food or EtOH-control food, and examined for rescue of the developmental
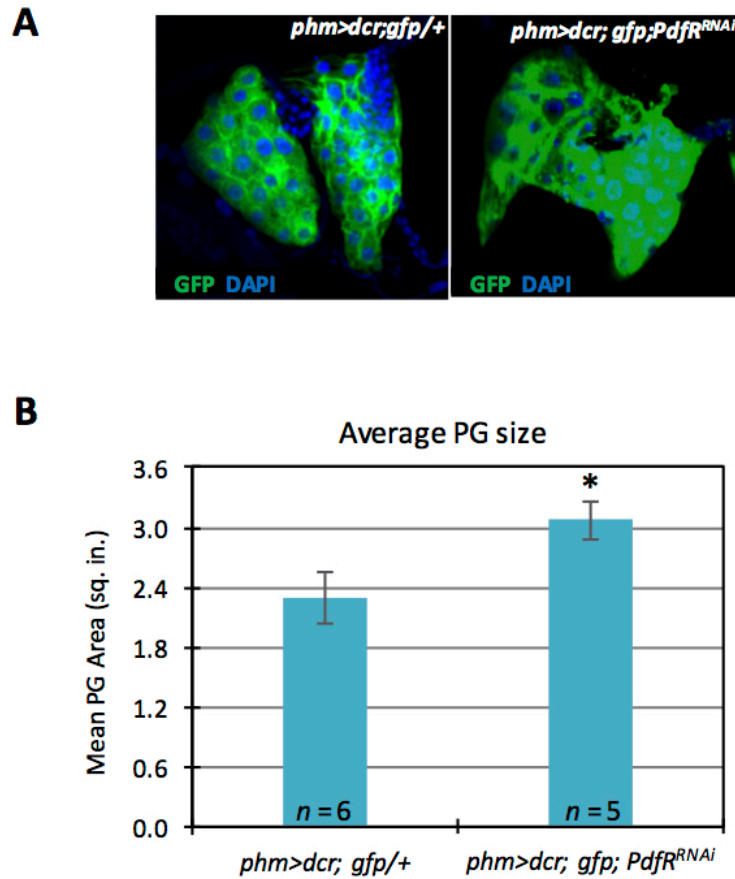
Figure 2.7. PG morphology is unaffected, but the PG is enlarged in *phm>PdfR^RNAi* larvae.

(A) *phm-Gal4* was used to drive *UAS-GFP* expression in all PG cells (**green**), and DAPI staining (**blue**) was used to mark all cell nuclei. *UAS-dicerII* was co-expressed to improve RNAi efficiency. PG-specific *PdfR* knockdown larvae exhibit normal PG morphology, but the PG is significantly enlarged compared with the PG from time-matched control larvae, quantified in B (*$p>0.05$, $n = 5$-6). The apparent lack of separation between the lobes, seen in the *PdfR* knockdown larvae, is an artefact of the dissection and mounting process.
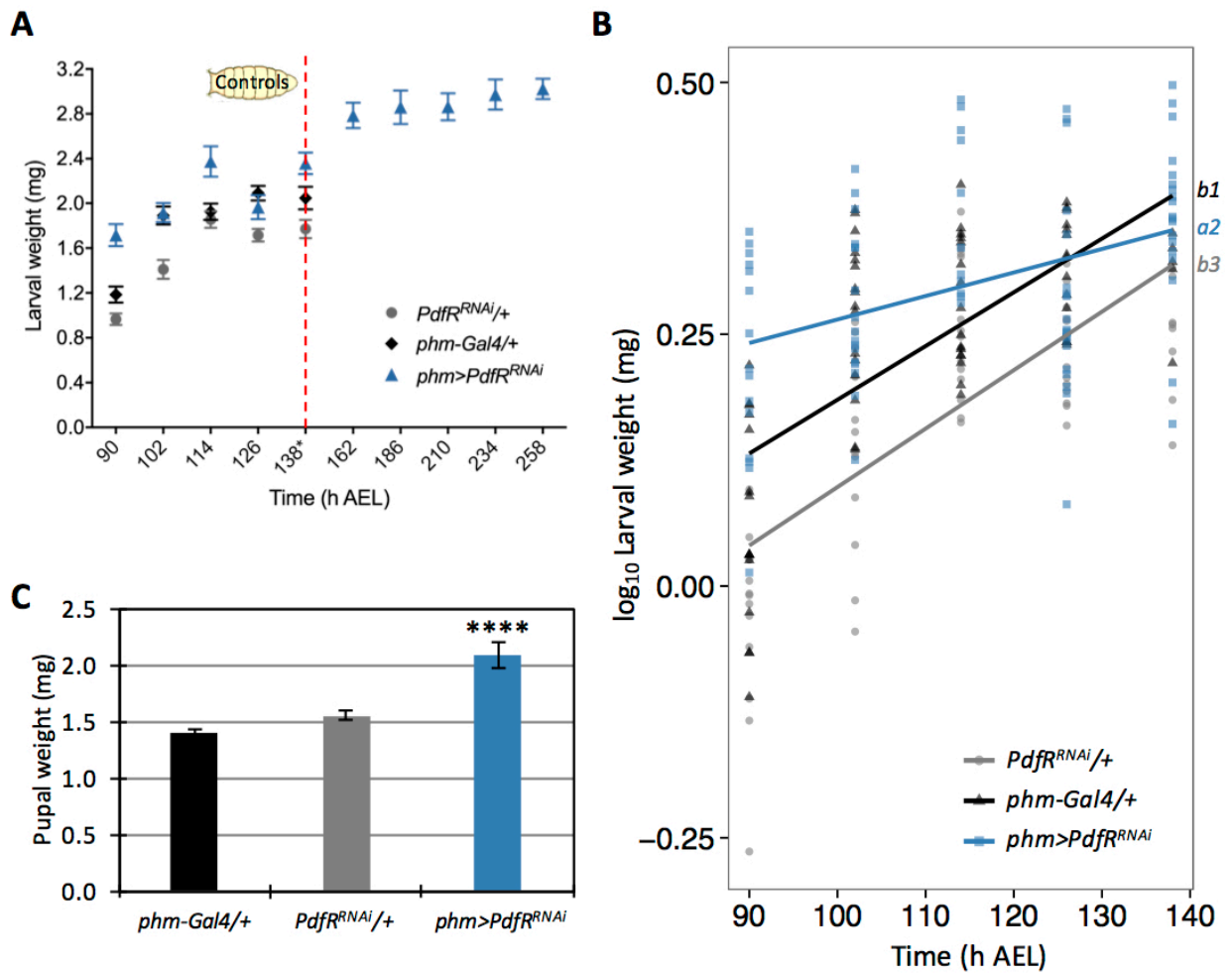
Figure 2.8. *phm>PdfR^RNAi* larvae grow for much longer than control larvae, but have a reduced larval growth rate.

(A) Larval weight over time, from 90h AEL to 258h AEL when *phm>PdfR^RNAi* larvae finally pupariated. Both sets of control larvae (*phm-Gal4/+* and *PdfR^RNAi/+*) had already pupariated at approximately 138h AEL, as indicated by the red dotted line. This clearly shows the dramatically increased duration of growth for the *phm>PdfR^RNAi* larvae. (B) Larval growth curve from 90h to 138h AEL, on the $\log_{10}$ transformed larval weight data. Both control genotypes have equivalent growth rates (*b*, ns), although *phm-Gal4/+* controls are heavier throughout their development (mean ±1 SEM, $p<0.05$). At the start of this period (90h AEL), *phm>PdfR^RNAi* larvae are bigger than both control genotypes, but due to a significantly reduced growth rate during this period (*a*, $p<0.001$), they are overtaken by the *phm-Gal4/+* controls by the end of this period (138h AEL). Given that the *phm>PdfR^RNAi* larvae continued to feed for another 120h after the controls pupariated, the *phm>PdfR^RNAi* larvae are substantially heavier than both of the control genotypes by the time they pupariated, as seen in (C) (****$p<0.0001$, $n = 14-23$).

45

delay phenotype. *phm>PdfR^{RNAi}* larvae raised on 20E-supplemented media pupariated at 141h AEL, significantly earlier than their EtOH-fed counterparts, which were delayed until 227h AEL (*p*<0.0001, Figure 2.9A). This demonstrates that exogenous supply of ecdysone during the third instar can completely rescue the developmental delay of *phm>PdfR^{RNAi}* animals, which is indicative of a defect in ecdysone production.

Given that the ecdysone-feeding results suggest that *phm>PdfR^{RNAi}* animals have an ecdysone production defect, it was investigated where in the ecdysone biosynthesis pathway *PdfR* is required. First, the ecdysone titres of all three genotypes were directly measured and compared between 34h and 50h after L3 ecdysis (AL3E), when the control larvae have relatively high ecdysone titres. The *phm>PdfR^{RNAi}* larvae were found to have significantly lower ecdysteroid titres across this 16-hour period when compared with both control genotypes (*p*<0.001, *n* = 5, Figure 2.9B, Appendix 2).

To determine if the reduced ecdysteroid titres are due to a perturbation in the transcription of ecdysone biosynthetic genes, qRT-PCR was used to measure the expression levels of two ecdysone biosynthetic genes, *disembodied* (*dib*) and *phantom (phm)*, as well as an ecdysone-response gene, *E74B*, in larvae collected at 42h AL3E. The expression level of *dib* was significantly reduced in *phm>PdfR^{RNAi}* larvae compared with control larvae (*p*<0.05, *n* = 3-6, Figure 2.9C). The expression of *phm* was significantly reduced in *phm>PdfR^{RNAi}* larvae compared to the *phm*-Gal4/+ control, but not when compared to the *PdfR^{RNAi}/+* control (*p*<0.05, ns, *n* = 3-5, Figure 2.9C). For *E74B*, no significant differences were detected between the control and experimental genotypes at this time-point, although the data did trend towards a reduction (ns, *n* = 3-5, Figure 2.9C). Given that expression levels of the ecdysone biosynthesis genes are highly temporally dynamic, it is possible that significant differences would be found at a different time-point. Taken together, these results suggest that the low ecdysone levels observed in *phm>PdfR^{RNAi}* larvae are caused by reduced transcriptional induction of at least one of the ecdysone biosynthesis genes. Bearing in mind that each of the ecdysone biosynthesis enzymes is rate-limiting (Gilbert *et al.* 2002; reviewed in Niwa and Niwa 2014a), even a significant reduction in just one enzyme would presumably impact the ability of the PG to synthesise ecdysone. However, these data do not rule out the possibility that PdfR also acts at the post-transcriptional or translational level to control ecdysone production.

48
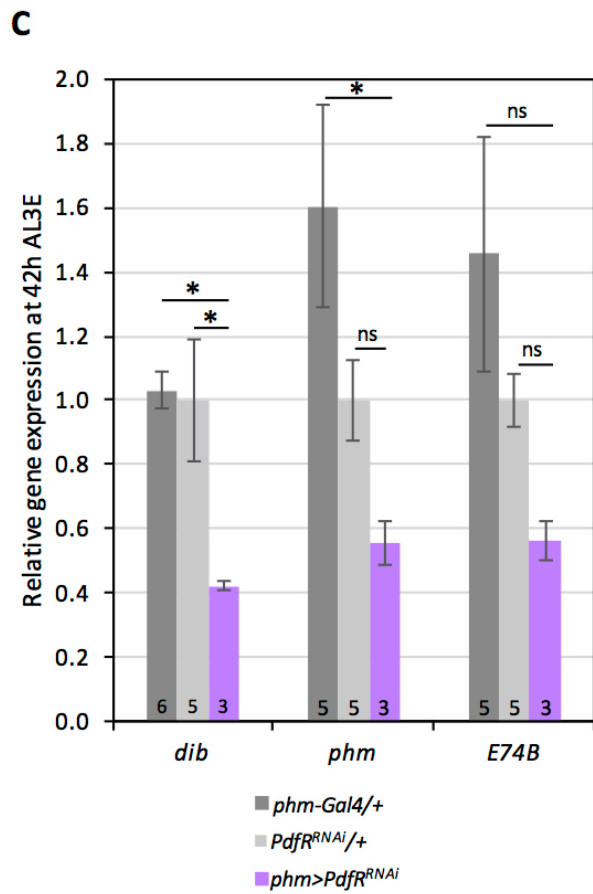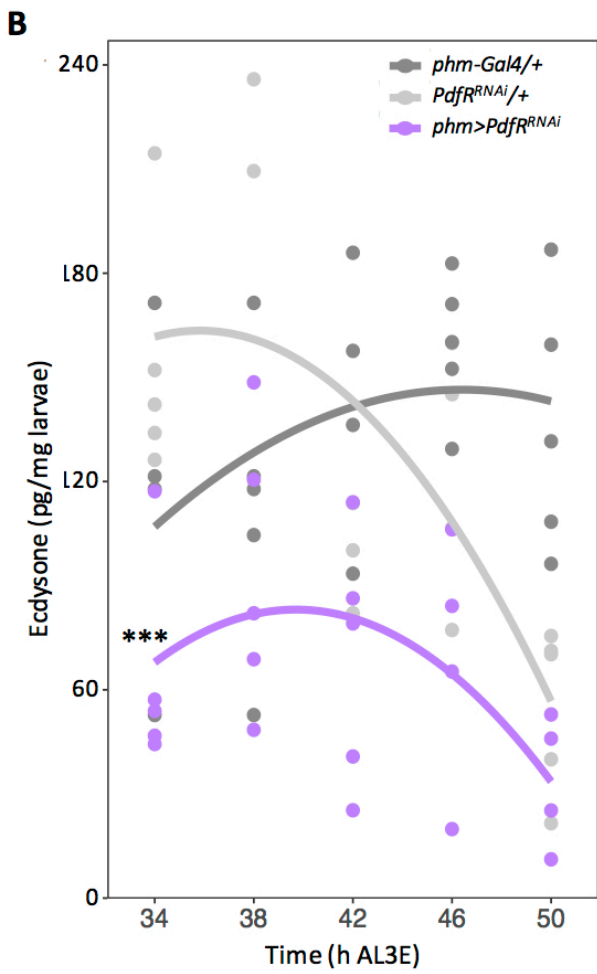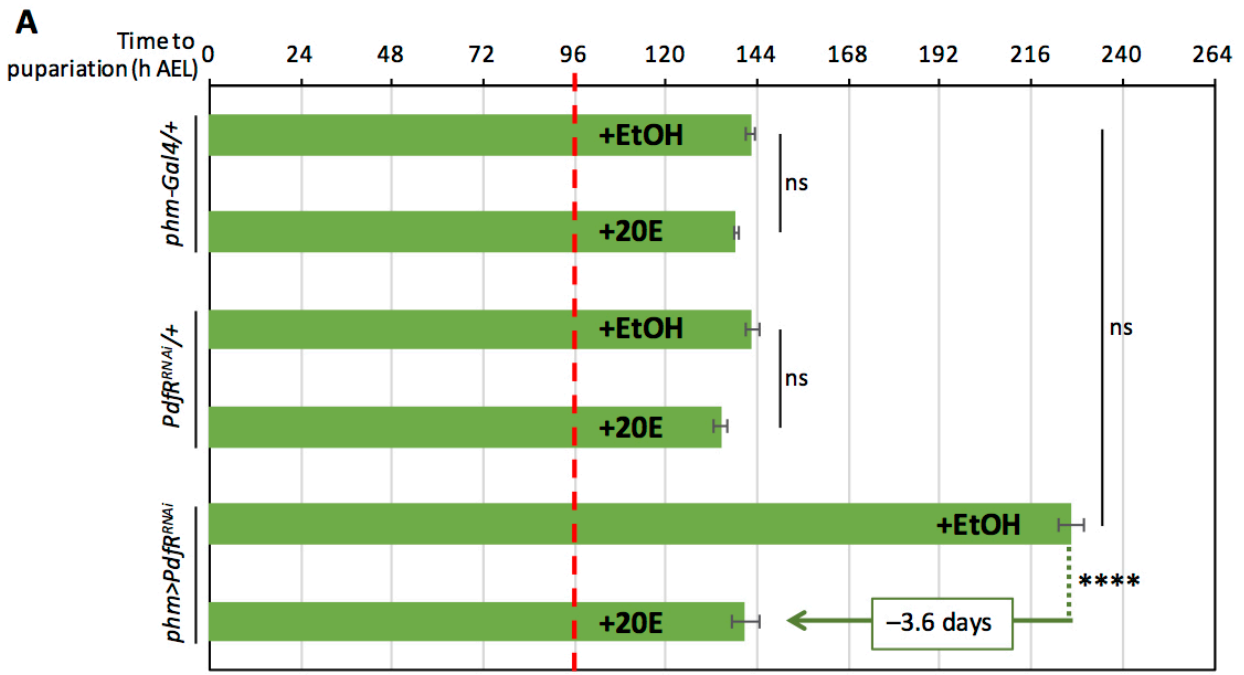
Figure 2.9. Low ecdysone titres are responsible for the developmental delay of *phm>PdfR^{RNAi}* larvae.

(A) Larvae were raised on 20E-supplemented media or control food (EtOH) from 96h AEL (red dotted line), and time to pupariation was measured. The developmental delay of *phm>PdfR^{RNAi}* larvae was rescued by feeding the larvae on 20E-supplemented media, with the time to pupariation returning to 141h AEL on average compared with the control-fed timing of 227h AEL on average (****$p>0.0001$). (B) Removal of *PdfR* from the PG results in a delayed rise in ecdysteroid titres. Ecdysteroid titre in pg/mg larvae was plotted against time after the third instar ecdysis (AL3E). Between 34h and 50h AL3E control larvae are preparing to wander and have high levels of ecdysteroid. This is not the case, however, for the *phm>PdfR^{RNAi}* larvae, which have significantly reduced ecdysteroid titres across this period compared with both the *phm-Gal4/+* and *PdfR^{RNAi}/+* control larvae (***$p<0.001$, analysis of curves, $n = 3-5$ per timepoint per genotype). (C) qRT-PCR analysis of the transcriptional levels of *phm, dib* and *E74B,* three genes required for ecdysteroid biosynthesis for *phm>PdfR^{RNAi}, phm-gal4/+, PdfR^{RNAi}/+* larvae (mean ±1 SEM). These levels were normalised to ribosomal protein L23 (*rpL23)* transcription levels in the same samples. All larvae were staged from the L3 moult and sampled 42h after this (at 42h AL3E), which is the central time-point of the time-course examined in the ecdysone titre experiment. The expression level of *dib* was significantly reduced in *phm>PdfR^{RNAi}* larvae compared with control larvae (*$p<0.05$, $n = 3-6$). The expression of *phm* was significantly reduced in *phm>PdfR^{RNAi}* larvae compared to the *phm*-Gal4/+ control, but not when compared to the *PdfR^{RNAi}/+* control (*$p<0.05$, ns, $n = 3-5$). For *E74B*, no significant differences were detected between the control and experimental genotypes at this time-point, although the data did trend towards a reduction (ns, $n = 3-5$).

2.3.3. AkhR is a novel regulator of developmental timing and growth in the PG

2.3.3.1 PG-specific AkhR knockdown causes late larval lethality, but whole-fly null animals are homozygous viable

AkhR is the receptor for adipokinetic hormone (Akh), a neuropeptide produced in and secreted by the CC cells that innervate both the heart and the PG. Akh acts to release energy-rich substrates from the fat body in response to nutritional requirements (Kim and Rulifson 2004), and is thus functionally analogous to human glucagon. The function of the Akh-producing processes of the CC that innervate the PG has not previously been demonstrated, and a role for AkhR in the PG has not previously been reported.

Null mutants for *AkhR* are homozygous viable, and display an obese and starvation resistant phenotype due to an inability to mobilise body fat stores (Grönke *et al.* 2007; Bharucha *et al.* 2008). However, the PG-specific knockdown of *AkhR* with the KK RNAi line resulted in developmental arrest and lethality (Figure 2.3). This seeming disparity between PG-specific knockdown and null mutant phenotype is not without precedent, as several other genes have been shown to cause developmental arrest and lethality when knocked down specifically in the PG even when whole-animal mutants of the same gene are viable (Gibbens *et al.* 2011; Ohhara *et al.* 2015). For example, the PG-specific knockdown of *tor* causes a major developmental delay to pupariation of 5.8 days on average, but *tor* null (*tor^XR1^*) mutants are delayed by only about 1 day on average (Rewitz *et al.* 2009; Johnson *et al.* 2013). One possible explanation for this is that in whole-animal nulls some type of compensatory change occurs in the other mutant tissues that ameliorates the effects of specific gene loss, such that only tissue-specific loss reveals the tissue-specific role.

However, it was also possible that the lethality observed in the *phm>AkhR^RNAi^* larvae was due to off-target effects of the RNAi. To address this, the KK RNAi line was first sequenced to confirm that the hairpin produced does in fact target the *AkhR* transcript (data not shown). Secondly, data available from the VDRC predicts that the evolutionarily related gene *Crustacean cardioactive peptide receptor (CCAP-R)* is a possible off-target for the AkhR KK RNAi construct. However, when *CCAP-R* was knocked down in the PG using a *CCAP-R*-specific RNAi line, no developmental delay or lethality was observed (Jade Kannangara, pers. comm.). This suggests that it is the PG-specific knockdown of *AkhR* that is causing the developmental arrest and lethality.

50

To confirm the RNAi phenotype with a second independent experiment, an independent GD RNAi line was obtained in an attempt to confirm the phenotype observed with the KK line and rule out any RNAi off targets or toxicity effects. However, this RNAi line did not cause larval lethality when expressed in the PG using *phm*-Gal4, nor did it alter developmental timing or result in any obvious phenotypes (data not shown). A recent study has shown that this GD RNAi construct achieves only 50% knockdown of *AkhR* levels when expressed in the fat body (Baumbach *et al.* 2014). It is therefore possible that the GD RNAi line failed to recapitulate the phenotype observed with the KK line because of inefficient *AkhR* knockdown in the PG. Taken together, these data are suggestive of a role for AkhR in the PG. However, it is difficult to reach definitive conclusions from RNAi data when no phenotype has been observed.

And so, in a further attempt to confirm the original RNAi phenotype, further investigations were undertaken on the whole-animal null mutants, which are homozygous viable. The *AkhR[1]* mutant was generated via P-element excision, which resulted in a deletion spanning several kilobases and removed the complete protein-coding region (Grönke *et al.* 2007). *AkhR[1]* homozygotes showed a significant delay of 54 hours to pupariation compared with their heterozygous counterparts (*p*<0.0001, Figure 2.10A). A role for AkhR is further supported by the fact that during this project another group observed a comparable developmental delay with *AkhR[1]* animals (Kim and Neufeld 2015). In addition, a null mutant for the ligand *Akh* was also obtained. The *Akh[4]* mutant was generated using CRISPR/Cas9-mediated genome editing and has a 6-bp deletion corresponding to the final two amino acids from this octapeptide (Gáliková *et al.* 2015). *Akh[4]* homozygotes were also significantly delayed to pupariation compared to their heterozygous counterparts, although the effect was milder (16.1 hrs, *p*<0.01, Figure 2.10A). The genetic loss of *Akh* and its receptor *AkhR* both resulted in a developmental delay phenotype.

Body size was also investigated for both *AkhR* and *Akh* mutants. Interestingly, *AkhR[1]* mutant pupae weighed significantly less than heterozygous controls, whereas *Akh[4]* mutant pupae weighed significantly more than heterozygous controls (*p*<0.0001 and *p*<0.001 respectively, Figure 2.10B). The genetic loss of *Akh* and its receptor *AkhR* appear to have differing phenotypic effects with respect to body size.
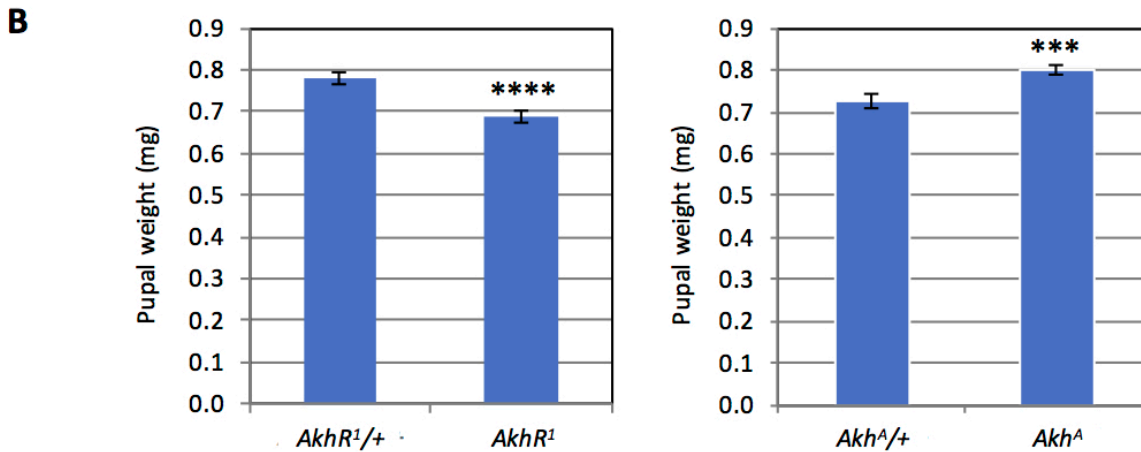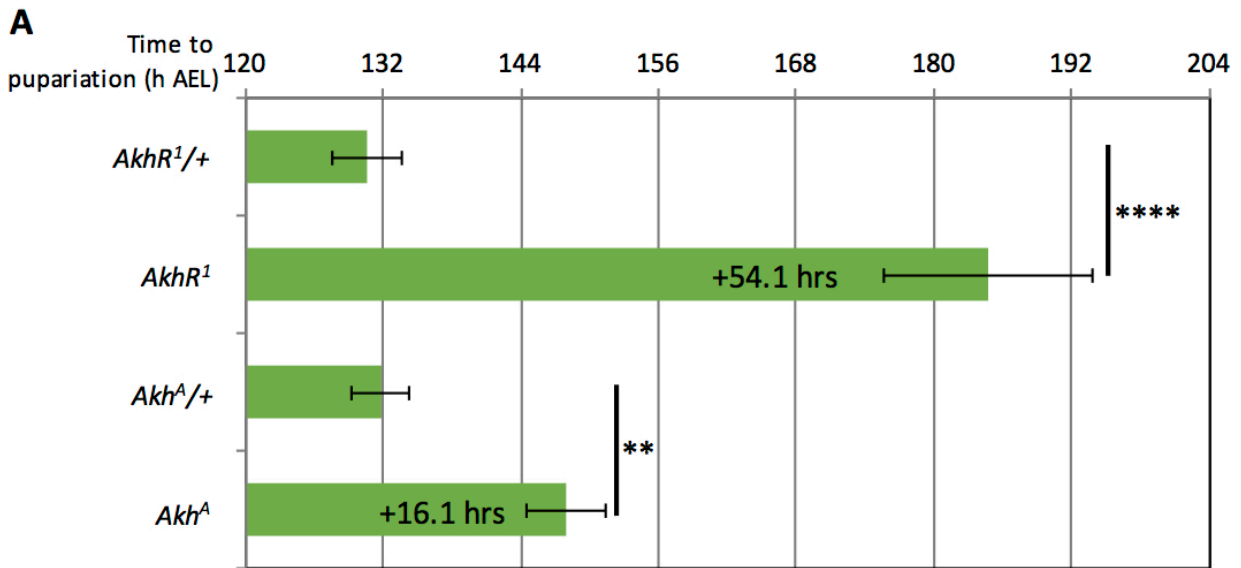
Figure 2.10. *AkhR¹* and *Akh^A* **mutants showed a delay in time to pupariation and altered body size.**

(A) *AkhR¹* mutants showed a significant delay in time to pupariation of 54 hours compared to heterozygous controls (****$p<0.0001$). *Akh^A* mutants showed a significant delay in time to pupariation of 16 hours compared to controls (**$p<0.01$). *n* = 12 with no fewer than 120 individuals tested for each genotype. Error bars represent ±1 SEM. h AEL = hours after egg lay. (B) *AkhR¹* mutant pupae were lighter on average than their heterozygous controls (****$p<0.0001$), n = 36-46. *Akh^A* mutant pupae, however, were heavier on average than their heterozygous controls (***$p<0.001$), n = 36-46. Error bars represent ±1 SEM.

In conclusion, the PG-specific knockdown of *AkhR* resulted in developmental arrest, which is consistent with the results from an independent genome-wide PG-specific RNAi screen performed by Danielsen *et al.* (2016). While this phenotype could not be replicated with an independent RNAi line, both *AkhR[1]* and *Akh[A]* mutant animals were also found to be developmentally delayed compared to heterozygous controls, supporting a role for AkhR in the regulation of growth and developmental timing in *Drosophila*. Further experiments on AkhR were not possible due to time-constraints, but the preliminary data presented here suggests that AkhR plays a novel role in the *Drosophila* PG, regulating growth and developmental timing.

2.4. Discussion

2.4.1. PdfR is a novel regulator of developmental timing and growth in the PG

2.4.1.1 PdfR function in Drosophila

Pdf signalling has many roles in the control of physiology and behaviour in *Drosophila* and other insects, including circadian rhythmicity (Renn *et al.* 1999), sleep and arousal (Parisky *et al.* 2008; Shang *et al.* 2008; Sheeba *et al.* 2008; Chung *et al.* 2009), geotaxis (Toma *et al.* 2002), mating behaviour and male pheromone production (Kim *et al.* 2013; Krupp *et al.* 2013), flight (Agrawal *et al.* 2013), visceral muscle contraction modulation (Talsma *et al.* 2012), and tracheal growth (Linneweber *et al.* 2014). The current understanding of PdfR function in its better characterised roles will be reviewed here, before hypotheses regarding the newly discovered function in the PG are presented.

By far the best-understood of Pdf's roles is in circadian rhythmicity, although even here the specifics of Pdf signalling are still being elucidated. The overall role of Pdf/PdfR in circadian rhythms is to synchronise the diverse clock neurons with each other and to coordinate their outputs to achieve specific behavioural activities. The approximately 150 clock neurons are clustered into discrete groups, including four groups of lateral neurons (LNs), which are further divided into two ventral clusters – large and small ventrolateral neurons (lLNvs and sLNvs), one group of dorsolateral neurons (LNds), and the lateral posterior neurons (LPNs). Amongst these clusters, and even within clusters, there is a large amount of heterogeneity, with the cells expressing different combinations of neuropeptides and neuropeptide receptors, as well as performing different functional roles.

Pdf is expressed by all of the LNvs except for a single laterally-represented Pdf-negative cell called the 5th sLNv (Helfrich-Förster 1995; Rieger *et al.* 2006). PdfR on the other hand is expressed only by a subset of clock neurons, spread across the different neuron classes, meaning that only certain subsets of clock neurons are actually receptive to Pdf (Yoshii *et al.* 2009). Thus, Pdf is hypothesised to synchronise the PdfR-expressing clock cells but desynchronise clusters of neurons consisting of both PdfR-positive and PdfR-negative cells (Shafer and Yao 2014). This explains why the absence of Pdf speeds up the molecular clock in certain clock cells, whilst slowing down others (Yao and Shafer 2014). Indeed, flies with mutations in either *Pdf* or *PdfR* have complex behavioural phenotypes, with an absence of the normal morning peak of activity and an early evening peak of activity in light:dark cycles (LD), but short-period rhythms that become arrhythmic very quickly under constant darkness (DD) (Renn *et al.* 1999; Lin *et al.* 2004; Hyun *et al.* 2005; Lear *et al.* 2005; Mertens *et al.* 2005). The complex nature of this phenotype can be broken down into the two specific groups of cells responsible for their regulation (reviewed in Dubowy and Sehgal 2017). The Pdf-positive LNvs are sufficient for free-running behaviour under DD cycles and for morning anticipation under LD cycles, but not for the evening peak of activity, and so are often referred to as the "morning" (M) cells. Alternatively, the Pdf-negative 5th sLNv and LNds are necessary for the evening anticipation under LD cycles, and so are often referred to as the "evening" (E) cells. Whilst these categorisations may be over-simplified, it provides a convenient system that has enabled investigations into the specifics of Pdf signalling.

The Pdf/PdfR signalling pathway found in clock neurons is summarised in Figure 2.11. Upon binding its ligand, PdfR activates Gαs (Choi *et al.* 2012; Zhang and Emery 2013), which in turn activates an adenylyl cyclase (AC) to produce cyclic AMP (cAMP) (Mertens *et al.* 2005; Shafer *et al.* 2008). The M cells signal specifically through AC3, but in the E cells, AC78C and an as-yet unidentified AC are activated by PdfR (Duvall and Taghert 2012, 2013). Whilst the main signalling components are now known, it is not yet clear whether Pdf signalling acts at the transcriptional, translational or post-translational level to regulate the core molecular clock. The increase in cAMP activates protein kinase A (PKA) in clock neurons, which acts to stabilise both the PERIOD (PER) and TIMELESS (TIM) proteins (Li *et al.* 2014; Seluzicki *et al.* 2014), indicating post-translational regulation by PdfR. PKA can also affect translation via TOR and 4E-BP (Tettweiler *et al.* 2005), although
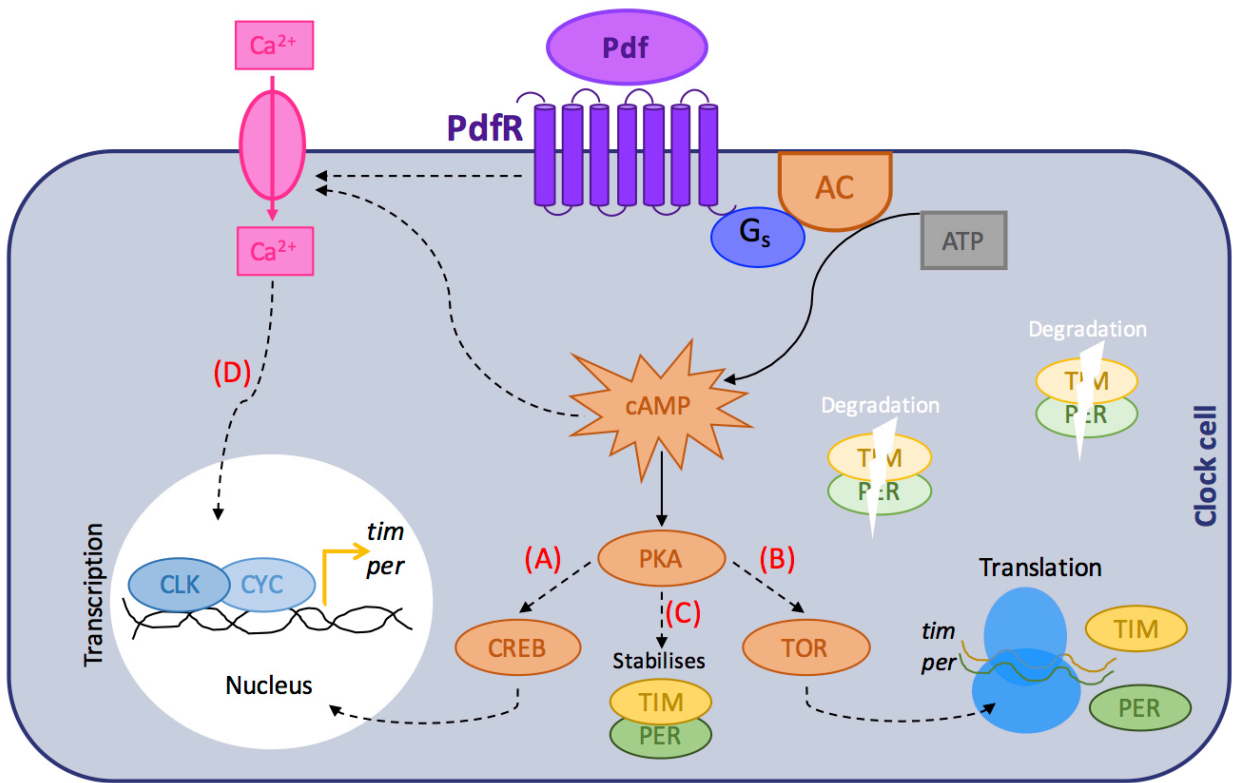
Figure 2.11. PdfR function in the core clock cells.

Upon binding its ligand, PdfR activates Gαs, which in turn activates an adenylyl cyclase (AC) to produce cyclic AMP (cAMP). The increase in cAMP activates protein kinase A (PKA) in clock neurons, which has several different possible cellular effects. (A) CREB2 acts downstream of cAMP and PKA to regulate the core molecular clock feedback loop, presumably at a transcriptional level. (B) PKA can also affect translation, although this does not appear to have been demonstrated for the *Drosophila* clock cells so far. (C) PKA acts to stabilise both the PER and TIM proteins, so that they can accumulate in the cytoplasm. (D) PdfR also acts to affect intracellular Ca^{2+} levels, either directly or via cAMP. This causes membrane depolarisation which in turn triggers an upregulation of CLK/CYC-mediated transcription, thereby maintaining high *per/tim* levels during the night-time.

this does not appear to have been demonstrated for the *Drosophila* clock cells. In addition, flies with a mutation in the cAMP response element-binding protein B (CREB2) resemble *Pdf* or *PdfR* mutants, suggesting that CREB2 may act downstream of the cAMP/PKA pathway to regulate the core molecular clock feedback loop, presumably at a transcriptional level (Belvin *et al.* 1999). Pdf also drives its own expression through the activation of PdfR in a positive autoregulation loop, as part of circadian clock synchronisation at least in the Pdf-positive morning cells (Mezan *et al.* 2016).

As well as signalling through increases in cAMP, PdfR also affects intracellular Ca^{2+} levels (Mertens *et al.* 2005; Seluzicki *et al.* 2014; Sabado *et al.* 2017), although there appears to be several different models for how this occurs. The first possibility is that the increase in cAMP levels directly activates a cyclic-nucleotide-gated channel to rapidly increase intracellular Ca^{2+} levels, thereby depolarising the cell and increasing the action potential firing rate (Seluzicki *et al.* 2014). Alternatively, intracellular Ca^{2+} levels increase via a cAMP-independent mechanism (Sabado *et al.* 2017). In this context, membrane depolarisation triggers an upregulation of CLK/CYC-mediated transcription, maintaining high *per/tim* levels during the night-time. However, independent experiments using fluorescent transcriptional reporters in *ex vivo* brain culture suggest that Pdf suppresses CLK activity (Mezan *et al.* 2016). These contradictory effects on CLK may be due to the different cell types investigated, as well as the different timescale of the experiments (Sabado *et al.* 2017). Nevertheless, both studies suggest that Pdf regulates clock gene transcription.

Further evidence for Pdf signalling being required for transcriptional regulation comes from its role in sex pheromone biosynthesis and mating behaviour in the *Drosophila* oenocytes (Krupp *et al.* 2013). In this context, Pdf signalling acts predominantly through transcriptional regulation of the *desat1* gene, which encodes a key enzyme required for the biosynthesis of male *Drosophila* sex pheromones. There was also some evidence of post-transcriptional regulation in this system, suggesting that Pdf signalling is capable of acting at multiple levels during the gene expression process via complex regulatory interactions (Krupp *et al.* 2013).

In summary, it is clear that there are cell type-specific differences in Pdf signalling, including the use of diverse downstream molecular components that enable regulation at

multiple levels of gene expression – transcriptional, translational, and post-translational. This is likely to be even more complex once other neuropeptide pathways and the crosstalk between these are factored into this network. In addition, the relationship between Pdf signalling and neuronal activity in different cell types will also need to be addressed in future studies.

2.4.1.2 A novel function for PdfR in the larval PG

Here, a novel role for PdfR in the regulation of growth and developmental timing in the *Drosophila* PG has been identified. PG-specific knockdown of *PdfR* caused a significant developmental delay to pupariation and increased overall body size. This finding is further supported by an independent genome-wide PG-specific RNAi screen performed by Danielsen *et al.* (2016) which identified a role for *PdfR* in the PG. In their study, they reported that *phm>PdfR^{RNAi}* larvae arrested development during the L3 stage, a more severe phenotype. The difference in severity of phenotype between the two studies is most likely due to different methodologies and/or environmental conditions, such as the different nutritional content of foods. For example, in the Danielsen *et al.* (2016) screen, females were allowed to lay for 24 hours and progeny were scored for developmental defects 11-13 days after this, whereas in this study, females were allowed to lay for just 3-4 hours, and the progeny were scored every 8 hours until all larvae had completed pupariation or died. In further support of a role for PdfR in growth and developmental timing, *PdfR^{5304}* homozygous mutant animals were also found here to be developmentally delayed and larger compared to heterozygous controls.

The findings presented in this chapter showed that the developmental delay of *phm>PdfR^{RNAi}* larvae can be rescued by feeding with 20E-supplemented media (Figure 2.9A), which is indicative of defects in ecdysone production. These larvae were shown to have significantly reduced ecdysone titres during the late third instar (Figure 2.9B). This reduction in ecdysone levels is likely due in whole or part to the reduced expression of at least one ecdysone biosynthetic gene (Figure 2.9C). Taken together, this suggests that PdfR acts at the transcriptional level to regulate ecdysone biosynthesis (Figure 2.12). The case for PdfR as a transcriptional regulator of ecdysone biosynthesis could be strengthened in future work by extending the qRT-PCR analysis across additional timepoints during larval development. Given that the expression of the ecdysone biosynthetic genes is highly-
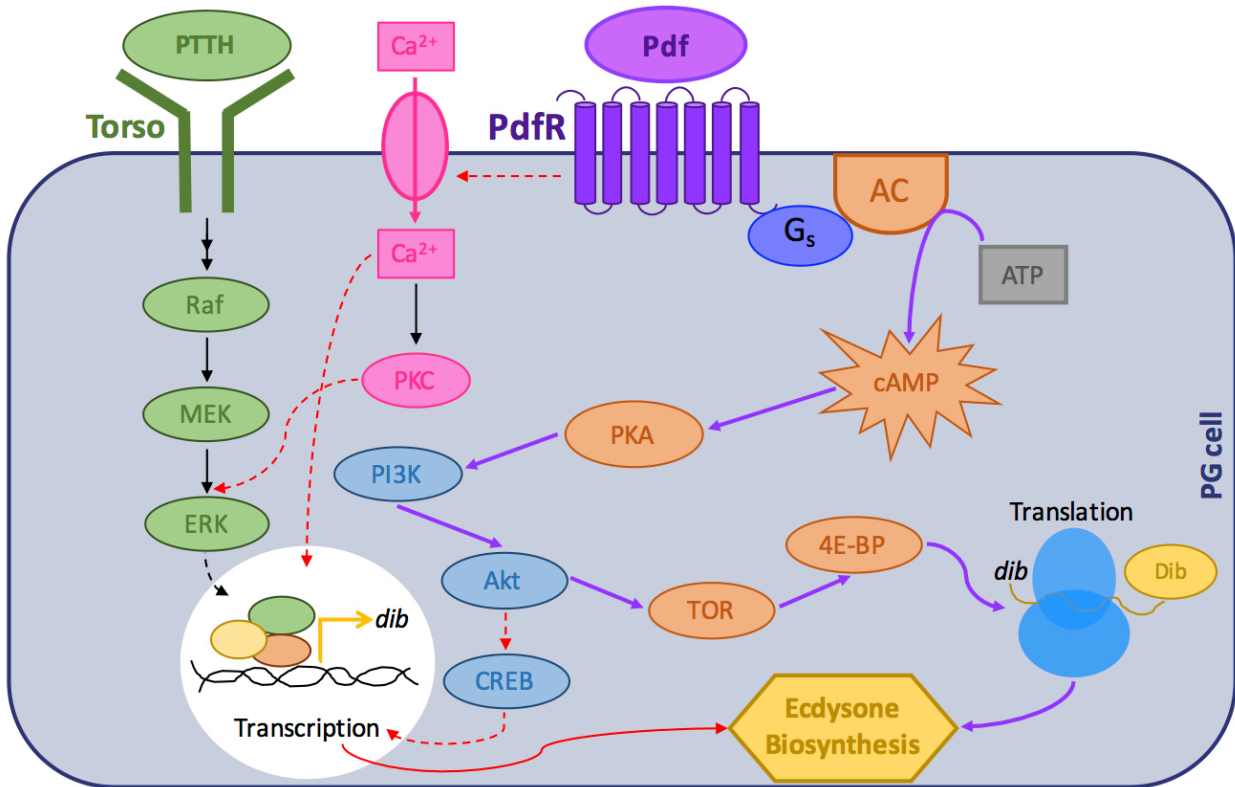
Figure 2.12. PdfR may function in the PG to regulate ecdysone biosynthesis at either the transcriptional or translational level.

(A) In this study, PdfR regulated at least one of the ecdysone biosynthetic genes at the transcriptional level. Red lines indicate proposed pathways for transcriptional regulation. (B) PdfR may also regulate ecdysone biosynthesis through translational regulation of the biosynthetic genes, as has been shown for the *Bombyx* PG. Purple lines indicate pathways used for translational regulation, as suggested by the *Bombyx* data (Iga *et al.* 2014). Solid lines indicate established and highly-likely pathways, whilst dashed lines indicate proposed and/or possible pathways. Figure adapted from Iga *et al.* (2014).

temporally dynamic, adding several more timepoints would improve temporal resolution, and be more consistent with the ecdysone titre data also presented here.

Even if PdfR does affect transcription of the ecdysone biosynthesis genes, it is also possible that it regulates ecdysone biosynthesis at the translational or post-translational level (Figure 2.12). This is supported by recent work in *Bombyx mori* that showed that cultured PGs respond to Pdf by stimulating ecdysone production, and that this effect is achieved through translational regulation of the ecdysone biosynthetic genes (Iga *et al.* 2014). In particular, PGs dissected from late final instar *Bombyx* larvae and pupae responded to Pdf by increasing cAMP levels, which suggests PKA involvement. Indeed, when PGs were treated with a PKA inhibitor their Pdf-induced ecdysone biosynthesis was suppressed. PKA has been implicated in both transcriptional and translational aspects of ecdysone biosynthetic gene regulation, via CREB proteins and eIF4e binding protein (4E-BP), respectively. To test the first possibility, transcription was pharmacologically inhibited, but this did not suppress Pdf-induced ecdysone biosynthesis. On the contrary, treatment with a translation inhibitor was able to suppress the Pdf-induced ecdysone biosynthesis, suggesting that translational regulation is occurring via 4E-BP. In support of this, p4E-BP was upregulated in PGs cultured with Pdf. In addition, treatment with a phosphatidylinositol 3-kinase (PI3K) inhibitor or a TOR inhibitor also suppressed the Pdf-induced ecdysone biosynthesis in cultured PGs, suggesting that the PKA-PI3K-TOR pathway phosphorylates 4E-BP for ecdysone biosynthesis in response to Pdf signalling. Taken together, these data suggest that the main role of Pdf signalling in the *Bombyx* PG is to cause translational upregulation of ecdysone biosynthesis genes.

In addition, it is possible that PKA and other intracellular kinases also undertake important post-translational modifications on components of the ecdysteroid biosynthetic pathway. This is consistent with Pdf signalling in the *Drosophila* molecular clock, where PKA-mediated phosphorylation stabilises both PER and TIM (Li *et al.* 2014; Seluzicki *et al.* 2014). Furthermore, Pdf signalling also appeared to partially regulate ecdysone biosynthesis through an extracellular Ca^{2+}-mediated pathway, potentially overlapping somewhat with the MAPK pathway downstream of PTTH (Iga *et al.* 2014), and thereby facilitating transcriptional regulation of the ecdysone biosynthesis genes.

Overall, the reduced *dib* expression observed in *phm>PdfR^{RNAi}* larvae (Figure 2.9C) suggests that PdfR functions at the transcriptional level in the *Drosophila* PG, but this does not necessarily preclude the translational regulation suggested by Iga *et al.* (2014) in the *Bombyx* PG, and PdfR could in fact function at multiple levels in the *Drosophila* PG. This could be due in part to the differences between how *Bombyx* and *Drosophila* regulate ecdysteroidogenesis, which are only now beginning to be elucidated. For example, the PG-innervating neurons of *Drosophila* supply PTTH to the PG, but this is not the case in *Bombyx,* where these neurons are not stained by a PTTH antibody (Tanaka 2011). In addition, several novel neuropeptides have recently been found to regulate ecdysteroidogenesis in *Bombyx* (reviewed in Tanaka 2011). *Bombyx* and *Drosophila* also have several key physiological differences, as well as different numbers and timing of life-stages. In particular, the *Drosophila* PG is part of a composite organ called the ring gland, whereas the *Bombyx* PG is a stand-alone organ, which is likely to affect the nature of communication between the various endocrine tissues of the developing larva. In summary, even when the same peptidergic system is being used in the PG to regulate ecdysteroidogenesis, the specific regulatory mechanisms may differ between diverse insect species (Tanaka 2011).

Alternatively, PdfR might affect several pulses of ecdysone, and might use different mechanisms to affect each pulse. This is already known to occur for insulin signalling (Gibbens *et al.* 2011). To investigate whether PdfR regulates ecdysone biosynthesis at the translational level in *Drosophila*, similar experiments to those performed with *Bombyx* PGs in culture could be performed with *Drosophila* brain-ring gland complexes. Culture methods for *Drosophila* brain-ring gland complexes have been developed and can be used for both larval and pupal brain-ring gland complexes as well as in co-culture with other organs such as fat body (Awad and Truman 1997; Britton and Edgar 1998; Koyama and Mirth 2016). Additionally, given that antibodies for the main ecdysone biosynthetic enzymes have now been developed, levels of these enzymes could be directly assayed in *Drosophila* PGs, such as in Ohhara *et al.* (2015).

A third hypothesis of how PdfR functions in the PG comes about because of a recent study that found that the PG-specific knockdown of circadian clock genes results in developmental arrest whereas whole animal mutants are viable (Di Cara and King-Jones 2016). This appears to be due to the lack of synchronisation between the PG cells, where

circadian function has been removed, and the rest of the wild-type animal, which still has a functional circadian clock. As well as the central clock, the PG has its own local clock, at least in *Drosophila* pupae and *Rhodnius* larvae, that regulates eclosion rhythms and ecdysone production respectively (Ampleford and Steel 1985; Emery *et al.* 1994; Myers *et al.* 2003). Di Cara and King-Jones (2016) demonstrated for the first time that TIM and PER proteins undergo nucleocytoplasmic oscillations in larval PG cells in a manner consistent with the pupal PG clock (Emery *et al.* 1997; Myers *et al.* 2003; Morioka *et al.* 2012), suggesting that the larval clock may be required for the circadian control of ecdysone production. Indeed, when the larval PG clock was perturbed, such as by the PG-specific knockdown of *tim*, the resulting L3 larvae failed to pupariate and continued to feed for several weeks, thereby substantially increasing overall body size (Di Cara and King-Jones 2016). This was due to the reduction of ecdysone titres and ecdysone biosynthetic gene expression, as well as reduced *tor* expression. Additionally, the insulin signalling pathway was required upstream of the clock genes for this activity. During the day when larvae are feeding, insulin signalling levels are high, which limits Glycogen Synthase Kinase 3 (GSK3) activity. At night, however, insulin signalling is reduced, which elevates GSK3 activity, thereby stabilising TIM protein levels, which in turn activates *torso* expression (Figure 2.13). Therefore, the larval PG clock acts to synchronise the activity of the insulin signalling pathway and the PTTH/Torso signalling pathway, thereby indirectly promoting ecdysone biosynthesis during the night by maximising *torso* expression and ensuring that the PG cells are competent to receive the PTTH signal (Di Cara and King-Jones 2016).

In several ways, these phenotypes parallel the PdfR data presented here, especially given PdfR's well-known role as a circadian regulator, suggesting that PdfR may act indirectly to regulate ecdysone production. Given that PdfR is required in the core clock cells to stabilise PER/TIM protein levels at night (Li *et al.* 2014; Sabado *et al.* 2017), it is possible that it plays a similar in the larval PG clock. If this is the case, PdfR would be facilitating TIM activity during the night to increase *torso* expression levels, thereby driving ecdysone production (Di Cara and King-Jones 2016). However, there are some key differences which make it seem unlikely that PdfR is acting in the same manner as described for the core clock gene TIM. Firstly, whilst PdfR is a *bone fide* clock gene, it is not part of the core clock such as TIM, PER or CLK, and so cannot be assumed to function in the same manner. Secondly, there is evidence for at least one of these genes, *tim*, that shows that PG-specific knockdown results in a small PG, whereas the PG of *phm>PdfR^{RNAi}* larvae is significantly
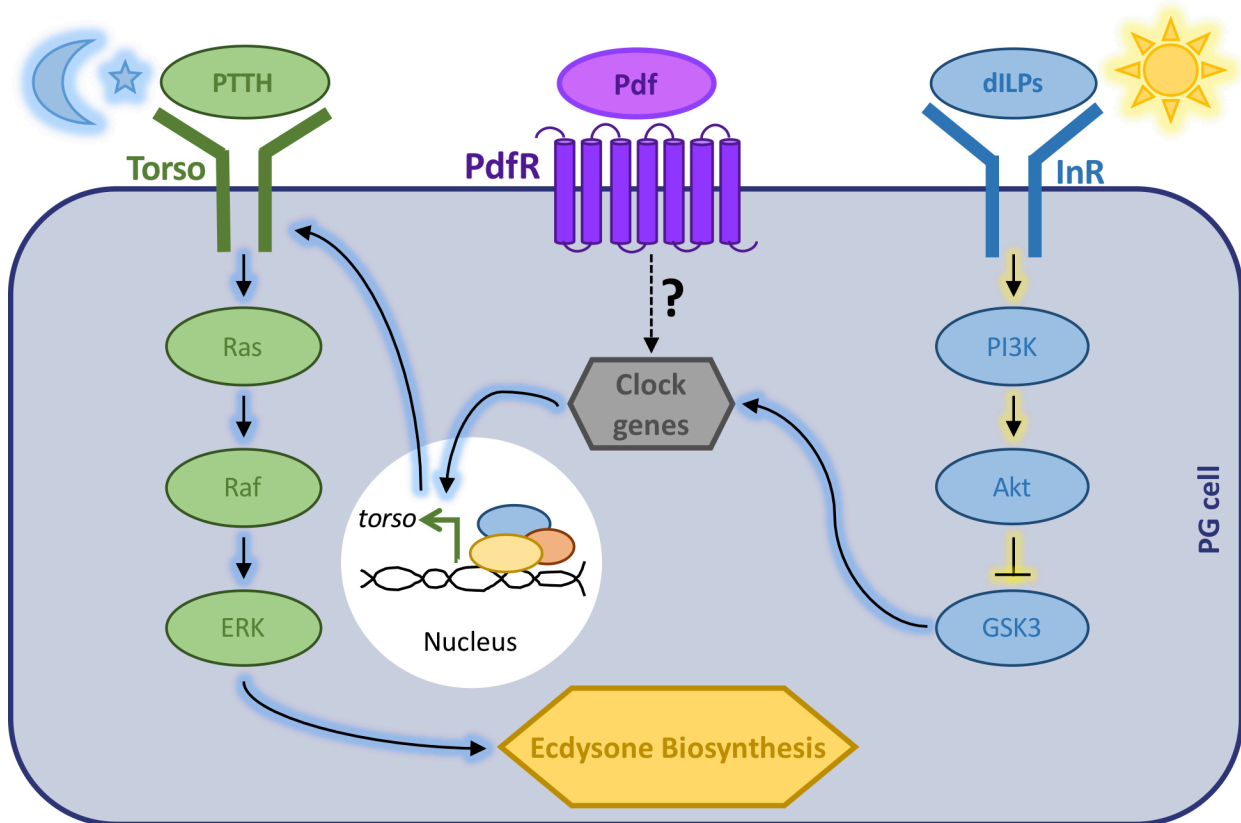
Figure 2.13. PdfR may regulate ecdysone biosynthesis indirectly via the PG clock and *torso* expression.

A third possible role for PdfR in the PG could be a more indirect one, as was recently proposed for the clock genes such as *timeless* (Di Cara and King-Jones 2016). Under this model, insulin signalling is particularly active during the day because the larva is feeding (indicated by the sun and yellow arrows). During the night (represented by the moon and blue arrows), insulin signalling is reduced, which removes repression on GSK3, thereby activating the core clock components such as TIM. This, in turn, drives *torso* expression, thereby activating PTTH/Torso signalling and driving ecdysone biosynthesis. Given that PdfR is required in the core clock cells to stabilise PER/TIM protein levels at night (Li *et al.* 2014; Sabado *et al.* 2017), it is possible that it plays a similar in the larval PG clock. If this is the case, PdfR would be facilitating TIM activity during the night to increase *torso* expression levels, thereby driving ecdysone production.

larger than the PG of time-matched controls (Figure 2.7). Thirdly, loss of PTTH/Torso signalling in the PG does not appear to alter the overall larval growth rate, as shown for both *ptth* null mutants (Shimell *et al.* 2018) and the PG-specific knockdown of *torso* (Jade Kannangara, pers. comm.), whereas *phm>PdfR^RNAi* larvae have a significantly reduced larval growth rate (Figure 2.8B). Finally, the model proposed by Di Cara and King-Jones (2016) is at least partially incompatible with the translational model proposed by Iga *et al.* (2014). For example, expression of either *Pi3K* or *Akt* were unable to rescue the developmental arrest observed with PG-specific *tim* knockdown, but PI3K-AKT-TOR signalling is downstream of Pdf signalling in the *Bombyx* PG. Nevertheless, it remains possible that PdfR has some partial indirect effect on ecdysone production by regulating the larval PG clock (Figure 2.13). Future experiments could directly investigate this hypothesis by performing genetic interactions between the Torso and/or insulin signalling pathways and PdfR within the PG. For example, if Torso acts downstream of PdfR as is the case for the core clock genes, then *torso* overexpression would be expected to rescue the developmental delay phenotype of *phm>PdfR^RNAi* larvae. In addition, *torso* expression would be reduced in *phm>PdfR^RNAi* larvae under this hypothesis.

2.4.2. AkhR is a novel regulator of developmental timing and growth in the PG

The second candidate receptor studied in this chapter was AkhR, which displayed a developmental arrest phenotype when knocked down specifically in the PG. This phenotype is consistent with the results from an independent genome-wide PG-specific RNAi screen performed by Danielsen *et al.* (2016), which utilised the same RNAi line as here. While this phenotype could not be replicated with an independent RNAi line, both *AkhR^1* and *Akh^A* mutant animals were also found to be developmentally delayed compared to heterozygous controls, supporting a role for AkhR in the regulation of growth and developmental timing in *Drosophila*. The developmental delay observed for both *AkhR* and *Akh* null mutants in this study was somewhat surprising given that several previously published studies have not reported developmental defects in animals in which the Akh-producing cells have been ablated or in *Akh* null animals (Kim and Rulifson 2004; Gáliková *et al.* 2015). This suggests that perhaps the effects of Akh signalling loss are potentially context-dependent and sensitive to environmental changes. Indeed, Akh signalling has repeatedly been associated with stress response in multiple insect species, especially metabolic stress (Bednářová *et al.* 2013). In support of this idea, a comparable developmental delay phenotype was observed for *AkhR^1* mutants by Kim and Neufeld

(2015) only when the larvae were raised on standard food, not protein-rich media (yeast-rich media), suggesting that the requirement for Akh signalling is partially nutrition-sensitive. This potentially explains the discrepancies between Akh/AkhR data from different research groups, if different food is being used.

In this study, genetic loss of *Akh* appeared to have different effects to the loss of its receptor with respect to body size, as *AkhR[1]* mutants weighed significantly less than heterozygous controls, whereas *Akh[A]* mutants weighed significantly more than heterozygous controls. This potentially suggests the presence of an additional ligand for *AkhR* in *Drosophila*, although no other ligands have been reported in the literature to date. The weight increase observed for *Akh* mutants is consistent with the literature. Animals homozygous for an independently generated *Akh* loss-of-function mutation have also been reported as heavier and/or bigger than controls, as have animals with ablated Akh-producing neurons (Sajwan *et al.* 2015). On the other hand, animals homozygous for an independently generated *AkhR* loss-of-function mutation displayed adult-onset obesity, defined as the excess accumulation of adipose fat, but were not tested for overall changes in body size or weight (Bharucha *et al.* 2008). Part of the discrepancy between the effect of *AkhR* loss and *Akh* loss on body weight may be due to changes in insulin signalling. On low-protein food, *AkhR[1]* animals resemble *dilp3* loss-of-function mutants, because AkhR is required for the secretion of dILP3 (Kim and Neufeld 2015). This reduced insulin signalling would potentially reduce overall growth, at the same time as loss of *AkhR* directly results in increased lipid accumulation, ultimately leading to adults with reduced overall weight. In contrast, *Akh[A]* mutants have increase expression of all three of the brain-derived *dilps* (*dilps 2, 3* and *5*), which may act to increase growth (Gáliková *et al.* 2017). The relationship between Akh/AkhR and dILP/InR signalling appears quite complex and is only now beginning to be elucidated. That *Akh* and *AkhR* null mutants may affect growth differently is confirmed by evidence that *Akh* null mutants have increased wing size, but *AkhR* null mutants do not (Gáliková *et al.* 2015). This also highlights the potential difficulties in using just one measure of growth, such as weight, to describe a biological process as complex as growth. Future studies could overcome this by measuring pupal length or volume as well as weight.

In this study, the PG-specific knockdown of *AkhR* caused late larval lethality, but whole-fly null animals were homozygous viable. One possible explanation for this is that in whole-

animal nulls some type of compensatory change occurs in the other mutant tissues that ameliorates the effects of specific gene loss. In support of this, there is evidence that Akh/AkhR signalling is not the only lipolytic pathway in *Drosophila*, and at least some level of compensation has been suggested (Grönke *et al.* 2007; Gáliková *et al.* 2015). Alternatively, it is possible that Akh production in the CC cells is normally regulated through a negative feedback system involving the PG, which when lost due to PG-specific knockdown of *AkhR*, causes Akh to accumulate to toxic levels. In support of this, it has become clear that processes from the CC do make contact with the PG cells, and a role for this has not yet been established. Since the main product of the CC is Akh, and it is likely that at least some of this product is delivered directly to the PG cells, it also makes sense that the sole receptor for Akh, AkhR, would be present in the PG cells. This is supported by evidence that *AkhR* expression is enriched in the ring gland compared with other larval tissues (Phil Batterham, pers. comm.; Christesen *et al.* 2017). Overall, it is becoming increasingly clear that the effects of tissue-specific knockdown can differ markedly from whole-animal mutants, particularly when the tissue involved is a central developmental and signalling hub like the larval PG.

Whether AkhR regulates the production and/or secretion of ecdysone, or affects the development of the PG itself, remains to be elucidated. However, if AkhR is indeed regulating ecdysone levels, how might it be achieving this? The first possibility is that AkhR acts at the transcriptional or post-transcriptional level to directly affect the ecdysone biosynthetic genes (Figure 2.14). In support of this hypothesis, Akh/AkhR signalling induces the transcription of at least one cytochrome P450 gene in the fat body of cockroaches (Bradfield *et al.* 1991), and many of the ecdysone biosynthetic genes also encode cytochrome P450s. To test this, experiments such as those described and performed for PdfR could be undertaken with AkhR in the future. Alternatively, immunohistochemistry could be used to assay protein levels of members of the ecdysteroidogenic pathway, such as by Ohhara *et al.* (2015).

A second possibility is that AkhR is not required for the production of ecdysone but rather for its secretion from the PG (Figure 2.14). Recent work by Yamanaka *et al.* (2015) has implicated at least one GPCR in the vesicle-mediated secretion of ecdysone, and specifically identified Gαq as the G-protein responsible for this process. Because there is evidence that AkhR can signal via Gαq (Baumbach *et al.* 2014), it is possible that AkhR is
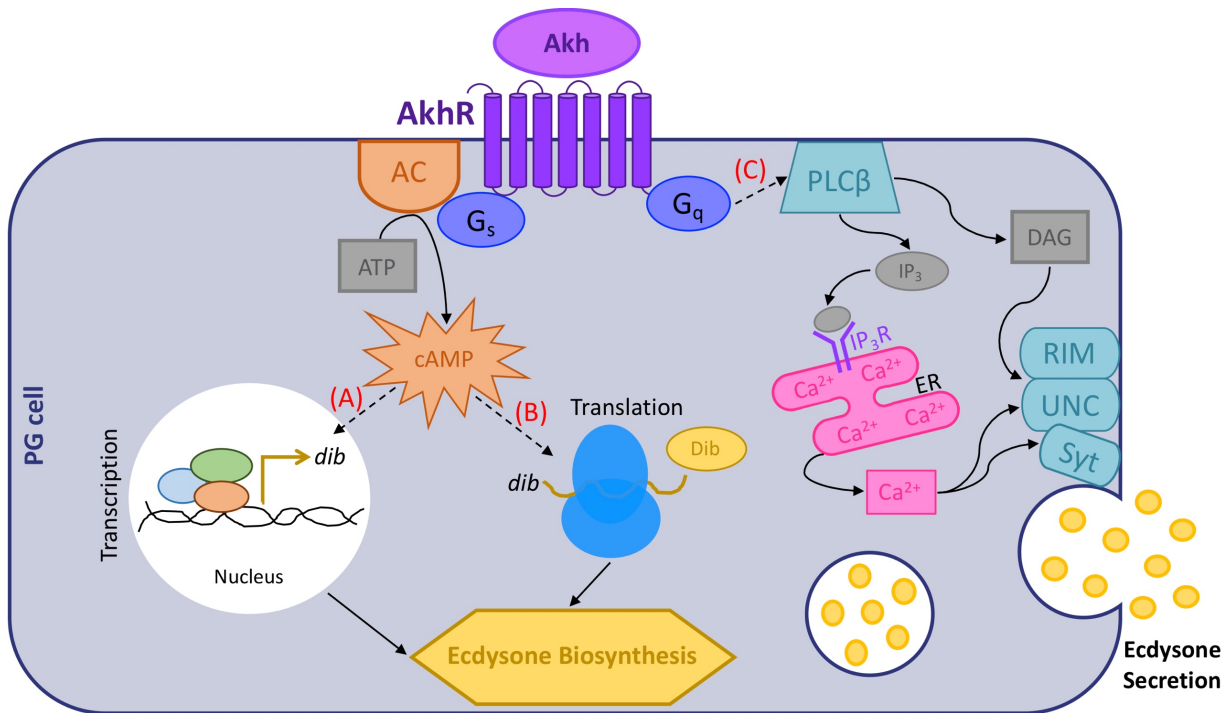
Figure 2.14. AkhR may function in the PG to regulate ecdysone biosynthesis and/or secretion.

AkhR may act at the transcriptional (A) or post-transcriptional (B) level to affect the ecdysone biosynthetic genes, thereby affecting ecdysone production. Alternatively, AkhR may be required for the vesicle-mediated secretion of ecdysone from the PG (C). It is also possible that AkhR acts at multiple levels to regulate both the production and secretion of ecdysone via different intracellular signalling pathways.

this GPCR. Moreover, a role for AkhR signalling in secretion is supported by a study that showed that AkhR controls the selective secretion of dILP3 from the insulin-producing cells in the larval brain in response to dietary sugars (Kim and Neufeld 2015). It is therefore possible that in the PG, AkhR acts to stimulate the release of ecdysone in response to nutritional cues sensed by the CC and transmitted to the PG through the release of Akh. To test this, the PG of *phm>AkhR^{RNAi}* larvae could be examined for vesicle accumulation using the *UAS-Syt-GFP* marker as described in Yamanaka *et al.* (2015). Genetically, it may also be possible to rescue the developmental arrest phenotype of *phm>AkhR^{RNAi}* larvae by co-expressing an activated form of Gαq (*Gαq.Q203L*) in the larval PG (Yamanaka *et al.* 2015).

A role for AkhR in the secretion of ecdysone does not necessarily preclude it from also having a role in ecdysone production. For example, there is evidence that the mammalian orthologue of AkhR, Gonadotropin-releasing hormone receptor, which regulates the onset of puberty in mammals, is required both for gonadotropin biosynthesis and secretion through multiple intracellular signalosomes (Naor 2009). Indeed, the diverse array of intracellular signalling cascades that are regulated by GPCRs and the promiscuous nature of GPCRs with regards to different combinations of heterotrimeric G proteins is now well-established (Gough 2016; Hilger *et al.* 2018). In particular, a single receptor is capable of interacting with multiple G proteins with distinct efficiencies and kinetics to achieve a range of cellular effects (Masuho *et al.* 2015). Thus, it is possible that AkhR acts at multiple levels to regulate both the production and secretion of ecdysone via different intracellular signalling pathways (Figure 2.14).

2.4.3. Conclusions and future directions

The data presented in this chapter confirms that there is still much to learn about the regulation of growth and developmental timing in insects. This is further supported by the recent publication of a genome-wide PG-specific RNAi screen which identified 1,906 candidate genes that resulted in developmental timing defects of some kind when knocked down in the PG (Danielsen *et al.* 2016). However, there are several caveats to large-scale screens of this kind, including: (i) no confirmation of the candidate genes was conducted using an independent RNAi, and (ii) no functional analysis, such as weight measurement, was carried out on the majority of these hits. Recently, three independent PG-

transcriptome data sets from *Drosophila* and *Bombyx mori* have also been published, which identify novel PG-specific and PG-enriched transcripts (Ou *et al.* 2016; Christesen *et al.* 2017; Nakaoka *et al.* 2017). Altogether, the identification and characterisation of PdfR and AkhR presented here, coupled with the recently published studies, confirms that there is much to still be discovered regarding growth control in insects. More generally, this work has confirmed that a multitude of complex cellular signalling pathways are required to coordinate the multiple developmental and environmental stimuli involved in growth regulation. As these pathways are further elucidated, we gain a deeper understanding of the fundamental processes that regulate growth. In the future, this may also affect our ability to diagnose and treat many human disorders such as cancer and obesity, which are fundamentally diseases caused by the dysregulation of growth.

Chapter 3: Investigating the function of non-*Drosophila* MACPF proteins in *Drosophila* development

3.1. Introduction

MACPF proteins are well known for their pore-forming roles in vertebrate immunity and bacterial pathogenesis. Indeed, much of their functional characterisation comes from work on the mammalian terminal complement components C6-C9 and the cellular immune effector Perforin. Whilst the immune functions of these particular mammalian proteins are relatively well characterised at both the biological and molecular level, the roles of other MACPF proteins, particularly those from more diverse species, remain to be elucidated. Therefore, our understanding of the functional diversity of MACPF proteins is currently rather limited.

Interestingly, studies of MACPF proteins across species indicate that some MACPF proteins play crucial roles in developmental processes (see section 1.2; also reviewed in Rosado *et al.* 2008; Berkowicz *et al.* 2017). Generally, the molecular functions of these developmental MACPF proteins are poorly understood, and they have been relatively understudied, especially *in vivo*. By far the best characterised to date is the *Drosophila* MACPF protein Torso-like (Tsl), best known for its essential role in embryonic terminal patterning. Tsl consists of a single MACPF domain, with no detectable accessory domains, and is the only *Drosophila* MACPF protein so far identified. This contrasts noticeably with higher eukaryotes, which usually have several MACPF members or more. As such, *Drosophila* offers a tractable model for *in vivo* studies of the MACPF domain to determine how it functions in developmental processes. That MACPF proteins from other species are capable of functioning similarly even across reasonably large evolutionary distances has recently been demonstrated for Tsl proteins from several distantly-related insect species. The Tsl proteins from both the honey bee (*Apis mellifera*) and the pea aphid (*Acyrthosiphon pisum*) can function in place of *Drosophila* Tsl to correctly pattern the termini, despite the fact that neither of these insects require Tsl for terminal patterning nor pattern their termini like dipterans in their endogenous setting (Duncan *et al.* 2013). This suggests that even if the developmental function of a protein is not conserved across evolution, its biochemical or molecular activity may still be similar. Additionally, *Drosophila* has proved an invaluable tool for genetic studies due to the range of mutants

and other reagents available for manipulating gene function, and the ease with which this can be done (Arias 2008).

Moreover, the high level of gene conservation between flies and humans means that evidence about gene function found using *Drosophila* can be highly informative with respect to human gene function and disease (Pandey and Nichols 2011). As such, the function of mammalian genes can be investigated *in vivo* by expressing them in *Drosophila* (reviewed in Pandey and Nichols 2011; Yamamoto *et al.* 2014). For example, the *human prostate tumour overexpressed*-1 gene was found to be a negative regulator of the Notch pathway when studied in *Drosophila* (Alaña *et al.* 2014). Moreover, unexpected and novel Notch ligands have been identified by overexpressing mammalian genes in *Drosophila*. The mammalian *Delta-like1* (*Dlk-1*) gene was found to negatively regulate the Notch pathway using this method (Bray *et al.* 2008). These studies show the value of *Drosophila* as a model organism to investigate novel gene function and disease-causing genes.

This chapter aimed to express MACPF proteins from different organisms in *Drosophila* for two purposes. Firstly, given that the only functional domain they share with Tsl is a MACPF domain, if they can function in the same manner as Tsl in embryonic patterning, this would strongly suggest that the MACPF domain is critical for Tsl function. A range of MACPF proteins were chosen for this purpose. The human immunity proteins perforin and Complement components C6-C9 were chosen as they comprise both lytic and non-lytic members and are both biologically and molecularly well-characterised. The mammalian MACPF proteins ASTN2 and BRINPs1-3 were also studied. They are implicated in neural development, but their mechanism of action is still poorly understood (Zheng *et al.* 1996; Adams *et al.* 2002; Kawano *et al.* 2004; Kobayashi *et al.* 2014). The final MACPF protein of interest, sea urchin Apx, has been implicated both in embryonic development and immunity based on expression data, but true functional characterisation has so far been lacking (Haag *et al.* 1999; Dheilly *et al.* 2011). Secondly, any phenotypes generated in *Drosophila* may provide important clues as to the function of these proteins in their endogenous setting. Together, these investigations aimed to provide insight into the distinct and diverse mechanisms by which MACPF proteins function in a developmental context.

3.2. Materials and Methods

3.2.1. Fly stocks and plasmid constructs

w^{1118} (BL3605), *patched*-Gal4 (BL2017), *actin*-Gal4 (BL25374), *tubulin*-Gal4 (BL5138), GMR-Gal4 (BL9146), *pannier*-Gal4 (BL3039), *elav*-Gal4 (BL5146), *c355*-Gal4 (BL3750), N^1 (BL6873), *UAS-E(spl)mβ* (BL26675) stocks were obtained from the Bloomington *Drosophila* Stock Centre. The *tsl* null mutant and *UAS-tsl* were as previously described (Johnson *et al.* 2013). Plasmid constructs used for expressing human MACPF proteins were cloned via gateway into pUASgHA.attB (Bischof *et al.* 2013), as part of our human ORFeome project (Travis Johnson, unpublished) and injected by BestGene Inc. onto the third *Drosophila* chromosome at the 86FB site (Bischof *et al.* 2007). The HeET-1 gene from *Heliocidaris erythrogramma*, which encodes the Apx protein, was synthesised by GenScript, and its variants (Apx^{MACPF} and Apx^C) were altered by GenScript to obtain truncated forms of the protein. All Apx constructs were injected by BestGene Inc. onto the second *Drosophila* chromosome at the 51C site (Bischof *et al.* 2007). All construct sequences are included in Appendix 3.

3.2.2. Cuticle preparations

Cuticle preparations were used to examine the phenotype of embryos, and were performed as previously described in Van der Meer (1977). Adults were allowed to lay on apple juice agar media supplemented with yeast paste for 24hr before being removed. Embryos were aged for a further 24hrs, before being collected and dechorionated in 50% (v/v) bleach, rinsed with distilled water, and mounted onto slides in a 1:1 (v/v) mixture of Hoyer's solution (Appendix 1) and lactic acid (BDH). Slides were incubated at 65°C overnight and visualised with dark field optics on a Leica DM LB compound microscope (with Leica DC300 camera).

3.2.3. Tissue immunohistochemistry

Antibodies used were anti-Cut (Ct, 2B10) and anti-Wingless (Wg, 4D4), obtained from the Developmental Studies Hybridoma Bank, and anti-Senseless (Sens), which was a gift from Hugo Bellen (Nolo *et al.* 2000). Third instar wandering larvae were collected and washed with distilled H_2O to remove any affixed fly media. Larvae were dissected in PBS on ice and fixed in 4% paraformaldehyde for 30 minutes at room temperature. Tissue was washed

five times in PTx (PBS with 0.1% Triton-X), before blocking with 5% goat serum (Sigma) for an hour. Tissue was incubated with primary mouse α-Cut or α-Wg (1 in 40) in 5% goat serum overnight with agitation at 4˚C. Dissected larvae were washed five times in PTx, then incubated with secondary antibody (α-mouse Alexa488, A11029; α-mouse 568, A11004; α-guinea pig 568, A11075 from Invitrogen) at a concentration of 1:1000 for an hour with shaking at room temperature. After a further five washes with PTx, larvae were incubated in H_2O with DAPI (1:3000) to stain the cell nuclei. Tissue was washed five times in PTx for an hour. Wing discs were dissected and mounted onto slides in VectaShield mounting medium (Vector Laboratories) and imaged using a spinning disk confocal microscope (Olympus CV1000). Apoptotic cells were detected by TUNEL staining using the *In Situ* Cell Death Detection Kit, TMR Red (Roche). n ≥ 15 wing discs for each genotype were used in these experiments. All images were processed using ImageJ (FIJI) software.

3.2.4. Adult wing mounting and imaging

Adult *Drosophila* wings were detached from the thorax and placed briefly in isopropanol and then mounted in Hoyer's mountant (Appendix 1) on microscope slides. A Leica DMLB compound microscope (with Leica DC300 camera) was used to image the wings. Each wing image is representative of wings observed from at least 20 individual adults.

3.3. Results

3.3.1. Mammalian MACPF proteins and sea-urchin Apx cannot function in the same manner as Torso-like in embryonic patterning

To investigate whether the MACPF proteins of interest can function in the same manner as Tsl in *Drosophila* embryonic development, transgenic flies containing coding sequences for Complement C6-9, perforin, BRINPs1-3, ASTN2 and Apx cloned behind UAS sequences were generated (Methods 3.2.1, Appendix 3). The MACPF proteins were tested to see if they could generate the same phenotype that Tsl causes when it is overexpressed in all follicle cells with the *c355*-Gal4 driver (Manseau *et al.* 1997); namely ectopic Torso activation and expansion of the termini at the expense of the central segments, the so-called "spliced" phenotype (Savant-Bhonsale and Montell 1993). To confirm the overexpression system was functional in these experiments, *tsl* was overexpressed using *c355*-Gal4. As expected, this caused ectopic Torso activation, as assessed by the spliced phenotype (Figure 3.1B; Savant-Bhonsale and Montell 1993; Martin *et al.* 1994). However,

72

none of the other MACPF proteins generated this spliced phenotype when expressed using *c355*-Gal4, resembling the *c355-Gal4/+* control instead (Figure 3.1C compared with 3.1A). These results indicate that these proteins are unable to function as Tsl does in terminal patterning.

3.3.2. Phenotypes caused by overexpression of MACPF proteins in *Drosophila*

Although none of the non-*Drosophila* MACPF proteins were able to function in the same manner as Tsl, an interesting and unexpected phenotype was observed upon expression of Apx. Driving Apx with *c355*-Gal4 resulted in notches at the adult wing margin and ectopic bristles on the scutellum (Table 3.1). The generation of this phenotype with the *c355*-Gal4 driver is most likely due to the fact that, in addition to expressing in the ovarian follicle cells (Section 3.3.1), *c355*-Gal4 also expresses in the larval wing pouch that ultimately goes on to form the adult wing, and also in a complex pattern in the presumptive wing notum (Hrdlicka *et al.* 2002). Given this finding with *Apx* expression, all of the MACPF constructs were expressed using a number of Gal4 drivers and the progeny analysed for any resulting phenotypes. Two ubiquitous drivers, *tubulin*-Gal4 (Lee and Luo 1999) and *actin*-Gal4 (Ito *et al.* 1997), which drive high and low levels of expression respectively, were utilised. In addition, several widely-used tissue-specific drivers were chosen to study expression in different tissues. *Elav*-Gal4 is a pan-neuronal driver (Lin and Goodman 1994), *GMR*-Gal4 expresses in post-mitotic neurons in the eye (Lee and Thomas 2011), and *pannier*-Gal4 expresses along the dorsal midline (Heitzler *et al.* 1996).

Expression of several of these MACPF proteins (Complement components C7, C8β and C9) gave no observable phenotypes with any of these drivers (Table 3.1). Ubiquitous expression of *Complement component C8α* was lethal, but more restricted expression did not generate any other observable phenotypes. Ubiquitous expression of *perforin* was also lethal, and *perforin* expression with *pnr*-Gal4 resulted in adults with very mild, partially penetrant bristle loss. The *pnr*-specific expression of *ASTN2* resulted in adults with a moderate thoracic cleft approximately 25% of the time (Figure 3.2A). Expression of *BRINP1* with *Elav*-Gal4 gave a fully penetrant mild rough eye phenotype, whereas *GMR>BRINP1* flies had a more severe rough eye phenotype (Figure 3.2B and C).
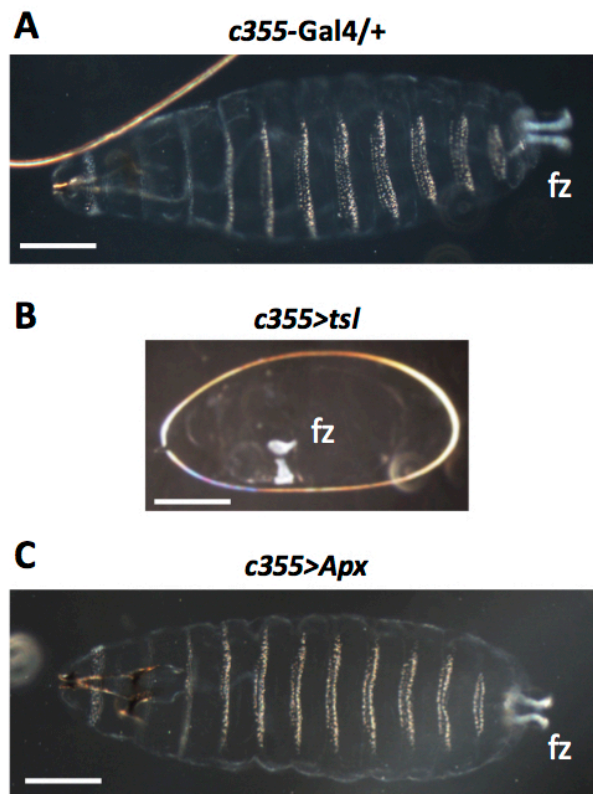
Figure 3.1. Non-*Drosophila* MACPF proteins cannot function in the same manner as Tsl in embryonic patterning.

(A) *c355*-Gal4/+ control larvae are wild-type, having eight abdominal segments and a filzkörper (fz) at the posterior. (B) Overexpression of *tsl* in all follicle cells using *c355*-Gal4 causes ectopic activation of Torso, resulting in embryos with expanded terminal structures at the expense of the abdominal segments, as indicated by a centralised filzkörper (fz). (C) None of the twelve MACPFs of interest were able to recapitulate this phenotype when expressed with *c355*-Gal4, and all resulting larvae were phenotypically wildtype. As an example, *c355>Apx* is shown here. Anterior is to the left for all panels. Each image is representative of ≥10 individual larvae/embryos. Scale bars represent 100μM.

Table 3.1. Summary of phenotypes caused by the expression of non-*Drosophila* MACPF proteins in various tissues of *Drosophila*.

MACPF protein	Tubulin (Ubiquitous)	Actin (Ubiquitous)	Elav (All neurons)	Pannier (Midline)	GMR (Eyes)	c355 (Follicle cells & others)	Patched (Wing imaginal disc)
	Gal4 Driver (Tissue type)						
hPf	Lethal	NOP	NOP	56% mild bristle loss	NOP	NOP	Not tested
hC6	NOP	NOP	NOP	NOP	100% mild rough eye	NOP	Not tested
hC7	NOP	NOP	NOP	NOP	NOP	NOP	Not tested
hC8α	Lethal	NOP	NOP	NOP	NOP	NOP	Not tested
hC8β	NOP	NOP	NOP	NOP	NOP	NOP	Not tested
hC9	NOP	NOP	NOP	NOP	NOP	NOP	Not tested
hBRINP1 (DBC1)	Reduced viability	NOP	100% mild rough eye (anterior)	90% mild bristle loss	100% severe rough eye	NOP	Not tested
hBRINP2 (FAM5B)	NOP	NOP	NOP	NOP	NOP	NOP	Not tested
hBRINP3 (FAM5C)	NOP	NOP	NOP	NOP	NOP	NOP	Not tested
hASTN2	NOP	NOP	NOP	25% moderate thorax cleft	NOP	NOP	Not tested
mMpeg1	Pupal lethal#*	Mild rough eye, ectopic bristles, wing notches#	Not tested	Not tested	Very mild rough eye (partially penetrant)#	Mild wing notches (partially penetrant)#	Ectopic bristles, wing notches#
HeApx	Lethal	Lethal	Reduced viability	90% ectopic bristles	Moderate rough eye	Ectopic & lost bristles, wing notches, vein thickening	Ectopic & lost bristles, wing notches, vein thickening

h = *Homo sapiens*, m = *Mus musculus*, He = *Heliocidaris erythrogramma* indicate endogenous species of MACPF protein; NOP denotes that no obvious phenotype was observed.

#indicates work that was completed by another PhD student, Lauren Forbes Beadle, and is summarised here.

*indicates that individuals died during pupal development. Upon dissection, ectopic bristles and rough eyes were observed.

Initial phenotypic screen of human MACPFs with the first five Gal4 drivers (columns 2-6) was conducted by our former RA, John Kotsanas.

Expression of *Apx* with both *tubulin*-Gal4 and *actin*-Gal4 resulted in lethality prior to pupariation, whilst expression with *Elav*-Gal4 severely reduced viability (Table 3.1). *GMR>Apx* flies showed a moderate rough eye phenotype with 100% penetrance (Figure 3.2F). *pannier>Apx* flies were observed to have ectopic bristles on the scutellum and along the midline of the thorax, with 90% penetrance (Figure 3.2A). Interestingly, another PhD candidate in our lab Lauren Forbes Beadle saw similar phenotypes to Apx when expressing murine *Mpeg1* with *c355*-Gal4 and these other Gal4s in *Drosophila*.

Mpeg1 is a highly conserved MACPF protein found from the earliest extant metazoans such as *Porifera* (sponges) through to mammals (D'Angelo *et al.* 2012). This MACPF protein was named Macrophage expressed gene 1 (Mpeg1) due to its seemingly exclusive expression in mature murine and human macrophages (Spilsbury *et al.* 1995). Early studies suggested a role for Mpeg1 in immunity because Mpeg1 expression was up-regulated during differentiation of mature macrophages in mice, and because of substantial sequence similarity to perforin (Spilsbury *et al.* 1995). Mpeg1 expression was also upregulated upon prion infection in the mouse brain, linking Mpeg1 to an infection state (Kopacek *et al.* 2000).

Expression of *Mpeg1* with *tubulin*-Gal4 resulted in lethality. However, as this occurred very late in the pupal stage, pupae could be removed from the pupal case and were observed to have rough eyes and ectopic bristles (Figure 3.2D). *actin>Mpeg1* flies had rough eyes, ectopic bristles and wing notches (Figure 3.2E). Expression with *GMR*-Gal4 caused a mild rough eye phenotype (Figure 3.2F). Due to the phenotypic similarities observed between *Apx*- and *Mpeg1*-expressing flies, which may be indicative of an underlying functional similarity, these two proteins were chosen for further study.

To investigate whether the MACPF domain is responsible for the phenotypes observed with *Apx* expression in *Drosophila*, a series of domain-specific *UAS-Apx* constructs were designed (Figure 3.3). These new constructs were tested in the same manner as the full length Apx described above. The *Apx^{MACPF}* construct contains the signal peptide and MACPF domain, but none of the sequence C-terminal to the MACPF domain. This was generated to eliminate any function attributed to the C-terminus and its predicted ApeC domain. A C-terminal domain only construct, *Apx^C*, was created to determine if the C-terminus alone

A *pannier*

+ ASTN2

B *Elav*

+ BRINP1

C *GMR*

+ BRINP1

D *tubulin*

+ Mpeg1

E *actin*

+ Mpeg1

F *GMR*

+ Mpeg1 Apx

78
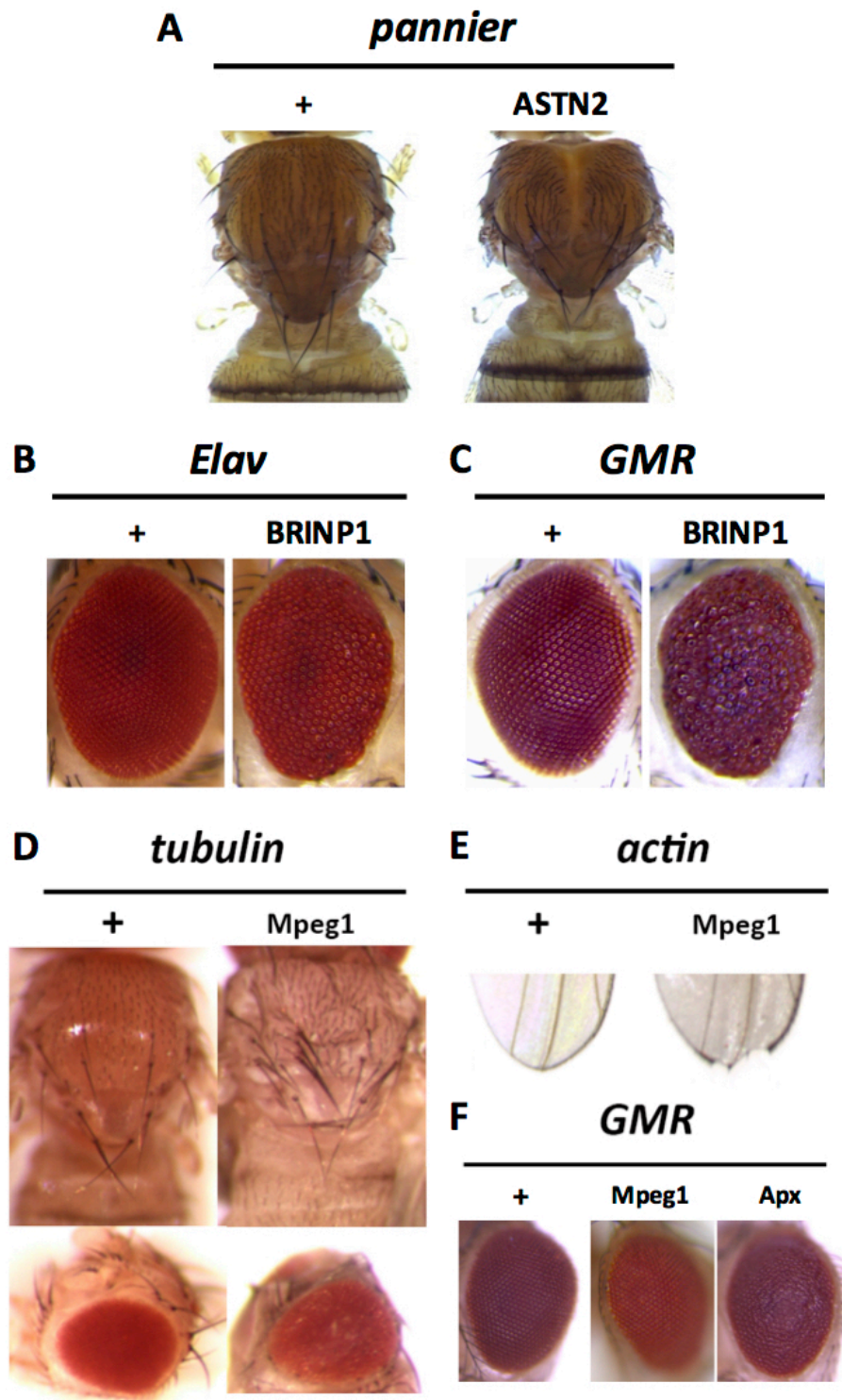
Figure 3.2. Phenotypes caused by the expression of non-*Drosophila* MACPFs in various tissues of *Drosophila*.

 (A) *pannier-Gal4* expresses along the dorsal midline. At least 25% of the *pnr>ASTN2* flies showed a moderate thoracic cleft. (B) *Elav-Gal4* is a pan-neuronal driver. When *Elav-Gal4* was used to express *BRINP1*, a mild rough eye phenotype was observed. (C) *GMR-Gal4* drives expression in the post-mitotic neurons of the eye. When *BRINP1* was expressed with *GMR-Gal4*, a severe rough eye phenotype was observed. (D) *tubulin*-Gal4 is a strong ubiquitous driver. *Mpeg1* expression with this driver caused lethality during pupal development. Upon dissection, ectopic bristles and rough eyes were observed. (E) *actin*-Gal4 is also a ubiquitous driver that expresses at a lower level than *tubulin*-Gal4. Expression of *Mpeg1* with *actin*-Gal4 had wing notches (shown), in addition to the ectopic bristle and rough eye phenotypes observed *with tubulin-Gal4*. *GMR>Mpeg1* flies showed a very mild rough eye phenotype, which was not fully penetrant. *GMR>Apx* flies showed a fully-penetrant moderate rough eye phenotype. Each image is representative of at least 15 individuals per genotype. All Mpeg1 data was completed by another PhD student, Lauren Forbes Beadle.

Apx variant	Tub-Gal4	act-Gal4	GMR-Gal4	ptc-Gal4
Apx (Full length) – 491 aa N C MACPF ApeC 29 395	Lethal	Lethal	Moderate rough eye	Ectopic & lost bristles, wing notches, vein thickening
Apx^{MACPF} (SP & MACPF) – 395 aa MACPF	Lethal	Lethal	Moderate rough eye	Ectopic & lost bristles, wing notches, vein thickening
Apx^C (SP & ApeC) – 143 aa ApeC	NOP	NOP	NOP	NOP

Figure 3.3. Domain structures of Apx variant constructs and the phenotypes caused by their overexpression.

The endogenous signal peptide (SP) sequence is used for all constructs (**dark pink**). Apx is the full-length protein sequence containing a MACPF domain (**purple**) and a C-terminal ApeC domain (**blue**). Apx^{MACPF} is the N-terminal region of the Apx sequence containing the SP and MACPF domain. Apx^C consists only of the signal peptide and the C-terminal sequence. The predicted protein length of each construct is shown in amino acids (aa). The phenotypes of flies expressing these Apx variants with several Gal4 drivers is shown to the right of each structure figure. NOP denotes that no obvious phenotype was observed

was functional. Expression of *Apx^MACPF* with various Gal4 drivers recapitulated the phenotypes observed with full-length *Apx* (Figure 3.3). Alternatively, expression of *Apx^C* resulted in viable flies and caused no observable phenotypes with any of the Gal4 drivers tested (Figure 3.3). These data suggest that the MACPF domain of Apx is responsible for the Apx phenotypes observed in *Drosophila*.

3.3.3. Apx and Mpeg1 overexpression phenotypes resemble those caused by reduced Notch signalling

The wing notching and ectopic bristle phenotypes observed by overexpression of Apx and Mpeg1 resemble the well-described phenotypes observed in mutants of the Notch signalling pathway (Shellenbarger and Mohler 1978). The Notch pathway is a highly conserved signalling pathway required for cell fate specification via lateral inhibition, controlling lineage decisions via asymmetric cell division and by specifying cell boundaries. In *Drosophila*, the Notch pathway controls multiple aspects of both wing and bristle development (reviewed in Bray 2006). The wing and bristle phenotypes of Mpeg1 and Apx were investigated further using a tissue-specific driver called *patched*-Gal4 (*ptc*-Gal4), which is expressed in a stripe of cells along the anterior/posterior boundary of the larval wing disc (Sun and Artavanis-Tsakonas 1997; Glise *et al.* 2002). This area of the wing disc develops into the area between veins L3 and L4 in the adult wing and also contributes tissue to both the scutellum and notum regions of the thorax. This driver has been used in the identification and characterisation of novel regulators of *Drosophila* Notch signalling (Dalton *et al.* 2011; Hori *et al.* 2011), and the phenotypes caused by using it to manipulate Notch signalling are well understood.

Expression of Apx in the *ptc* domain resulted in a severe loss of tissue at the wing margin with 100% penetrance (n>50, Figure 3.4D compared to A and B). Apx expression also resulted in mild vein thickening and fusion of the L3 and L4 veins at the proximal end of the wing in all individuals sampled (Figure 3.4D). Both ectopic bristle and bristle loss phenotypes were observed in *ptc>Apx* flies (n>80, Figure 3.4G and H compared to E). Expression of Mpeg1 with *ptc*-Gal4 resulted in wing notches, but to a lesser extent than with Apx expression, and with approximately 89% penetrance (n=47, Figure 3.4C). Mild bristle duplications were observed in 46% of *ptc>Mpeg1* flies (n>40, Figure 3.4F). No vein thickening or fusion of L3 and L4 veins was observed in *ptc>Mpeg1* wings. Neither the
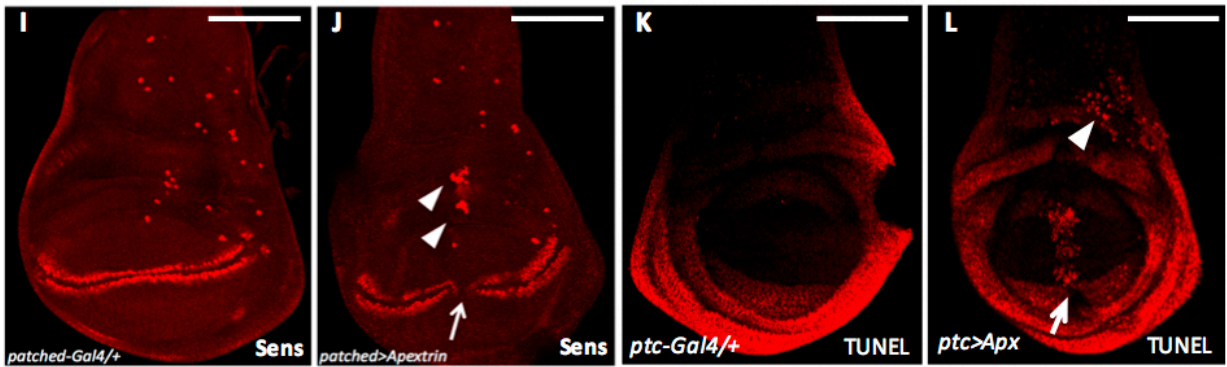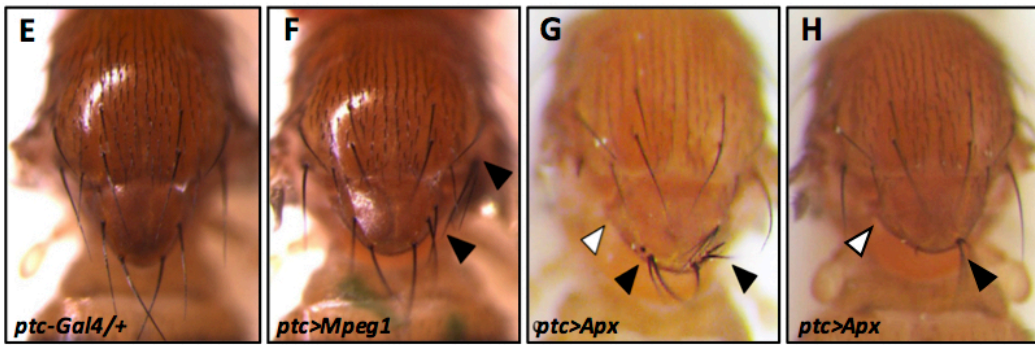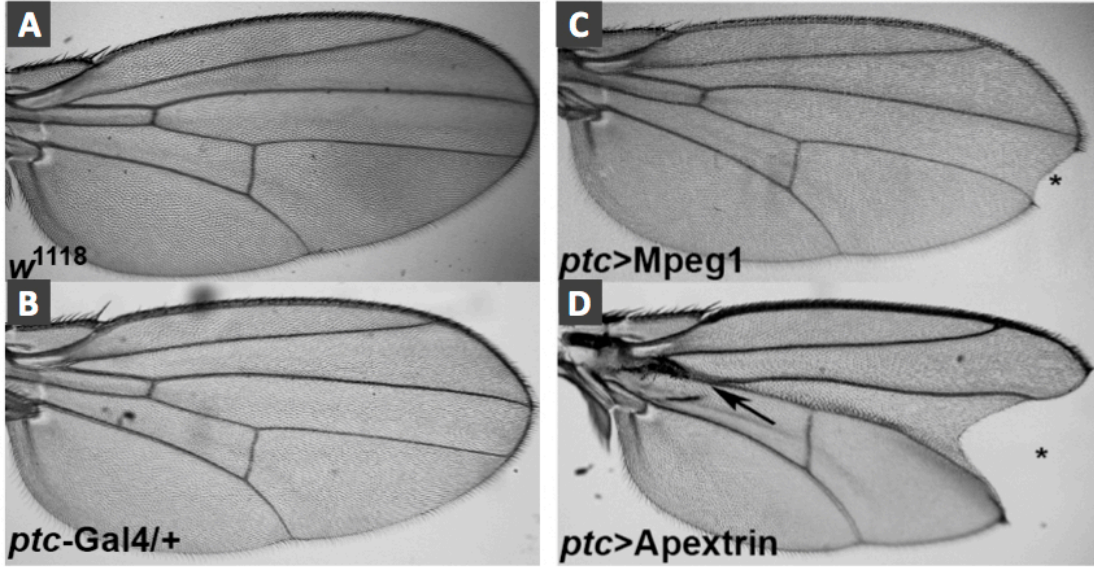
Figure 3.4. Expression of Apx and Mpeg1 in the wing disc causes wing notching and a complex bristle phenotype, including more Senseless-positive cells and increased apoptotic cell death.

(A) A control wing from the w^{1118} strain. Proximal is to the left and distal is to the right of each panel. (B) The *ptc*-Gal4 driver control wing. (C) *ptc*-Gal4>*Mpeg1* causes a loss of wing tissue at the margin in the distal region with 89% penetrance (asterisk). (D) *ptc>Apx* wings have a more severe loss of wing tissue at the distal margin (asterisk) and fusion of the L3 and L4 wing veins in the proximal region (arrow). (E) The *ptc-Gal4/+* controls can have minor bristle duplications but generally have wild type bristles. (F) *ptc*-Gal4>*Mpeg1* flies have mild bristle duplications (black arrowheads). (G-H) *Apx* expression in the *ptc* domain leads to severe bristle duplications on the scutellum (black arrowheads) and/or loss of scutellar bristles (open arrowhead), but is variable across animals. (I-J) Senseless expression is inhibited at the D/V boundary (arrow), which is indicative of a disrupted margin, and clusters of Senseless-positive cells are observed in Apx-expressing discs (arrowheads), which is indicative of ectopic sensory organ precursor cells. Scale bars represent 100μM. (K-L) TUNEL staining is noticeably increased in the *ptc* domain (arrow) where *Apx* is expressed, compared with the *ptc-Gal4/+* control discs, which show very little cell death in the pouch of the wing disc. Additionally, TUNEL staining can be seen in parts of the presumptive notum where the bristle precursor cells arise (arrowhead). Scale bars represent 100μM.

control *w[1118]* flies nor the *ptc-Gal4/+* flies were observed to have wing notches or wing vein fusion (n≥50, Figure 3.4A and B, respectively).

The bristle phenotypes observed in the *ptc>Apx* flies were interesting because the Notch signalling pathway is required at multiple stages during bristle development, both in the specification of the sensory organ precursor (SOP) cells and in deciding the fates within each bristle lineage (Shellenbarger and Mohler 1978; Hartenstein and Posakony 1990). Due to the dual roles of Notch signalling in bristle development, bristle loss can be brought about by both decreased and increased Notch activity. To determine if the effects of Apx expression on bristle number were due to reduced Notch signalling, a marker of SOP cells (Senseless) was examined (Nolo *et al.* 2000). If Apx expression was reducing Notch activity, we would expect an increase in the number of SOP cells in the wing disc. Indeed, there was a noticeable increase in the number of Senseless-positive cells within the *ptc* domain, indicating an increase in SOP cells (Figure 3.4J compared to 3.4I). The increase in SOP cells corresponds to the ectopic bristles seen on the *ptc>Apx* flies and supports an effect for Apx on SOP specification. Additionally, Senseless staining along the dorso-ventral (DV) boundary was absent in the *ptc* domain, which is indicative of altered Notch signalling at the presumptive wing margin (Figure 3.4J).

However, if more precursor cells are being specified, what then underlies the bristle loss phenotype observed, often concurrently with ectopic bristles, in *ptc>Apx* flies (Figure 3.4G and H)? The first possibility is that Apx reduces Notch signaling to increase the number of bristle precursors but not all of them are developing their neuronal fate to actually form the external bristle structure. Another possibility for the bristle loss phenotype is that Apx expression is inducing cell death in the wing disc. For example, apoptosis can be triggered in specific cells within the neural lineages as a result of ectopic activated Notch expression (Orgogozo *et al.* 2002). Moreover, the severity of the wing notching phenotype indicates a substantial amount of tissue loss is occurring in adult wings as a result of Apx expression. To investigate this, TUNEL staining was conducted on third instar wing discs expressing Apx in the *ptc* domain. Compared with the *ptc-Gal4/+* control, there was a marked increase in cell death where Apx was expressed (Figure 3.4L compared to K). This increased cell death may be the cause of bristle loss, however, whether this is the sole cause of bristle loss requires further investigation. The complexities of the bristle phenotype also suggest that further analysis of this particular phenotype may not provide clear insight into Apx

function in *Drosophila*. Taken together, the wing notching and ectopic bristle phenotypes observed by overexpression of Apx and Mpeg1, together with the increase in Senseless-positive cells and the disruption at the DV boundary in the *ptc* domain, phenocopy well Notch loss-of-function (Shellenbarger and Mohler 1978).

3.3.4. Apx and Mpeg1 overexpression phenotypes are enhanced by reduced Notch signalling

In order to determine whether the *Apx* and *Mpeg1* overexpression phenotypes were exacerbated when Notch levels were reduced, genetic interaction experiments were performed using the N^1 allele. N^1 is a loss of function mutation in Notch that shows dominant defects in tissues such as the adult wing and thorax (Jack and DeLotto 1992; de Celis and García-Bellido 1994b). The genetic lesion in N^1 is unknown and homozygotes cannot be tested as N^1 is recessive lethal (Poulson 1937; Lehmann *et al.* 1983). Notch alleles such as N^1 have been used extensively to test for N pathway interactions. For example, the transmembrane protein Uif was shown to genetically interact with the Notch signalling pathway through experiments with the N^1 allele (Xie *et al.* 2012).

Consistent with previous studies (Barry *et al.* 2011), heterozygous N^1 females showed loss of wing tissue (notching), slight broadening of the veins at the margin (called deltas), and occasional duplications of scutellar macrochaetae bristles (n≥20, Figure 3.5A). Wing notching was enhanced in N^1/+ females when *Mpeg1* was expressed using *ptc*-Gal4 in all individuals observed (n≥20, Figure 3.5C compared to 3.4C). *Apx* expression in the N^1 mutant background also exacerbated the wing notching in all observed cases (Figure 3.5D compared to 3.4D), although this was not as severe as observed for Mpeg1. This is perhaps because *ptc>Apx* alone already causes severe tissue loss at the wing margin. The fusion of the L3 and L4 wing veins observed in the *ptc>Apx* flies was also exacerbated in the N^1 background (Figure 3.5D). The veins themselves appeared thickened and the area of fusion extended further towards the posterior crossvein when compared to the *ptc>Apx* wings. The bristle phenotype also appeared more severe in N^1/+; *ptc>Apx* flies, with the bristle loss phenotype now predominating over ectopic bristles (Figure 3.5G). This suggests that the bristle loss phenotype is more severe than the duplication phenotype. Overall, these observations suggest that Apx and Mpeg1 expression may be reducing Notch pathway activity in *Drosophila*.
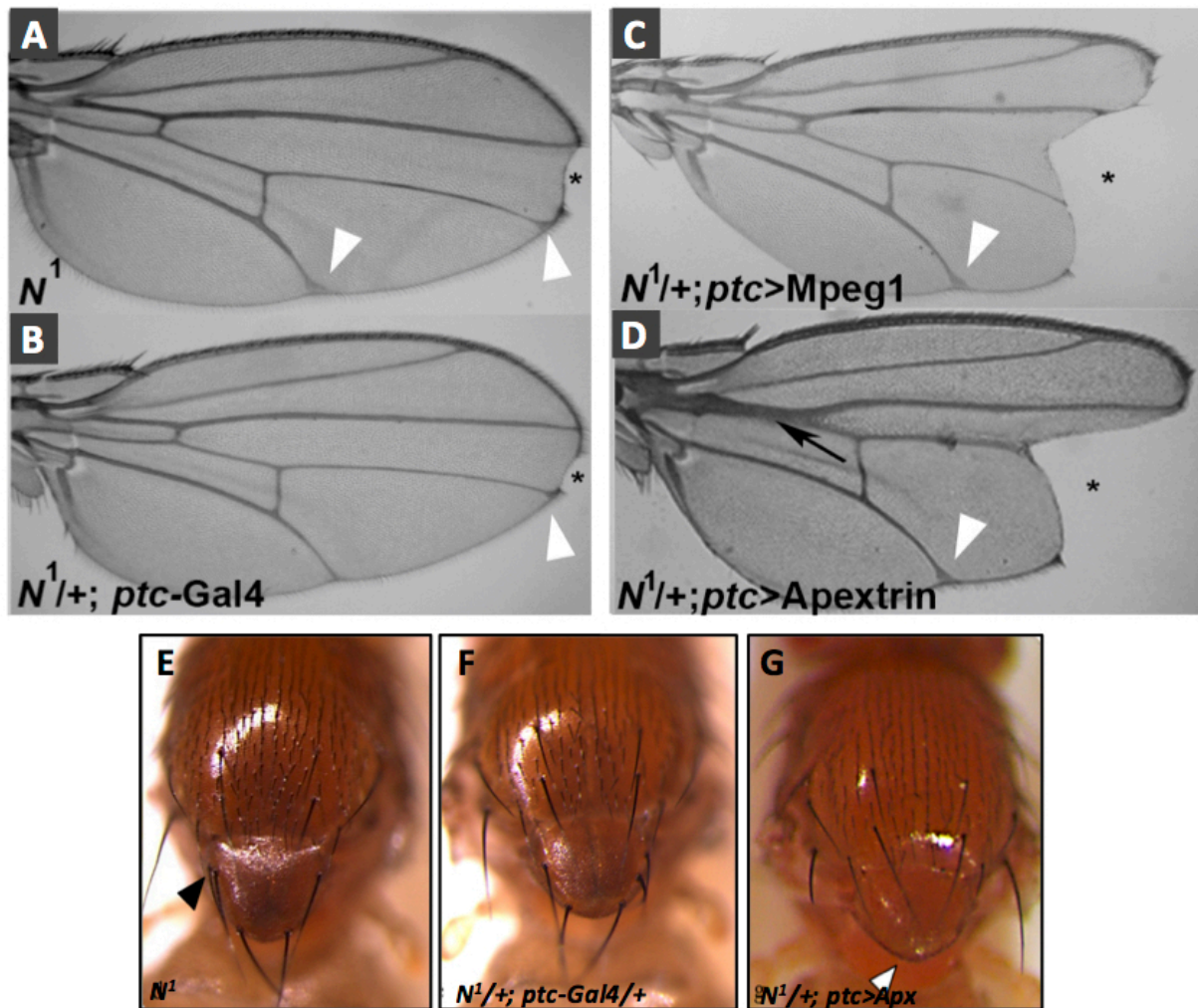
Figure 3.5. Reduction of Notch levels by the *N¹* allele enhances the wing and bristle defects caused by Apx and Mpeg1 expression in the *Drosophila* wing.

(A) *Notch¹* (*N¹*) is a hypomorphic mutation of *Notch* that causes tissue loss at the distal wing margin (asterisk) and wing vein deltas (arrowhead). (B) *ptc*-Gal4 driver in the *Notch¹* mutant background. (C) Expression of *Mpeg1* using *ptc*-Gal4 in the *N¹* background causes severe wing notching (asterisk), with wing vein deltas also present (arrowhead). (D) *ptc>Apx* expressed in the *N¹* background also exacerbated the wing notching (asterisk) and wing vein fusion (arrow) phenotypes. Deltas are still present (arrowhead). Each image represents ≥ 15 adult wings. Experiments carried out jointly with Lauren Forbes Beadle. (E) Bristle duplications are characteristic of *Notch* hypomorphic mutants such as *N¹* (arrowhead). (F) The *ptc*-Gal4 driver in the *N¹* background has wild type bristles. (G) Expression of *Apx* in the *N¹* background enhances the bristle loss phenotype (open arrowhead).

3.3.5. Notch target genes are disrupted by Apx and Mpeg1 expression in the larval wing disc

To further confirm that *Apx* and *Mpeg1* overexpression reduces Notch pathway activity, the expression of two transcriptional targets of Notch pathway activity was analysed in developing wing discs. These were the transcription factor Cut (Ct) and the secreted morphogen Wingless (Wg), which are both required in the presumptive wing margin (along the D/V boundary) to drive wing margin differentiation (Neumann and Cohen 1996; Micchelli *et al.* 1997). In w^{1118} control wing discs, Ct and Wg are expressed in a 2-to-5-cell layer at the margin (Figure 3.6A and B, respectively). When Notch activity is decreased in the wing disc, Ct and Wg expression is also reduced (Micchelli *et al.* 1997).

In *ptc>Apx* wing discs, the 2-to-5-cell layer of Ct-and Wg-expressing cells was severely disrupted within the *ptc* domain (Figure 3.6C and D, respectively). Expression of Mpeg1 in the wing disc using *ptc*-Gal4 also caused a thinning or disruption to both Ct and Wg staining (Figure 3.6E and F). This disruption was milder than that seen in *ptc>Apx* discs (Figure 3.6C and D), and is consistent with the milder wing notching observed in *ptc>Mpeg1* adult wings (Figure 3.4C). This loss of Ct and Wg expression strongly supports the idea that Apx and Mpeg1 expression in the developing *Drosophila* wing margin reduces Notch activity.

3.3.6. Expression of a Notch pathway target gene suppresses Apx-induced wing notches

Although the previous experiments suggested that Apx and Mpeg1 were interacting with the Notch signalling pathway, it remained possible that these proteins were affecting Notch signalling indirectly. For instance, it is possible that these proteins are damaging or killing the cells such that they cannot differentiate. If these proteins are in fact downregulating Notch signalling directly, then expressing downstream Notch target genes should suppress the defects caused by Apx and Mpeg1 expression in the wing. Previous studies have utilised Notch *enhancer of split*, *E(spl)*, target genes to this end (Ligoxygakis *et al.* 1999; Escudero *et al.* 2003; Xie *et al.* 2012). For example, co-expression of *E(spl)mβ* in the wing disc using *A9-Gal4* significantly alleviated the thickened vein phenotype caused by the ectopic expression of a neomorphic form of Uif, a transmembrane protein containing EGF-like repeats (Xie *et al.* 2012).
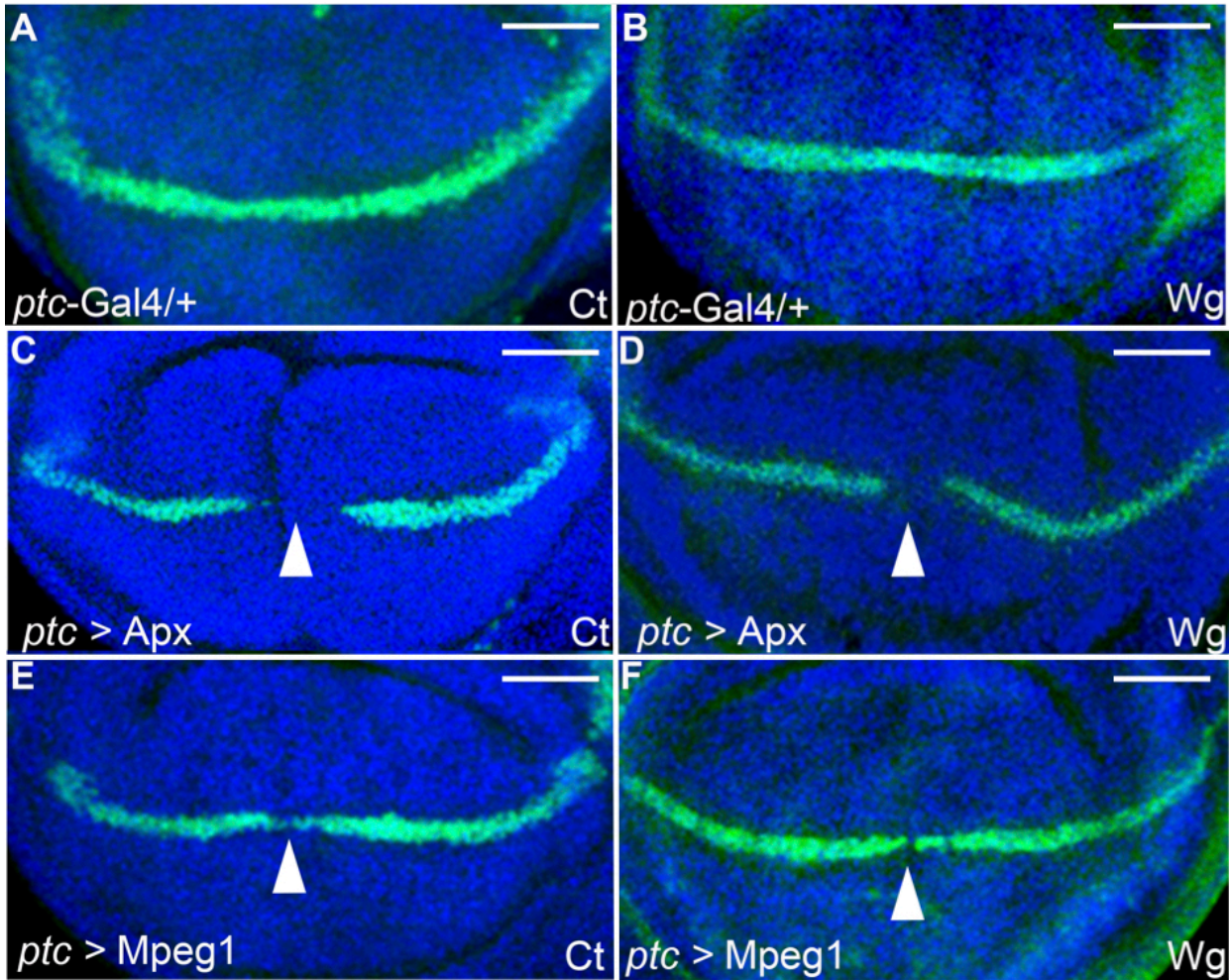
Figure 3.6. Apx and Mpeg1 expression disrupt Notch target genes at the wing margin.

Cut (Ct) and Wingless (Wg) are Notch targets that are expressed in a two-to-five-cell layer at the wing margin of the larval wing disc (green). (A) Ct expression is seen in the wing margin cells of the wing disc in *ptc*-Gal4 control larvae. (B) Wg has a matching expression pattern to Ct in the wing margin cells of the larval wing disc. *Apx* expression causes a break in Ct (C) and Wg (D) expression in the *ptc*-Gal4 domain (all breaks in expression indicated by the white arrowhead). This break was observed in all wing discs that were examined. (E) *ptc>Mpeg1* larvae showed a break and thinning of the Ct expression domain at the wing margin (40% penetrance). (F) *Mpeg1* also caused a break in Wg expression in the *ptc*-Gal4 domain in approximately 30% of wing discs examined. All wing discs were also stained with DAPI (blue) to mark the cell nuclei. Each panel is representative of n ≥ 15 wing discs for each genotype. Scale bars represent 50μM. Experiments carried out jointly with Lauren Forbes Beadle.

Expression of *E(spl)mβ* with *ptc*-Gal4 caused a partial loss of the anterior crossvein, consistent with previous studies (Figure 3.7B, Ligoxygakis *et al.* 1999). Remarkably, expression of *E(spl)mβ* in the *ptc>Apx* flies significantly restored the wing tissue at the margin (n≥20, Figure 3.7F, compared to E). The intervein tissue loss in the proximal region of the *ptc>Apx* flies was also restored with the co-expression of *E(spl)mβ* (Figure 3.7F), but the anterior crossvein remains absent, consistent with the phenotype of the control (*ptc>E(spl)mβ*, Figure 3.7B). Taken together, these results suggest that Apx reduces Notch signalling when expressed in *Drosophila*.

Incongruously, expression of *E(spl)mβ* in the *ptc>Mpeg1* flies failed to suppress the wing margin tissue loss (Figure 3.7D, compared to C). Thus, *E(spl)mβ* is not sufficient to suppress the wing notching phenotype in *Mpeg1*-expressing flies. This suggests that despite their functional similarity, Mpeg1 and Apx differ slightly in their effects on specific Notch targets in this context.

3.4. Discussion

Taken together, the data presented here show that non-*Drosophila* MACPF proteins cannot function in the same manner as Tsl for embryonic patterning. However, these data reveal the surprising finding that Apx and Mpeg1, two ancient and related MACPF proteins, may have functional similarity, identified here through their common ability to affect the highly conserved Notch signalling pathway.

Apx and Mpeg1 overexpression caused phenotypes including wing notches and ectopic bristles, similar to phenotypes caused by Notch loss of function mutations. The apparently contradictory effects of Apx expression on bristle formation, with both duplications and loss observed concurrently, can potentially be explained by the requirement for Notch signalling at multiple stages during bristle development (Shellenbarger and Mohler 1978; Hartenstein and Posakony 1990). Notch signalling is required during SOP specification via lateral inhibition, and later during asymmetric cell division for cell fate specification in each bristle lineage. Reduced Notch signaling during SOP specification increases the number of SOP cells, thereby increasing total bristle number. Alternatively, increased Notch activity during SOP specification, results in less SOP cells and therefore less bristles (de Celis and García-Bellido 1994a). When Notch signalling is reduced during asymmetric
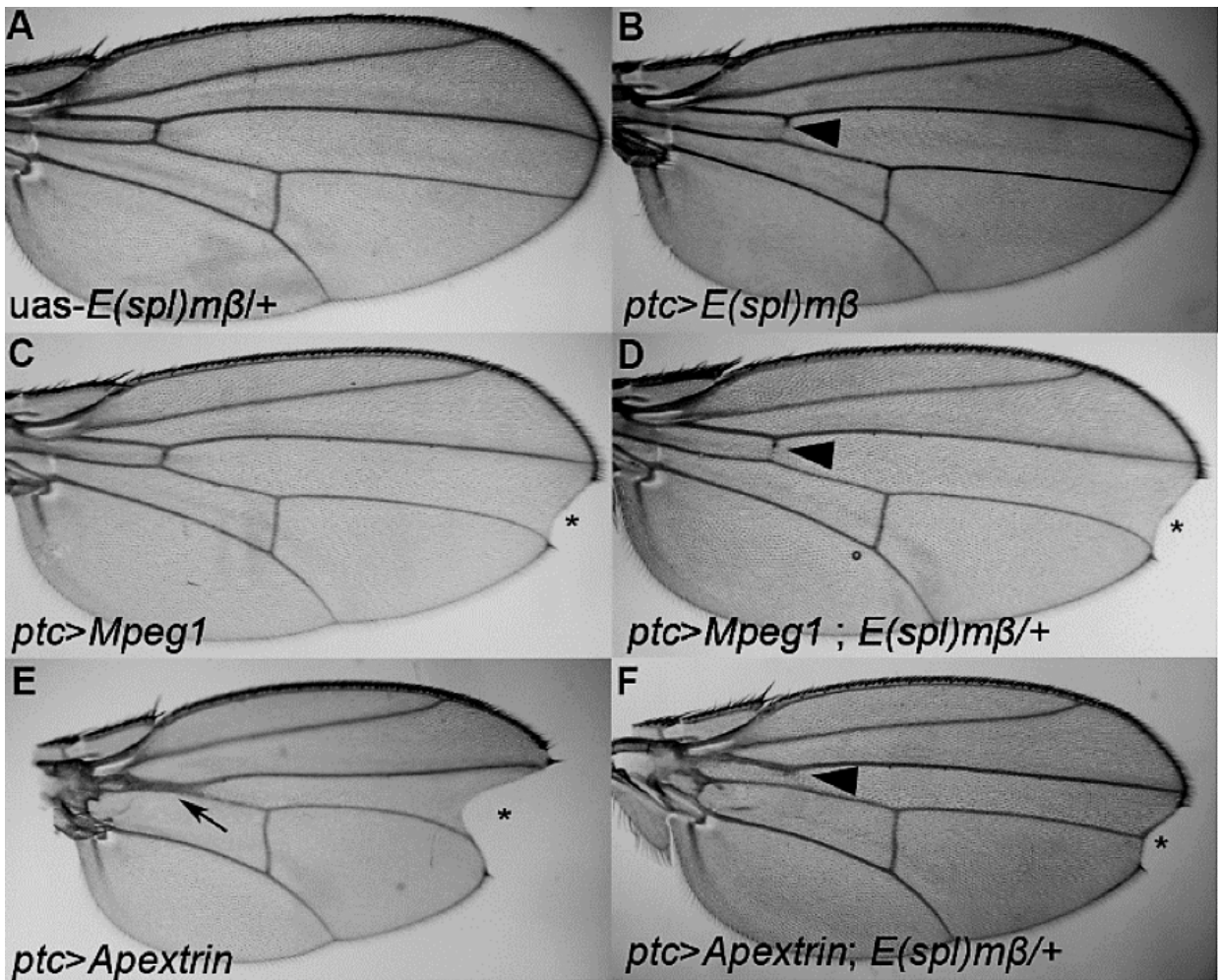
Figure 3.7. Expression of the Notch target gene *E(spl)mβ* rescues Apx-induced defects in the *Drosophila* wing.

(A) A control wing from the UAS-*E(spl)mβ*/+ strain. (B) Expression of *E(spl)mβ* with the *ptc*-Gal4 driver produced wings with a wild type margin but a reduced anterior crossvein (arrowhead). (C) *ptc>Mpeg1* caused tissue loss at the wing margin in the *ptc* domain (asterisk). (D) Expression of *E(spl)mβ* in the *ptc>Mpeg1* flies did not rescue the tissue loss at the wing margin and these wings also had the partial anterior crossvein loss. (E) *ptc>Apx* wings have a more severe loss of tissue at the wing margin (asterisk) as well as vein fusion in the proximal region (arrow). (F) *E(spl)mβ* expression in *ptc>Apx* wings considerably rescued both the tissue loss (asterisk) and the vein fusion phenotypes. Intervein tissue between the L3 and L4 wing veins was restored in these flies and the amount of tissue lost at the margin was significantly reduced. The loss of the anterior crossvein was still observed in these wings (arrowhead). Each image represents ≥ 15 adult wings. Experiments carried out jointly with Lauren Forbes Beadle.

cell division, all daughter cells adopt an internal fate, thereby appearing as an absence of bristles. Reduced Notch activity can therefore cause both bristle duplications and bristle loss (Hartenstein and Posakony 1990), which is consistent with the complex bristle phenotype observed in *ptc>Apx* flies. This was further supported by the increase in Senseless-positive cells observed in the *ptc>Apx* wing discs, which showed that more SOP cells were specified as a result of Apx expression.

Moreover, Apx- and Mpeg1-induced overexpression phenotypes were enhanced in the N^1 mutant background. Two Notch target genes, Ct and Wg, were also disrupted by Apx and Mpeg1 expression in the *ptc* domain of *Drosophila* wing discs. The Apx, but not the Mpeg1, overexpression defects could be partially rescued by expression of a downstream target of the Notch signalling pathway. Taken together these results suggest that Apx and Mpeg1 act to downregulate Notch signalling when expressed in *Drosophila*, but that there are potentially some differences in where they act.

The endogenous role of Apx has been difficult to ascertain given the challenges around conducting functional *in vivo* studies in sea urchins. It is known that the Notch receptor is localised specifically on the basolateral membrane of cells during multiple stages of *Lytechinus variegatus* sea urchin development (Sherwood and McClay 1997). On the other hand, Apx is apically localised in these cells (Haag *et al.* 1999). It is therefore possible that Apx acts to downregulate Notch signalling specifically at the apical membrane, which maintains high Notch signalling at the basal membrane, where it acts in embryonic development.

There are many ways that Notch signalling is regulated, including proteolytic processing, post-translational modifications such as ubiquitination and glycosylation, and recycling and trafficking by the endocytic machinery of the receptor and its ligands (Figure 3.8; reviewed in Bray 2006). For instance, when Notch receptor trafficking or recycling by the endocytic machinery is disrupted, Notch can be prevented from reaching the cell membrane, which is the normal site of the ligand-induced proteolytic cleavage required for the release of Notch intracellular domain (N^{ICD}), which then translocates to the nucleus to activate transcription (reviewed in Bray 2006).
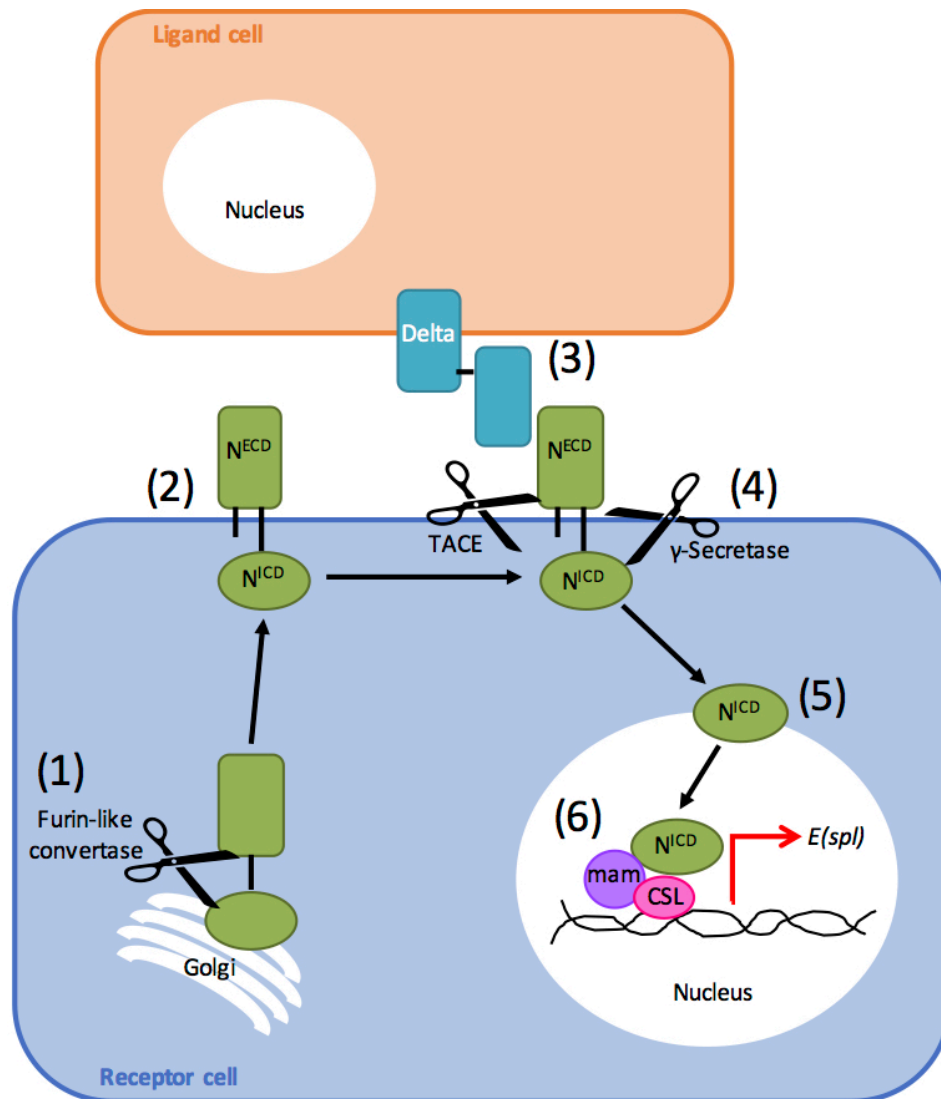
Figure 3.8. Notch signalling in *Drosophila*.

The Notch receptor (green) undergoes multiple cleavage events and post-translational modifications during its maturation in the Golgi apparatus, where it is assembled into a heterodimer (1), before translocating to the cell membrane where it is available for signalling (2). Binding of the Notch ligand Delta (teal) or Serrate to the Notch receptor (3) induces a series of cleavage events of Notch first by TACE and then γ-Secretase (4). These cleavage events culminate in the release of the Notch intracellular domain (N^{ICD}) which translocates to the nucleus (5). N^{ICD} binding releases transcriptional repressors, and in conjunction with CSL (CBF, Su(H) and Lag-1, pink) and mastermind (mam, purple) activates the expression of Notch target genes such as the *E(spl)* genes (6). Notch target gene expression regulates multiple developmental processes including lateral inhibition, cell boundary specification and lineage decisions. Modified from Sainson & Harris, 2007.

Interestingly, recent studies on the MACPF-related pore-forming CDC proteins have revealed that the formation of pores by these proteins can trigger rapid endocytosis through membrane damage and calcium influx (Cassidy and O'Riordan 2013). This raises the possibility that Apx and Mpeg1 may be causing membrane disruption, thereby promoting the endocytosis of Notch, and thus reducing the amount of Notch receptor available at the membrane for signalling. This parallels the current model proposed for Tsl function in the terminal patterning system. In this model Tsl acts on the embryonic membrane to induce secretion of the active Trk ligand from the embryo into the extracellular space, where Trk can then bind to the Torso receptor and activate the downstream signalling pathway required for correct specification of the termini.

Previous studies have shown the crucial role of endocytosis in Notch signalling (Gupta-Rossi *et al.* 2004; Sakata *et al.* 2004; and reviewed in Sala *et al.* 2012; Palmer and Deng 2015), and various mutants of endocytic machinery proteins show phenotypes indicative of negative regulation of this pathway. A particular example of this negative regulation is illustrated by *lethal (2) giant discs (lgd)* which acts cell autonomously to regulate Notch signalling (Childress *et al.* 2006). Lgd belongs to an as-yet-uncharacterised protein family, members of which possess one C2 domain and four repeats of a DM14 domain of unknown function (Jaekel and Klein 2006). Loss-of-function mutants of *lgd* cause an increase in Notch signalling, and the Lgd protein interacts with the endocytic machinery, suggesting that Lgd normally downregulates Notch signalling through the endocytosis and degradation of the full-length Notch receptor (Childress *et al.* 2006; Jaekel and Klein 2006; Troost *et al.* 2012). In line with these findings, weak overexpression of *lgd* in the wing results in loss of wing margin tissue and ectopic scutellar bristles (Jaekel and Klein 2006) and partial vein thickening (Troost *et al.* 2012), similar to the phenotypes observed for Apx and Mpeg1 overexpression.

A second example of this negative regulation involves the gamma-secretase-dependent cleavage of Notch, which is crucial for Notch activation and the release of the N^{ICD}. Once released, the N^{ICD} translocates to the nucleus, where it releases transcriptional repressors and aids in the activation of Notch target genes (Figure 3.8). Gamma-secretase is localised to the phagosome in both fly cells and murine macrophages throughout their maturation into phagolysosomes, where they play an essential role in the inflammatory response (Jutras *et al.* 2005). Recent work has shown that Mpeg1 is predominantly contained in

endosome-like vesicles that rapidly fuse with lysosomes in response to proinflammatory signals, such as TNF-α, in turn activating the NF-κB pathway (Xiong *et al.* 2017). Interestingly, Apextrin-like proteins in the lancelet (amphioxus) have also been implicated in NF-κB activation in response to bacterial infection (Huang *et al.* 2014). Perhaps when expressed in *Drosophila*, Mpeg1 and Apx are localised to the phagolysosome, where they disrupt the normal activity of this organelle, thereby also impacting Notch function.

Therefore, the effect of Apx and Mpeg1 on Notch signalling could be occurring via membrane disruption and the promotion of Notch endocytosis, thereby reducing the amount of Notch receptor available at the membrane for signalling. Alternatively, Mpeg1 and Apx could be localised to a specific organelle required for the proteolytic cleavage of Notch, such as the phagolysosome. For instance, Mpeg1 is an integral membrane protein that is specifically and rapidly incorporated into phagolysosomes in mammalian macrophages (Podack and Munson 2016). It is therefore possible that when Mpeg1 and Apx are expressed in the *Drosophila* wing disc, these proteins are incorporated into a related vesicle, thereby disrupting the cleavage event(s) of Notch and reducing the ability of cells to activate Notch signalling

While earlier work on Mpeg1 and Apx suggested developmental roles, it is important to note that recent functional studies have provided substantial support for antibacterial roles. Knockdown of *Mpeg1* in macrophage and MEF cell lines renders these cells incapable of preventing bacterial proliferation following infection (McCormack *et al.* 2013). In addition, ectopic expression of an RFP-tagged Mpeg1 in HeLa cells resulted in the clearance of bacteria from these cells within 24 hours of infection, which is consistent with Mpeg1 disrupting and killing bacterial cells (Fields *et al.* 2013). Moreover, knockout Mpeg1 mice quickly perish following methicillin-resistant *Staphylococcus aureus* and *Salmonella typhimurium* infection, due to systemic spreading of the bacteria (McCormack *et al.* 2015). Coupled with the fact that their control littermates are not killed by these pathogens, this suggests that Mpeg1 functions to clear intracellular bacterial infection (McCormack *et al.* 2015). This study also showed that Mpeg1 co-localises with bacteria in infected cells and forms pores on the bacterial membrane, as visualised using negative staining transmission electron microscopy. This pore-forming function of Mpeg1 facilitates the bactericidal activity of reactive oxygen and nitrogen species and other hydrolytic enzymes (McCormack *et al.* 2015). Subsequently, McCormack *et al.* (2016) have shown

94

that Mpeg1 also restricts the proliferation of the intracytosolic pathogen *Listeria monocytogenes*, potentially by preventing the acidification of *Listeria*-containing vacuoles, which deprives the bacteria of the conditions needed for vacuole escape into the cytosol, ultimately preventing its replication. Taken together, these studies provide substantial *in vivo* evidence of a lytic, bactericidal function for Mpeg1.

Furthermore, there is mounting evidence that Apx plays an important role in defence against bacterial infection, as differential expression occurs in response to infection or damage (Huang *et al.* 2007; Dheilly *et al.* 2011). At the moment, it is difficult to reconcile the evidence for Mpeg1 and Apx as immunity effectors with the Notch phenotype caused by their expression in the *Drosophila* wing. One idea to reconcile these findings is that Apx and Mpeg1 act to disrupt cell membranes, promoting the rapid endocytosis of the Notch receptor, thereby reducing the amount of Notch available at the membrane for signalling. This model is compatible with these proteins having an additional lytic role as immune effectors. This is supported by the recent evidence that both the human MAC and perforin can have both lytic and non-lytic effects on cells in different contexts and concentrations.

Future experiments to confirm a role for Apx and Mpeg1 in Notch signalling are required. Now that a knockout mouse model for Mpeg1 has been generated (McCormack *et al.* 2015), it may be possible to examine these animals for defects in Notch signalling. Alternatively, there is a well-established mammalian cell culture model for Notch signalling pathway function, which has been used successfully to investigate the mammalian Notch ligands Delta-like 1 and 3 (Geffers *et al.* 2007). This system utilises a Notch-responsive luciferase reporter construct stably expressed in the mouse myogenic C2C12 cell line to measure Notch activation (Kato *et al.* 1996; Chapman *et al.* 2006; Geffers *et al.* 2007). Transfection of Mpeg1 or Apx into the Notch-expressing cell (in *cis*) or in a co-cultured cell line (in *trans*) could determine their ability to activate Notch signalling.

In conclusion, this study has identified a new putative function of the MACPF proteins Apx and Mpeg1 in Notch signalling. This work adds to the expanding knowledge of the distinct and diverse mechanisms by which MACPF proteins function in development and immunity. Associations between the Notch pathway and immunity and the role of MACPF proteins such as Apx and Mpeg1 in these processes is an exciting direction for future study.

Chapter 4: Characterisation of genes that interact with the *Drosophila* MACPF protein Torso-like

4.1. Introduction

Although Tsl is known to be essential for correct embryonic terminal patterning, the molecular mechanism by which Tsl acts in development is currently unclear (Savant-Bhonsale and Montell 1993; Johnson *et al.* 2017a). Moreover, Tsl is unique amongst MACPF proteins so far studied, in possessing a single MACPF domain without any other apparent functional domains. This is atypical of MACPF proteins which generally utilise various N- or C-terminal domains both to interact with other binding partners for oligomeric complex formation and for initial membrane interaction. Given the absence of any detectable accessory domains in Tsl, it is highly likely that a number of as yet unidentified protein-interaction partners are required for Tsl function. In addition, previous genetic screens to identify terminal patterning genes were designed such that only mutations that were zygotically homozygous viable were recovered (Nüsslein-Volhard *et al.* 1987). Therefore, any terminal patterning genes that have other essential developmental roles, such that mutations are homozygous zygotic lethal, remain to be identified. To surmount this difficulty, the Warr lab designed and conducted a genome-wide genetic suppressor screen to identify novel terminal patterning genes, including those that are essential for life (Johns *et al.* 2018).

The suppressor screen utilised the previously reported spliced cuticle phenotype that results from the ectopic expression of *tsl* in all follicle cells. This phenotype is due to ubiquitous Torso (Tor) activation and the subsequent loss of embryo segmentation caused by the expansion of the terminal regions (Savant-Bhonsale and Montell 1993, Figure 4.1). The principle of this screen was that if a particular gene is required for Tsl to activate Tor signalling, then halving the dosage of that gene could cause suppression of the spliced phenotype. As proof of principle, halving the dosage of *trk* suppressed the spliced phenotype from 100% to just 2% (Figure 4.1). The Bloomington Deficiency kit, a set of nearly contiguous, molecularly mapped chromosomal deletions spanning 98.4% of the *Drosophila* genome (Cook *et al.* 2012) was used to systematically halve the dosage of groups of genes at a time in a *tsl* overexpression background.

After screening 92% of the genome using this approach, 59 suppressor regions were
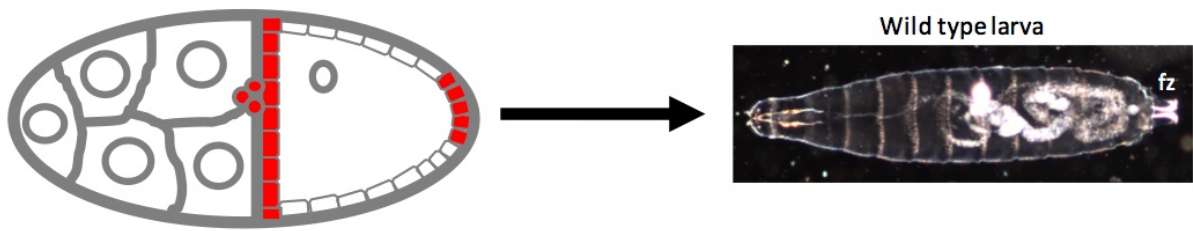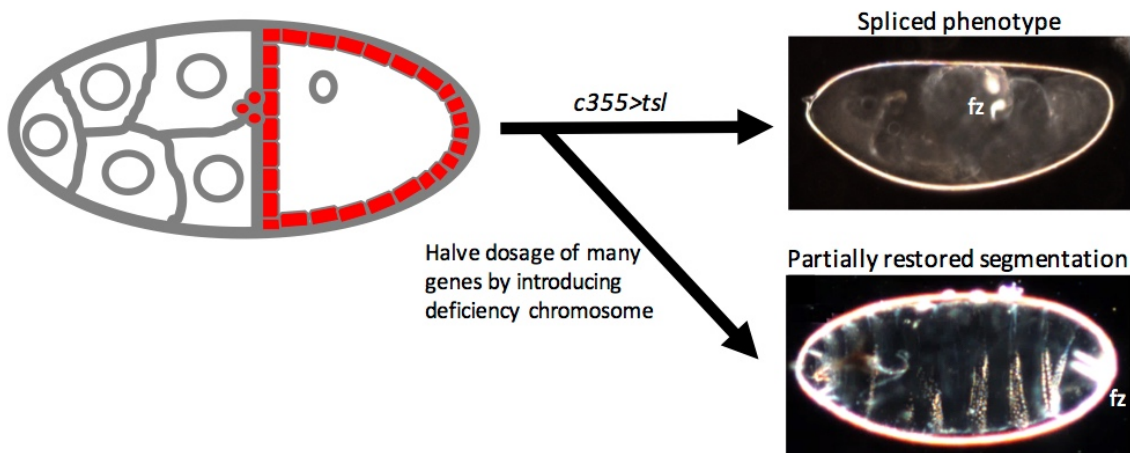
Figure 4.1. Genetic suppressor screen to identify novel terminal patterning genes.

(A) Tsl is expressed by a subpopulation of somatic follicle cells at the anterior and posterior poles of the oocyte (red), which leads to localised Torso (Tor) activation. This results in a wild type larva with eight abdominal denticle belts and well-defined terminal structures, most notable by the posterior filzkörper (fz). (B) Over-expression of *tsl* in all follicle cells using *c355*-Gal4 causes ubiquitous Tor activation and generates the spliced phenotype in which the central portions of the embryo develop terminal structures, most notable by the centralised filzkörper (fz). The suppressor screen involved halving the dosage of many genes at once by introducing individual deficiency chromosomes from the Bloomington Deficiency Kit into this background and looking for suppression of the spliced phenotype. This approach was validated by the strong suppression observed when the terminal patterning gene *trk* was halved in dosage using a null mutant (*trk*$^\Delta$).

confirmed, including 11 that contain known terminal class genes, further validating our screening approach (Johns *et al.* 2018). Of the remaining 48 suppressor regions, 29 were narrowed down to less than 15 genes through additional mapping with smaller available deficiency lines, and the causative suppressor gene was identified in six others. Two of these regions, corresponding to regions #35 and #54 in Johns *et al.* (2018), were chosen here for further investigation. Region 35 was mapped to a single gene called *Protein disulphide isomerase* (*Pdi*). Region 54 was mapped down to just two genes: an uncharacterised gene denoted as *CG13827* and *oo18 RNA-binding protein* (*orb*).

This chapter aimed to characterise the role of the confirmed candidate *Pdi* by seeking to understand whether *Pdi* interacts with Tsl and what specific role *Pdi* plays in terminal patterning. This chapter also aimed to determine which of the two genes remaining in candidate region 54 are required for terminal patterning and whether this gene interacts with Tsl.

4.2. Materials and Methods

4.2.1. Fly stocks, maintenance and crosses

w^{1118} (BL3605), *tubulin*-Gal4 (BL5138), *c355*-Gal4 (BL3750), *P{lacW}l(3)j2A2^{j2A2}/TM3* (here referred to as *Pdi^{j2A2}*; BL12090), *P{ovoD1-18}3L P{FRT(w^{hs})}2A/st^1 βTub85D^D ss^1 e^s/TM3* (for generating germline clones on 3, BL2139), *P{hsFLP}1, y^1 w^{1118}; Dr^{Mio}/TM3* (FLP source on X for clones on 3, BL7), *P{PZ}orb^{dec}/TM3* (BL10326), *P{EPgy2}orb^{EY08547}* (BL19931), *Mi{MIC}orb^{MI04761}/TM3* (BL37978) stocks were obtained from the Bloomington *Drosophila* Stock Centre. The following UAS-*RNAi* stocks were obtained from the Vienna *Drosophila* Resource Center: *CG13827* (GD24481), *Pdi* (GD23358). The *PBac{RB}CG13827^{e01415}* (*CG13827^{e01415}*) stock was obtained from Exelixis at Harvard Medical School. The screen line (*c355-Gal4; Gal80ts; UAS-tsl*) was generated and validated as described in Johns *et al.* (2018). All stocks were maintained on standard fly media (Appendix 1) in 30mL vials at 22°C with a 12-hour alternating light/dark cycle. Virgin females from the screen line (*c355-Gal4; Gal80ts; UAS-tsl*) were crossed with either heterozygous mutant males or males homozygous for RNAi constructs. All crosses involving the screen line were performed at 22°C and then shifted to 29°C approximately 92 hr after egg lay (h AEL). From each cross, at least 10 F1 females of the correct genotype were collected and placed in a vial containing apple juice agar supplemented with yeast

paste and allowed to mate with w^{1118} males. All other crosses were performed at 25°C, unless otherwise stated.

4.2.2. Cuticle preparations

Cuticle preparations were used to examine the phenotype of embryos, and were performed as previously described in Van der Meer (1977). Adults were allowed to lay on apple juice agar media supplemented with yeast paste for 24hr before being removed. Embryos were aged for a further 24hrs, before being collected and dechorionated in 50% (v/v) bleach, rinsed with distilled water, and mounted onto slides in a 1:1 (v/v) mixture of Hoyer's solution (Appendix 1) and lactic acid (BDH). Slides were incubated at 65°C overnight and visualised with dark field optics on a Leica DM LB compound microscope (with Leica DC300 camera).

4.2.3. cDNA synthesis and Reverse Transcription-PCR (RT-PCR)

Ten pairs of gravid ovaries were dissected from adult females and snap frozen before RNA was extracted using TRIsure reagent (Bioline) and treated with DNase (Promega) to remove genomic DNA. The Tetro cDNA Synthesis Kit (Bioline) was used to generate complementary DNA (cDNA) as per the manufacturer's protocol. Both oligo-dT and random hexamers were used to prime 5mg of RNA. GoTaq Flexi DNA Polymerase (Promega) was then used for RT-PCR using primers specific for *CG13827* (F-5'-GGAACTAGCCAAGCGATACG-3', R-5'-GTGAGATCCGAACGATGGAC-3'), *orb* (F-5'-GGATCGCACAAAATTGGAGT-3', R-5'-ACACGCTAAAGCTCCTGCAT-3'), and *tsl* (F-5'-TACCGCTCAATGACAACTCG-3', R- 5'-CACCACCCTCACCAAAACAT-3') as a control gene.

4.2.4. RNA *in situ* hybridisation

RNA *in situ* hybridisation on whole-mount dissected and fixed (4% paraformaldehyde in phosphate buffered saline) ovaries was performed using DIG-labelled sense and anti-sense RNA probes transcribed from pGEM-T Easy (Promega) clones of *CG13827* (544bp, primers as for RT-PCR, but amplified from ovary cDNA), *orb* (614bp, primers as for RT-PCR, but amplified from ovary cDNA), and *Pdi* (502bp, F-5'-CTCCTCCTCCTCCTCGGTCT-3', R-5'-GGACATGGCCAAGTACAAGC-3'), following standard protocols (Tomancak *et al.* 2002). In brief, probes were hybridised to ovaries overnight at 55°C and washed in hybridisation buffer (4x saline sodium citrate buffer, 50% v/v formamide, 0.1% v/v Tween-20, 50

mg/ml heparin) for 36 hr, before incubation with alkaline phosphatase conjugated anti-digoxygenin and colour development with 5-bromo-4-chloro-3-indolyl phosphate and nitro blue tetrazolium chloride. Following probe detection, individual egg chambers were dissected from ovaries and mounted on slides in 75% glycerol before imaging with differential interference contrast (DIC) optics on a Leica DM LB compound microscope.

4.2.5. Generation of germline clones

The Pdi^{j2A2} allele was recombined with $P\{FRT(w^{hs})\}$ at 79D-F to enable the use of the FLP-FRT dominant female sterile (DFS) technique (Perrimon 1998; reviewed in Selva and Stronach 2007) to generate germline clones of Pdi. Virgin females homozygous for $hsFLP$ on the X were crossed to ovo^{D1}, $FRT(w^{hs})$ males to generate males carrying both heat-shock FLP and $ovoD1$, $FRT(w^{hs})$ balanced over $TM3$ ($hs\text{-}FLP/y;+/+;ovo^{D1}$, $FRT(w^{hs})/TM3$). Ten to fifteen of these males were crossed to 30-40 virgin females carrying Pdi^{j2A2}, $FRT(w^{hs})$ balanced over $TM6B$ (+;+;Pdi^{j2A2}, $FRT(w^{hs})/TM6B$), and allowed to lay for 48 hours. Third instar larvae were heat-shocked at 37°C degrees for 1 hr on consecutive days (Day 5 and 6) and virgin females were collected and mated to w^{118} males. Only females in which recombination has occurred will have a homozygous mutant germline and be fertile (due to the loss of ovo^{D1}). Adults were allowed to lay on apple juice agar media supplemented with yeast paste for 24 hours. The embryos were aged for a further 24 hours before phenotypic examination was conducted as previously described (4.2.2).

4.2.6. Bioinformatics

The sequence of each CG13827 polypeptide was obtained from FlyBase (Gramates *et al.* 2017), release FB2014_01, and run using PSI-BLAST (Altschul *et al.* 1997), available through the NCBI platform, to identify related proteins and therefore predict biochemical function.

4.3. Results

4.3.1. Manipulation of maternal Pdi expression

Region 35 provided a strong consistent level of suppression, with the gain of multiple central segments (Johns *et al.* 2018). A P-element insertion in the first intron of Pdi (here named Pdi^{j2A2}), which generates a loss-of-function allele, also strongly suppressed the spliced phenotype and phenocopied the original deficiency well (Johns *et al.* 2018).

Expression of *Pdi* in the *Drosophila* ovary was investigated here using RNA *in situ* hybridisation, which showed strong ubiquitous expression in all three cells types: the nurse cells, follicle cells and the oocyte (Figure 4.2A).

Pdi proteins catalyse the formation of intramolecular disulphide bridges and are thought to stabilise the tertiary and quaternary structures of many secreted and cell surface proteins (Freedman 1989; Noiva and Lennarz 1992). They reside in the lumen of the endoplasmic reticulum (ER) in mammals (Freedman 1979), plants (Roden *et al.* 1982; Andreae *et al.* 1988), and *Drosophila* (McKay *et al.* 1995). It is thought that this family of proteins has a broad role in protein folding, and may even have many non-ER localisations and functions (Turano *et al.* 2002; Ellgaard and Helenius 2003). Genes encoding proteins involved in protein trafficking and secretory pathways are of particular interest because they may play a part in transporting proteins required for Tor signalling. Alternatively, they may also be involved in the transport and secretion of Tsl itself.

A *Pdi RNAi* line expressed in the screening background (*i.e.* follicle cells) failed to suppress the spliced phenotype (Figure 4.2B), suggesting that Pdi is acting in the nurse cells or oocyte, not the follicle cells at least for the suppression phenotype. However, it is also possible that this RNAi line is not knocking down *Pdi* expression enough to generate suppression. This is particularly likely given the high level of *Pdi* expression present in the ovary. To further investigate this, *Pdi RNAi* was expressed ubiquitously with *tubulin-Gal4* as this would recapitulate the early lethality observed for whole fly mutants, if the RNAi line is reasonably efficient. Whilst this resulted in considerable lethality at the late larval and pupal stages, some individuals made it to adulthood, suggesting that *Pdi* knockdown is incomplete with this RNAi line.

Ideally, the best way to confirm that *Pdi* is a genuine terminal patterning gene would be to examine the embryos laid by homozygous mutant mothers for terminal patterning defects. However, as *Pdi* is homozygous zygotic lethal, it is not possible to obtain homozygous mutant mothers in order to examine maternally-deficit embryos. Thus, the germline clone technique (Perrimon 1998; Selva and Stronach 2007) was utilised to generate a homozygous mutant germline within an otherwise heterozygous background, thereby allowing mutant embryos to be laid. The effect of removing the maternal contribution on embryonic development can thus be assayed. However, when this experiment was
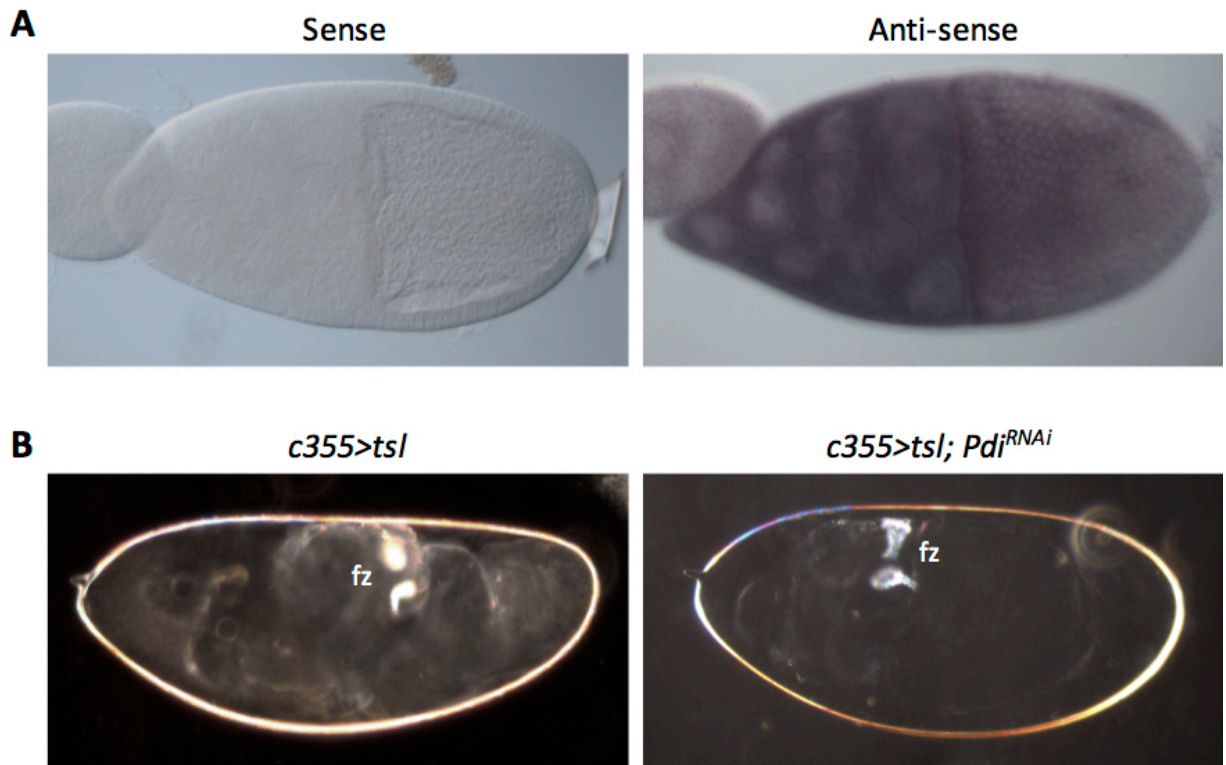
Figure 4.2. *Pdi* expression is ubiquitous in the wild type ovary.

(A) RNA *in situ* hybridisation of whole mount ovaries was performed using DIG-labelled RNA probes corresponding to the sense and anti-sense strands of *Pdi*. *Pdi* expression is ubiquitous and very strong throughout the egg chamber, in all three cell types. (B) Expression of *Pdi GD RNAi* in the follicle cells failed to suppress the ectopic *tsl* phenotype, as indicated by the centralised filzkörper (fz). Anterior is to the left in all panels.

conducted, the resulting females did not lay any embryos, suggesting that Pdi is required for oogenesis, and that the tissue is not viable without Pdi. Therefore, this method was not useful here.

4.3.2. Candidate region 54

This region contains only two genes – *CG13827* and *orb* (*oo18 RNA-binding protein*). *CG13827* is an uncharacterised gene, although bioinformatic analysis suggests that it is a peroxisomal biogenesis factor (Pex11 family) important for peroxisome division. *orb* is required for both antero-posterior and dorso-ventral patterning during *Drosophila* oogenesis, by regulating the translation of localised mRNAs such as *oskar* and *gurken* (Christerson and McKearin 1994; Chang *et al.* 1999; Chang *et al.* 2001). It is therefore possible that *orb* is also involved in terminal patterning specification, and perhaps this has not been discovered previously due to the severe defects in the other patterning systems and earlier developmental defects observed in *orb* mutants.

To investigate whether both genes are indeed expressed in the ovary, reverse transcriptase (RT)-PCR and RNA *in situ* hybridisation experiments were performed. Ovary-specific RT-PCR showed that both genes were expressed in the ovary (Figure 4.3A). RNA *in situ* hybridisation showed strong *orb* expression in the oocyte and weaker expression in the nurse cells (Figure 4.3B), which is consistent with previously reported expression patterns (Christerson and McKearin 1994; Lantz and Schedl 1994). The *in situ* for *CG13827* was unfortunately not successful, and was therefore uninformative (data not shown). Taken together, both genes remained candidates after the expression analysis.

To identify which of these two genes is responsible for the observed suppression in this region, available known loss-of-function and potential loss-of-function mutant alleles, such as transposable element lines, were tested to see whether these too could suppress the ectopic *tsl* phenotype. Three such lines were obtained for *orb*: a PZ *P*-element inserted in the 5'UTR (exon 2) of the two female-specific transcripts; an *EPgy P*-element also inserted in the 5'UTR but closer to the start codon than the PZ *P*-element; and a *Minos* element inserted in intron 2 of the same two female-specific transcripts (Figure 4.4). It has been shown in *Drosophila* that *orb* has two different types of transcripts and polypeptides: longer ovarian/early-embryonic transcripts and polypeptides, and shorter male/larval-
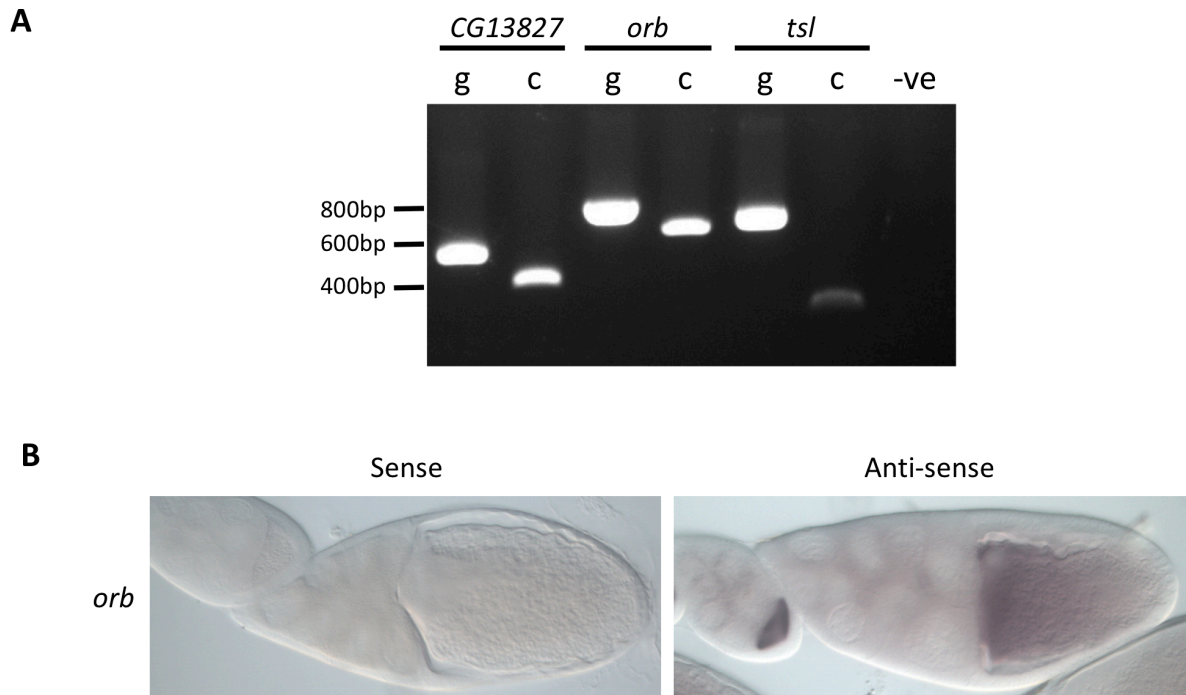
Figure 4.3. Candidate gene expression in wild type ovaries.

(A) RT-PCR of the candidate genes in region 54 using cDNA (lane 'c') from wild type ovaries indicates that both *CG13827* and *orb* are expressed. Genomic DNA (lane 'g') was tested concurrently as a positive control for each primer set since primers are intron-spanning. For *CG13827* expect bands of 544bp (g) and 425bp (c), and for *orb* expect bands of 729bp (g) and 614bp (c). Primers specific to *tsl* were used as a positive control for cDNA synthesis as this gene is known to be expressed in the ovary at relatively low levels: expect bands of 668bp (g) and 320bp (c). (B) RNA *in situ* hybridisation of whole-mount ovaries was performed using DIG-labelled RNA probes corresponding to the sense and anti-sense *orb* strands. *orb* expression can be seen strongly in the oocyte, with some weaker expression in the nurse cells. Anterior is to the left in all panels.
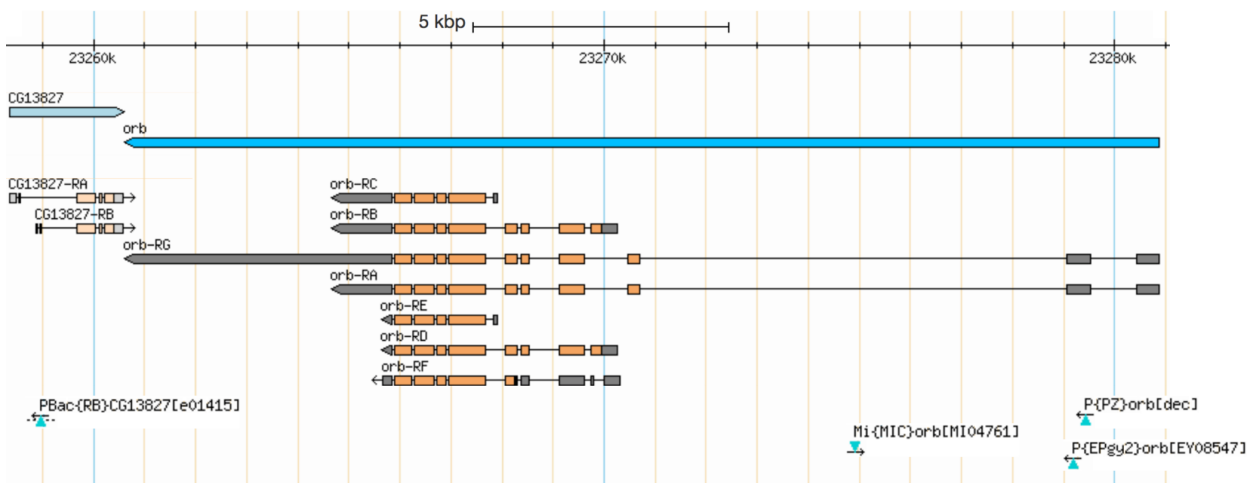
Figure 4.4. Genomic view of suppressor region 54, showing the current gene models and locations of transposable element insertions for candidates *CG132827* and *orb*.

A *piggyBac* element inserted in intron 2 of *CG13827,* isoform B, is a splice trap. The *PZ* P-element in the 5'UTR (exon 2) of *orb*'s female-specific transcripts (isoforms A & G) is a previously characterised strong loss-of-function allele called *orb^{dec}* (Christerson and McKearin 1994). An *EPgy* P-element is also inserted in the *orb* 5'UTR but closer to the start codon than the *PZ* P-element. A *Minos* element is inserted in the middle of the long intron 2 of the same two female-specific transcripts. Orange blocks are coding exons, grey blocks are UTRs, and lines are introns. Figure adapted from FlyBase (http://flybase.org/).

pupal transcripts and polypeptides (Lantz *et al.* 1992). The mutants known to cause patterning defects are those affecting the maternal/early embryonic transcripts. This is the case with the PZ allele, which is a strong loss-of-function allele (*orb^{dec}*) that produces little to no mRNA transcript and therefore no protein in homozygous females (Christerson and McKearin 1994). None of these *orb* alleles were able to suppress the spliced phenotype (Figure 4.5B-D). Since, the male/larval-pupal transcripts cannot functionally replace maternal transcript loss, any male transcripts still present in the three transposable element lines are unlikely to be masking suppression of the spliced phenotype caused by the loss of maternal *orb*. This suggests that *orb* is not the gene responsible for suppression in this region. By a process of elimination, this implicates *CG13827* as the causative gene in this suppressor region.

As an uncharacterised gene, there were less reagents available for *CG13827*, and none had been validated. Nevertheless, a line was obtained that contained a *piggyBac* element inserted in intron 2 of *CG13827*, which is predicted to act as a splice trap (Figure 4.4). This line did not suppress the spliced phenotype (Figure 4.5E). However, it remains possible that the *piggyBac* insertion does not remove enough CG13827 function to cause suppression of the spliced phenotype. A *CG13827 RNAi* line expressed in the screening background (*i.e.* follicle cells) also failed to suppress the spliced phenotype (Figure 4.5F), suggesting that if *CG13827* is the suppressor gene in this region, it is acting in the nurse cells or oocyte, not the follicle cells. One caveat to this, however, is that this *CG13827* RNAi may not have caused sufficient knockdown to generate a phenotype. Nevertheless, taken together, this data suggests that *CG13827* is most likely the causative gene in this suppressor region.

4.4. Discussion

4.4.1. Pdi is a new terminal patterning gene

Pdi encodes one of the two major protein disulphide isomerases in *Drosophila*. That it was such a strong suppressor in our screen suggests Pdi plays an important role in terminal patterning. This remains true despite the difficulties we encountered when trying to demonstrate that terminal patterning defects occur in embryos laid by mothers with homozygous mutant ovaries.
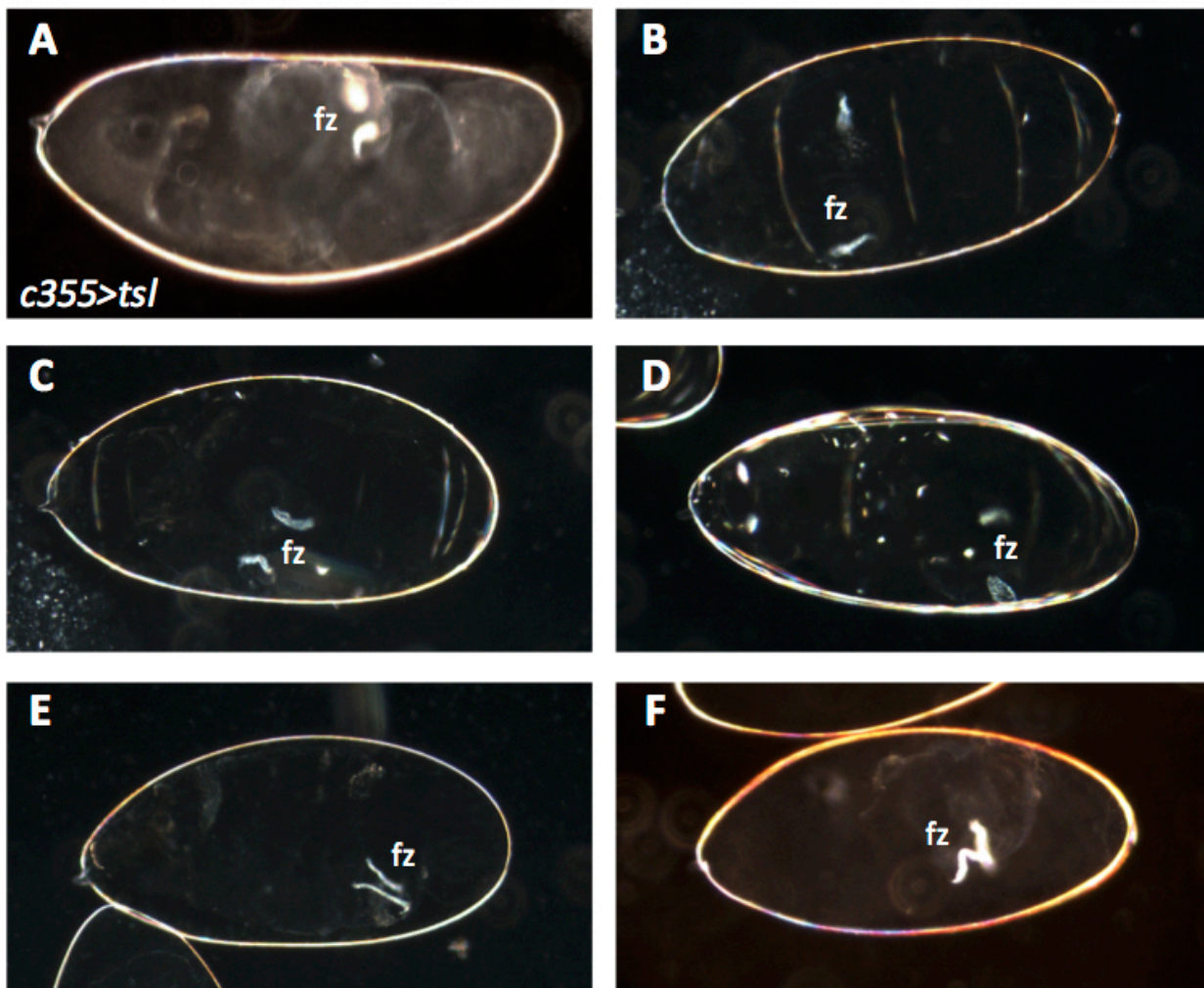
Figure 4.5. Testing available mutant alleles and RNAi reagents of *orb* and *CG13827* for suppression of spliced.

(A) Over-expression of *tsl* in all follicle cells using *c355*-Gal4 generated the spliced phenotype in which the central portions of the embryo develop terminal structures, most notable by the centralised filzkörper (fz). (B-D) Loss-of function *orb* mutants were crossed into the screening background, and the embryos laid by the resulting F1 females were examined for suppression of the spliced phenotype. Neither the known loss-of-function allele, *orb^dec^* (B), nor two putative loss-of-function alleles, *orb^EY08547^* (C) and *orb^MI04761^* (D), suppressed the ectopic *tsl* phenotype. The putative loss-of-function allele for *CG13827*, *CG13287^e01415^*, was unable to suppress the ectopic *tsl* phenotype (E). Likewise, expression of *CG13827 GD RNAi* also failed to suppress the spliced phenotype (F). Anterior is to the left in all panels.

108

So, how might Pdi function in terminal patterning? One possibility comes about through parallels with the dorso-ventral patterning system. In this system, a Pdi-like protein called Windbeutel is required to traffic Pipe through the ovarian follicle cell ER, as part of localising the signal for dorso-ventral patterning (Sen *et al.* 1998). This suggests that Pdi may be required for the correct folding and/or transport of key components of the Tor signalling pathway, particularly Tsl which is produced exclusively by the terminal follicle cells. There is at least some evidence that Pdi does not work in the follicle cells to cause suppression, as Pdi RNAi was unable to suppress the ectopic *tsl* phenotype. However, it is also possible that this RNAi line is not knocking down *Pdi* expression enough to generate suppression. Nevertheless, even if Pdi is not required in the follicle cells for the suppression phenotype, it is still possible that Pdi and Tsl interact. It is possible that their interaction occurs in the perivitelline space after Tsl has departed the follicle cells, or at the embryonic plasma membrane where Tsl potentially acts to trigger Trk secretion (Johnson *et al.* 2015), or aids in the dimerisation and activation of Tor (Amarnath *et al.* 2017). In support of this, immunoprecipitation-mass spectrometry (IP-MS) experiments performed in our lab on S2 cells expressing Tsl-3xmyc-eGFP suggest an *in vivo* physical interaction between Tsl and Pdi (Daniel Bakopoulos, pers. comm.). Moreover, Pdi has been demonstrated to perturb the lytic activity of another MACPF protein, perforin, in *in vivo* mouse models (Tamang *et al.* 2009).

Alternatively, evidence from several protein-protein interaction (PPI) datasets suggest that Pdi physically interacts with several downstream members of the terminal patterning pathway. From the Transcription Factor-Gene interactions identified as part of modEncode project, Pdi was predicted to interact with Groucho, a transcriptional repressor that is derepressed by Tor activation (Paroush *et al.* 1997). In the BioGRID project, which used yeast systems to predict protein-protein interactions, Pdi was predicted to interact with both Rolled, the terminal component of the MAPK cascade, and twins, a B subunit of the protein phosphatase 2A, which was also a candidate gene identified in this screen. In support of this, Pdi is heavily enriched in the fusome and is actively transported into the oocyte, suggesting that it may act to regulate the signalling cascade downstream of Tor activation. Indeed, it is possible that Pdi is required at multiple levels of the terminal patterning pathway, and this may be why it was such a strong suppressor of the spliced phenotype in our screen.

4.4.2. *CG13827*: The last gene standing?

The two candidate genes in suppressor region 54 are both expressed in the ovary. None of the reagents available to reduce *orb* expression were able to recapitulate the suppression seen with the original deficiency, suggesting that *orb* is not the causative gene in this suppressor region. However, the one putative loss-of-function allele for *CG13827* also failed to suppress the spliced phenotype. It remains possible, though very unlikely, that *orb* is the suppressor gene in this region. Thus, *CG13827* appears to be the better candidate gene for causing the suppression seen in this screen region.

So, how might *CG13827* function in terminal patterning? Peroxisome function is increasingly recognised as being important for a range of physiological processes, ranging from lipid and fat metabolism to innate immunity and muscle function (Mast *et al.* 2015). Indeed, peroxisomes are important centres for a range of enzymatic activity and produce a plethora of signalling molecules required for normal cellular processes. It is not surprising therefore that peroxisome biogenesis disorders are lethal genetic conditions in humans, and have in fact been modelled in *Drosophila* (Mast *et al.* 2011; Faust *et al.* 2012). For the *Drosophila* terminal patterning system, it seems likely that CG13827 is required for the production and/or transport of one or more components of the Tor signalling cascade or even for components required for the activation of the Trk ligand.

In conclusion, this work has identified at least one new gene involved in *Drosophila* terminal pattering, *Pdi*, and most likely a second, *CG13927*. In the future, biochemical experiments may help elucidate what proteins Pdi is specifically interacting with in the terminal patterning system. In addition, further genetic experiments, particularly the generation of a loss-of-function mutant for *CG13827*, are required to determine what role CG13827 plays in the terminal patterning system.

Chapter 5: Final discussion and future directions

The majority of MACPF proteins functionally characterised to date are known to act in vertebrate immunity as pore-forming effectors at the cell membrane. However, a number of MACPF proteins have been shown to play important but poorly understood roles in embryonic and neural development. Moreover, it is becoming clear that MACPF proteins can disrupt membranes to cause non-lytic cellular effects through multiple signalling pathways (Benzaquen *et al.* 1994; Cole and Morgan 2003; Leslie and Mayor 2013). For example, sublytic concentrations of the MAC have been implicated in the cell cycle and cell proliferation, through both the mitogen-activated protein kinase (MAPK) and phosphoinositide 3-kinase (PI3K) pathways (Rus *et al.* 1997; Niculescu *et al.* 1999; Qiu *et al.* 2012). Thus, some of the findings of this thesis are discussed in this context.

5.1. MACPF proteins appear to control multiple developmental signalling pathways

Tsl has now been shown to function in at least three separate developmental pathways in addition to Tor signalling, and these will now be discussed here. Recent work from our lab has shown a second role for maternal Tsl in *Drosophila* development, which is independent of its role in terminal patterning. Females homozygous for a *tsl* null mutant lay embryos with a ventral cuticle hole phenotype due to defects in mesoderm invagination (Johnson *et al.* 2017b). More specifically, the ventral cell apices fail to constrict in a coordinated manner, resulting in incomplete ventral furrow formation. This causes a portion of the presumptive posterior mesoderm to be left behind on the surface of the embryo. The key signalling pathway required for initiating apical constriction involves the secreted protein Folded Gastrulation (Fog), the G-protein coupled receptor (GPCR) Mesoderm-invagination signal transducer (Mist), the GTPase Rho1 and its guanine nucleotide exchange factor RhoGEF2 (Costa *et al.* 1994; Barrett *et al.* 1997; Manning *et al.* 2013). Indeed, *tsl* mutants appear to phenocopy *fog* mutants, which also display uncoordinated ventral cell apical constriction, leading to a disorganised ventral furrow, and the failure to complete invagination (Costa *et al.* 1994; Oda and Tsukita 2001). Furthermore, *tsl* mutants are not only sensitive to *RhoGEF2* gene dosage, but also suppress the effects of ectopic *fog* expression. Taken together, Johnson *et al.* (2017b) showed that Tsl regulates the extracellular activity of Fog to synchronise and coordinate the cell shape changes necessary for timely ventral morphogenesis in *Drosophila* gastrulation.

In other recent work from our lab, Tsl was shown to play an important role in *Drosophila* immune system development (Forbes-Beadle *et al.* 2016). In *tsl* mutants there is a dramatic reduction in the number of circulating immune cells, which normally act to clear pathogens by phagocytosis (Forbes-Beadle *et al.* 2016). Rather than acting as a traditional MACPF immune effector, Tsl therefore appears to function in the development of the immune cells themselves. The platelet-derived growth factor and vascular endothelial growth factor receptor (Pvr) pathway, is a good candidate for Tsl to work with here (Forbes-Beadle *et al.* 2016). Like Tor, Pvr is a receptor tyrosine kinase (RTK), and this pathway plays a crucial role in *Drosophila* hemocyte proliferation, differentiation and survival (Heino *et al.* 2001; Munier *et al.* 2002; Brückner *et al.* 2004). In addition, *pvr* mutant embryos have a significantly reduced number of immune cells compared with wildtype embryos (Brückner *et al.* 2004), which is not dissimilar to that observed for *tsl* mutants (Forbes-Beadle *et al.* 2016). Recent work from our lab suggests that Tsl may function upstream of Ras in Pvr-mediated hemocyte proliferation (Lauren Forbes-Beadle, pers. comm.). Given that Tsl is present in the larval hemolymph (Henstridge *et al.* 2018), it is likely that this is the origin of Tsl required for hemocyte development.

Dr. Michelle Henstridge in our group showed that Tsl works with the insulin signalling pathway to regulate growth and developmental timing in the PG (Henstridge *et al.* 2018). For example, *tsl* null mutants closely resemble mutants with impaired insulin signalling in several key biochemical and physiological characteristics. Tsl genetically interacts with the insulin signalling pathway, as shown by the observation that larvae mutant for both *tsl* and *dilps 2, 3*, and *5*, had a similar developmental delay to *dilp 2-3[A]*, *dilp5[3]* mutants alone (Henstridge *et al.* 2018). Furthermore, *tsl* null larvae have been shown to accumulate both dILP2 and dILP5 in their insulin-producing cells (IPCs) during larval development, and also have increased *dilp2/5* expression, both of which are characteristic of a systemic reduction in insulin signalling (Henstridge *et al.* 2018). In addition, this same work has shown that Tsl is specifically required in the PG to regulate growth and developmental timing, and is present in the larval hemolymph. Taken together, this supports a role for Tsl in regulating systemic insulin signalling, thereby affecting larval growth and developmental timing.

Collectively, these findings have confirmed that Tsl is not just a specialised cue for Tor signalling, but has a broader significance for developmental cell signalling in multiple

tissues throughout *Drosophila* development. In each of the developmental contexts found so far to require Tsl function, it is likely that Tsl interacts with different signalling pathways, not only with multiple RTKs but also with a GPCR.

This thesis adds to these findings by suggesting that two poorly understood MACPF proteins (Apx and Mpeg1) regulate the Notch signalling pathway. Apx and Mpeg1 expression in *Drosophila* resulted in phenotypes that resembled Notch loss-of-function mutants. Genetic interaction experiments further supported the finding that these phenotypes were due to a downregulation of the Notch pathway. In summary, developmental MACPF proteins have so far been shown to regulate at least three RTKs, one GPCR and the Notch pathway. How a MACPF protein might work with so many different types of receptors and in such diverse developmental contexts remains to be elucidated.

5.2.   How could MACPF proteins be regulating membrane receptors and their signalling pathways in development?

One mechanism that has been suggested is a role in the secretion of growth factors, which will be discussed here. At least two lytic MACPF proteins (*e.g.* MAC and Streptolysin O) have been shown to induce the secretion of inflammatory cytokines (Hansch *et al.* 1987) and several developmental growth factors (Benzaquen *et al.* 1994) when present at sublytic concentrations. For example, sublytic MAC attack regulates interleukin-1β (IL-1β), interleukin-6 (IL-6) and interleukin-8 (IL-8) release from human lung epithelial cells (Triantafilou *et al.* 2013). IL-1β secretion has also been observed from macrophages and liposomes exposed to the pore-forming protein gasdermin D (Acosta *et al.* 1996; He *et al.* 2015; Evavold *et al.* 2018). At these sublytic levels, pore-formation results in membrane damage and subsequent remodelling and repair through lysosome release rather than cell lysis (Tan *et al.* 2016).

In addition, platelet-derived growth factor (PDGF) has been shown to be released from both human umbilical vein endothelial cells and bovine aortic endothelial cells following sublytic MAC attack (Benzaquen *et al.* 1994). This very rapid release of PDGF suggests that secretion of this growth factor occurs as a direct result of MAC pore-formation and membrane damage. Sublytic levels of the MAC have also been shown to regulate the

release of vascular endothelial growth factor (VEGF) in ARPE-19 retinal pigment epithelium cells that are under oxidative stress (Thurman *et al.* 2009). In a subsequent study, VEGF secretion was triggered quite rapidly in response to MAC attack, and appeared to involve the Ca^{2+}-mediated activation of Ras and Erk, which are both components of the MAPK signalling pathway (Kunchithapautham and Rohrer 2011).

It is important to note that these data are from *in vitro* models, and that the pore-induced release of growth factors in *in vivo* models has not yet been established. On the contrary, at least one developmental MAPCF protein, *Drosophila* Tsl, has been shown to regulate growth factor activity *in vivo*. However, molecular characterisation of the developmental MACPF proteins is almost entirely absent, and so it remains unclear whether they function in a similar manner to their immunity counterparts, through pore-formation and membrane disruption.

Recent work from our lab demonstrated that Trk cleavage occurs independently of Tsl, as Trk cleavage products were unaffected in a *tsl* mutant background (Henstridge *et al.* 2014). In addition, two related proteases, Furin 1 and Furin 2, act in a redundant manner inside the oocyte to cleave Trk prior to its secretion (Johnson *et al.* 2015). Given that Tsl accumulates at the embryonic plasma membrane (Mineo *et al.* 2015), but is not present inside the oocyte, this makes it highly unlikely that Tsl is involved in the intracellular cleavage of Trk. Johnson *et al.* (2015) has also shown that levels of a fluorescently tagged N-terminal Trk reporter (which mimics cleaved Trk) in the perivitelline space were substantially reduced at the embryo termini in *tsl* mutants. Taken together, these data suggest a model whereby Tsl acts on the embryonic plasma membrane to promote the localised secretion of Trk via a pore-forming or membrane-damaging mechanism (Johnson *et al.* 2015).

This is complemented by further work from our lab which has shown that Tsl works with the insulin signalling pathway to regulate growth and developmental timing in the PG (Henstridge *et al.* 2018). In particular, *tsl* null larvae have been shown to accumulate both dILP2 and dILP5 in their IPCs during larval development, which suggests that the regulated secretion of dILPs is perturbed in the absence of Tsl.

The evidence presented earlier regarding Tsl function in development, coupled with the tractability of *Drosophila* as a model, suggests that Tsl is the ideal *in vivo* system to investigate the secretion model of developmental MACPF function in the future. In particular, the dynamics of Trk trafficking and secretion could be monitored in embryos in real time using fluorescently-tagged proteins. Similarly, Ca^{2+} influx can also be assayed *in vivo* using fluorescent calcium indicators like GCaMP3. If Tsl is required in the embryo to promote Trk secretion via membrane damage and remodelling, it is possible that the delivery of a genuine cytolytic pore-former such as Streptolysin O into the perivitelline space would rescue the terminal patterning defects observed in *tsl* null mutants. Similarly, if Tsl is required during larval development for regulating dILP secretion, then it is possible that artificially stimulating dILP secretion would rescue the developmental timing and growth defects observed in *tsl* null mutants (Henstridge *et al.* 2018). Moreover, by conducting biophysical and biochemical analyses on purified Tsl it may be possible to determine whether it is capable of pore-formation and/or membrane disruption. Similar efforts with at least some of the vertebrate developmental MACPF proteins would also go a long way in increasing our understanding of their mechanism of action.

5.3. Final conclusions

Together with the recent evidence from other MACPF proteins, these findings emphasise the diverse and complex ways that MACPF proteins can function in development through interactions with multiple signalling pathways. Perhaps different concentrations and the different cellular/developmental contexts enables the non-lytic cell-signalling role as opposed to lytic pore-formation. Future experiments will further facilitate the elucidation of the mechanism of action used by developmental MACPF proteins. In addition, as part of a search for Tsl signalling pathways, this thesis identified two neuropeptide receptors, PdfR and AkhR, as novel regulators of growth in the *Drosophila* PG.

References

Acosta, JA, Benzaquen, LR, Goldstein, DJ, Tosteson, MT, Halperin, JA (1996) The transient pore formed by homologous terminal complement complexes functions as a bidirectional route for the transport of autocrine and paracrine signals across human cell membranes. *Molecular Medicine* **2**, 755-65.

Adams, NC, Tomoda, T, Cooper, M, Dietz, G, Hatten, ME (2002) Mice that lack astrotactin have slowed neuronal migration. *Development* **129**, 965-72.

Agrawal, T, Sadaf, S, Hasan, G (2013) A genetic RNAi screen for IP_3/Ca^{2+} coupled GPCRs in *Drosophila* identifies the PdfR as a regulator of insect flight. *PLoS Genetics* **9**, e1003849.

Alaña, L, Sesé, M, Cánovas, V, Punyal, Y, Fernández, Y, Abasolo, I, de Torres, I, Ruiz, C, Espinosa, L, Bigas, A, y Cajal, SR, Fernández, PL, Serras, F, Corominas, M, Thomson, TM, Paciucci, R (2014) Prostate Tumor OVerexpressed-1 (PTOV1) down-regulates HES1 and HEY1 notch targets genes and promotes prostate cancer progression. *Molecular Cancer* **13**, 74.

Aleshin, AE, Schraufstatter, IU, Stec, B, Bankston, LA, Liddington, RC, DiScipio, RG (2012) Structure of complement C6 suggests a mechanism for initiation and unidirectional, sequential assembly of membrane attack complex (MAC). *Journal of Biological Chemistry* **287**, 10210-22.

Altschul, SF, Madden, TL, Schaffer, AA, Zhang, J, Zhang, Z, Miller, W, Lipman, DJ (1997) Gapped BLAST and PSI-BLAST: a new generation of protein database search programs. *Nucleic Acids Research* **25**, 3389-402.

Amarnath, S, Stevens, LM, Stein, DS (2017) Reconstitution of Torso signaling in cultured cells suggests a role for both Trunk and Torso-like in receptor activation. *Development* **144**, 677-686.

Ampleford, EJ, Steel, CG (1985) Circadian control of a daily rhythm in hemolymph ecdysteroid titer in the insect *Rhodnius prolixus* (Hemiptera). *General and Comparative Endocrinology* **59**, 453-9.

Anderluh, G, Kisovec, M, Krasevec, N, Gilbert, RJ (2014) Distribution of MACPF/CDC proteins. *Subcellular Biochemistry* **80**, 7-30.

Andreae, M, Blankenstein, P, Zhang, YH, Robinson, DG (1988) Towards the subcellular localization of plant prolyl hydroxylase. *European Journal of Cell Biology* **47**, 181-192.

Arias, AM (2008) *Drosophila melanogaster* and the Development of Biology in the 20th Century. In '*Drosophila*: Methods and Protocols.' (Ed. C Dahmann.) pp. 1-25. (Humana Press: Totowa, NJ)

Awad, TA, Truman, JW (1997) Postembryonic development of the midline glia in the CNS of *Drosophila*: proliferation, programmed cell death, and endocrine regulation. *Developmental Biology* **187**, 283-97.

Barrett, K, Leptin, M, Settleman, J (1997) The Rho GTPase and a putative RhoGEF mediate a signaling pathway for the cell shape changes in *Drosophila* gastrulation. *Cell* **91**, 905-15.

Barry, KC, Abed, M, Kenyagin, D, Werwie, TR, Boico, O, Orian, A, Parkhurst, SM (2011) The *Drosophila* STUbL protein Degringolade limits HES functions during embryogenesis. *Development* **138**, 1759-69.

Baumbach, J, Xu, Y, Hehlert, P, Kuhnlein, RP (2014) *Galphaq*, *Ggamma1* and *Plc21C* control *Drosophila* fat body storage. *Journal of Genetics and Genomics* **41**, 283-92.

Bayly-Jones, C, Bubeck, D, Dunstone, MA (2017) The mystery behind membrane insertion: a review of the complement membrane attack complex. *Philosophical Transactions of the Royal Society of London B: Biological Sciences* **372**,

Bednářová, A, Kodrík, D, Krishnan, N (2013) Unique roles of glucagon and glucagon-like peptides: Parallels in understanding the functions of adipokinetic hormones in stress responses in insects. *Comparative Biochemistry and Physiology, Part A: Molecular & Integrative Physiology* **164**, 91-100.

Belvin, MP, Zhou, H, Yin, JCP (1999) The *Drosophila dCREB2* gene affects the circadian clock. *Neuron* **22**, 777-87.

Benzaquen, LR, Nicholson-Weller, A, Halperin, JA (1994) Terminal complement proteins C5b-9 release basic fibroblast growth factor and platelet-derived growth factor from endothelial cells. *Journal of Experimental Medicine* **179**, 985-92.

Berkowicz, SR, Giousoh, A, Bird, PI (2017) Neurodevelopmental MACPFs: The vertebrate astrotactins and BRINPs. *Seminars in Cell & Developmental Biology*

Bharucha, KN, Tarr, P, Zipursky, SL (2008) A glucagon-like endocrine pathway in *Drosophila* modulates both lipid and carbohydrate homeostasis. *Journal of Experimental Biology* **211**, 3103-10.

Bischof, J, Björklund, M, Furger, E, Schertel, C, Taipale, J, Basler, K (2013) A versatile platform for creating a comprehensive UAS-ORFeome library in *Drosophila*. *Development* **140**, 2434-42.

Bischof, J, Maeda, RK, Hediger, M, Karch, F, Basler, K (2007) An optimized transgenesis system for *Drosophila* using germ-line-specific ΦC31 integrases. *Proceedings of the National Academy of Sciences of the USA* **104**, 3312-7.

Blumenthal, R, Millard, PJ, Henkart, MP, Reynolds, CW, Henkart, PA (1984) Liposomes as targets for granule cytolysin from cytotoxic large granular lymphocyte tumors. *Proceedings of the National Academy of Sciences of the USA* **81**, 5551-5.

Böhni, R, Riesgo-Escovar, J, Oldham, S, Brogiolo, W, Stocker, H, Andruss, BF, Beckingham, K, Hafen, E (1999) Autonomous control of cell and organ size by CHICO, a *Drosophila* homolog of vertebrate IRS1-4. *Cell* **97**, 865-75.

Bradfield, JY, Lee, Y-H, Keeley, LL (1991) Cytochrome P450 family 4 in a cockroach: molecular cloning and regulation by regulation by hypertrehalosemic hormone. *Proceedings of the National Academy of Sciences of the USA* **88**, 4558-62.

Bray, SJ (2006) Notch signalling: a simple pathway becomes complex. *Nature Reviews Molecular Cell Biology* **7**, 678-89.

Bray, SJ, Takada, S, Harrison, E, Shen, S-C, Ferguson-Smith, AC (2008) The atypical mammalian ligand Delta-like homologue 1 (Dlk1) can regulate Notch signalling in *Drosophila*. *BMC Developmental Biology* **8**, 11.

Britton, JS, Edgar, BA (1998) Environmental control of the cell cycle in *Drosophila*: nutrition activates mitotic and endoreplicative cells by distinct mechanisms. *Development* **125**, 2149-58.

Brogiolo, W, Stocker, H, Ikeya, T, Rintelen, F, Fernandez, R, Hafen, E (2001) An evolutionarily conserved function of the *Drosophila* insulin receptor and insulin-like peptides in growth control. *Current Biology* **11**, 213-21.

Brönner, G, Jäckle, H (1991) Control and function of terminal gap gene activity in the posterior pole region of the *Drosophila* embryo. *Mechanisms of Development* **35**, 205-11.

Browne, KA, Blink, E, Sutton, VR, Froelich, CJ, Jans, DA, Trapani, JA (1999) Cytosolic delivery of granzyme B by bacterial toxins: evidence that endosomal disruption, in addition to transmembrane pore formation, is an important function of perforin. *Molecular and Cellular Biology* **19**, 8604-15.

Brückner, K, Kockel, L, Duchek, P, Luque, CM, Rørth, P, Perrimon, N (2004) The PDGF/VEGF receptor controls blood cell survival in *Drosophila*. *Developmental Cell* **7**, 73-84.

Burns, JS, Abdallah, BM, Guldberg, P, Rygaard, J, Schrøder, HD, Kassem, M (2005) Tumorigenic heterogeneity in cancer stem cells evolved from long-term cultures of telomerase-immortalized human mesenchymal stem cells. *Cancer Research* **65**, 3126-35.

Caldwell, PE, Walkiewicz, M, Stern, M (2005) Ras activity in the *Drosophila* prothoracic gland regulates body size and developmental rate via ecdysone release. *Current Biology* **15**, 1785-95.

Casali, A, Casanova, J (2001) The spatial control of Torso RTK activation: a C-terminal fragment of the Trunk protein acts as a signal for Torso receptor in the *Drosophila* embryo. *Development* **128**, 1709-15.

Casanova, J, Furriols, M, McCormick, CA, Struhl, G (1995) Similarities between trunk and spatzle, putative extracellular ligands specifying body pattern in *Drosophila*. *Genes & Development* **9**, 2539-44.

Casanova, J, Struhl, G (1989) Localized surface activity of *torso*, a receptor tyrosine kinase, specifies terminal body pattern in *Drosophila*. *Genes & Development* **3**, 2025-38.

Casanova, J, Struhl, G (1993) The *torso* receptor localizes as well as transduces the spatial signal specifying terminal body pattern in *Drosophila*. *Nature* **362**, 152-5.

Cassidy, SK, O'Riordan, MX (2013) More than a pore: the cellular response to cholesterol-dependent cytolysins. *Toxins (Basel)* **5**, 618-36.

Chang, JS, Tan, L, Schedl, P (1999) The *Drosophila* CPEB homolog, Orb, is required for oskar protein expression in oocytes. *Developmental Biology* **215**, 91-106.

Chang, JS, Tan, L, Wolf, MR, Schedl, P (2001) Functioning of the *Drosophila orb* gene in *gurken* mRNA localization and translation. *Development* **128**, 3169-77.

Chapman, G, Liu, L, Sahlgren, C, Dahlqvist, C, Lendahl, U (2006) High levels of Notch signaling down-regulate Numb and Numblike. *The Journal of Cell Biology* **175**, 535-540.

Chen, C, Jack, J, Garofalo, RS (1996) The *Drosophila* insulin receptor is required for normal growth. *Endocrinology* **137**, 846-56.

Chia, J, Yeo, KP, Whisstock, JC, Dunstone, MA, Trapani, JA, Voskoboinik, I (2009) Temperature sensitivity of human perforin mutants unmasks subtotal loss of cytotoxicity, delayed FHL, and a predisposition to cancer. *Proceedings of the National Academy of Sciences of the USA* **106**, 9809-14.

Childress, JL, Acar, M, Tao, C, Halder, G (2006) Lethal giant discs, a novel C2-domain protein, restricts notch activation during endocytosis. *Current Biology* **16**, 2228-33.

Choi, C, Cao, G, Tanenhaus, AK, McCarthy, EV, Jung, M, Schleyer, W, Shang, Y, Rosbash, M, Yin, JCP, Nitabach, MN (2012) Autoreceptor control of peptide/neurotransmitter corelease from PDF neurons determines allocation of circadian activity in *Drosophila*. *Cell Reports* **2**, 332-44.

Christerson, LB, McKearin, DM (1994) *orb* is required for anteroposterior and dorsoventral patterning during *Drosophila* oogenesis. *Genes & Development* **8**, 614-28.

Christesen, D, Yang, YT, Somers, J, Robin, C, Sztal, T, Batterham, P, Perry, T (2017) Transcriptome analysis of *Drosophila melanogaster* third instar larval ring glands points to novel functions and uncovers a cytochrome p450 required for development. *G3 (Bethesda)* **7**, 467-479.

Chung, BY, Kilman, VL, Keath, JR, Pitman, JL, Allada, R (2009) The GABA$_A$ receptor RDL acts in peptidergic PDF neurons to promote sleep in *Drosophila*. *Current Biology* **19**, 386-90.

Cole, DS, Morgan, BP (2003) Beyond lysis: how complement influences cell fate. *Clinical Science (London)* **104**, 455-66.

Colombani, J, Bianchini, L, Layalle, S, Pondeville, E, Dauphin-Villemant, C, Antoniewski, C, Carre, C, Noselli, S, Leopold, P (2005) Antagonistic actions of ecdysone and insulins determine final size in *Drosophila*. *Science* **310**, 667-70.

Cook, RK, Christensen, SJ, Deal, JA, Coburn, RA, Deal, ME, Gresens, JM, Kaufman, TC, Cook, KR (2012) The generation of chromosomal deletions to provide extensive coverage and subdivision of the *Drosophila melanogaster* genome. *Genome Biology* **13**, R21.

Costa, M, Wilson, ET, Wieschaus, E (1994) A putative cell signal encoded by the *folded gastrulation* gene coordinates cell shape changes during *Drosophila* gastrulation. *Cell* **76**, 1075-89.

Cote, M, Menager, MM, Burgess, A, Mahlaoui, N, Picard, C, Schaffner, C, Al-Manjomi, F, Al-Harbi, M, Alangari, A, Le Deist, F, Gennery, AR, Prince, N, Cariou, A, Nitschke, P, Blank, U, El-Ghazali, G, Menasche, G, Latour, S, Fischer, A, de Saint Basile, G (2009) Munc18-2 deficiency causes familial hemophagocytic lymphohistiocytosis type 5 and impairs cytotoxic granule exocytosis in patient NK cells. *Journal of Clinical Investigation* **119**, 3765-73.

Cullen, SP, Brunet, M, Martin, SJ (2010) Granzymes in cancer and immunity. *Cell Death and Differentiation* **17**, 616-23.

D'Angelo, ME, Dunstone, MA, Whisstock, JC, Trapani, JA, Bird, PI (2012) Perforin evolved from a gene duplication of MPEG1, followed by a complex pattern of gene gain and loss within *Euteleostomi*. *BMC Evolutionary Biology* **12**, 59.

Dalton, HE, Denton, D, Foot, NJ, Ho, K, Mills, K, Brou, C, Kumar, S (2011) *Drosophila* Ndfip is a novel regulator of Notch signaling. *Cell Death and Differentiation* **18**, 1150-60.

Danielsen, ET, Moeller, ME, Rewitz, KF (2013) Nutrient signaling and developmental timing of maturation. *Current Topics in Developmental Biology* **105**, 37-67.

Danielsen, ET, Moeller, ME, Yamanaka, N, Ou, Q, Laursen, JM, Soenderholm, C, Zhuo, R, Phelps, B, Tang, K, Zeng, J, Kondo, S, Nielsen, CH, Harvald, EB, Faergeman, NJ, Haley, MJ, O'Connor, KA, King-Jones, K, O'Connor, MB, Rewitz, KF (2016) A *Drosophila* genome-wide screen identifies regulators of steroid hormone production and developmental timing. *Developmental Cell* **37**, 558-70.

David, E, Tanguy, A, Pichavant, K, Moraga, D (2005) Response of the Pacific oyster *Crassostrea gigas* to hypoxia exposure under experimental conditions. *FEBS Journal* **272**, 5635-52.

de Celis, JF, García-Bellido, A (1994a) Modifications of the Notch function by *Abruptex* mutations in *Drosophila melanogaster*. *Genetics* **136**, 183-94.

de Celis, JF, García-Bellido, A (1994b) Roles of the *Notch* gene in *Drosophila* wing morphogenesis. *Mechanisms of Development* **46**, 109-22.

Dheilly, NM, Haynes, PA, Bove, U, Nair, SV, Raftos, DA (2011) Comparative proteomic analysis of a sea urchin (*Heliocidaris erythrogramma*) antibacterial response revealed the involvement of apextrin and calreticulin. *Journal of Invertebrate Pathology* **106**, 223-9.

Di Cara, F, King-Jones, K (2016) The circadian clock Is a key driver of steroid hormone production in *Drosophila*. *Current Biology*

Dietzl, G, Chen, D, Schnorrer, F, Su, K-C, Barinova, Y, Fellner, M, Gasser, B, Kinsey, K, Oppel, S, Scheiblauer, S, Couto, A, Marra, V, Keleman, K, Dickson, BJ (2007) A genome-wide transgenic RNAi library for conditional gene inactivation in *Drosophila*. *Nature* **448**, 151-6.

DiScipio, RG, Linton, SM, Rushmere, NK (1999) Function of the factor I modules (FIMS) of human complement component C6. *Journal of Biological Chemistry* **274**, 31811-8.

Dourmashkin, RR, Deteix, P, Simone, CB, Henkart, P (1980) Electron microscopic demonstration of lesions in target cell membranes associated with antibody-dependent cellular cytotoxicity. *Clinical and Experimental Immunology* **42**, 554-60.

Dubowy, C, Sehgal, A (2017) Circadian rhythms and sleep in *Drosophila melanogaster*. *Genetics* **205**, 1373-1397.

Dudkina, NV, Spicer, BA, Reboul, CF, Conroy, PJ, Lukoyanova, N, Elmlund, H, Law, RH, Ekkel, SM, Kondos, SC, Goode, RJ, Ramm, G, Whisstock, JC, Saibil, HR, Dunstone, MA (2016) Structure of the poly-C9 component of the complement membrane attack complex. *Nature Communications* **7**, 10588.

Duncan, EJ, Benton, MA, Dearden, PK (2013) Canonical terminal patterning is an evolutionary novelty. *Developmental Biology* **377**, 245-61.

Duncan, EJ, Johnson, TK, Whisstock, JC, Warr, CG, Dearden, PK (2014) Capturing embryonic development from metamorphosis: how did the terminal patterning signalling pathway of *Drosophila* evolve? *Current Opinion in Insect Science* **1**, 45-51.

Duvall, LB, Taghert, PH (2012) The circadian neuropeptide PDF signals preferentially through a specific adenylate cyclase isoform AC3 in M pacemakers of *Drosophila*. *PLoS Biology* **10**, e1001337.

Duvall, LB, Taghert, PH (2013) E and M circadian pacemaker neurons use different PDF receptor signalosome components in *Drosophila*. *Journal of Biological Rhythms* **28**, 239-48.

Edmondson, JC, Liem, RK, Kuster, JE, Hatten, ME (1988) Astrotactin: a novel neuronal cell surface antigen that mediates neuron-astroglial interactions in cerebellar microcultures. *Journal of Cell Biology* **106**, 505-17.

Ellgaard, L, Helenius, A (2003) Quality control in the endoplasmic reticulum. *Nature Reviews Molecular Cell Biology* **4**, 181-91.

Emery, IF, Bedian, V, Guild, GM (1994) Differential expression of *Broad-Complex* transcription factors may forecast tissue-specific developmental fates during *Drosophila* metamorphosis. *Development* **120**, 3275-87.

Emery, IF, Noveral, JM, Jamison, CF, Siwicki, KK (1997) Rhythms of *Drosophila period* gene expression in culture. *Proceedings of the National Academy of Sciences of the USA* **94**, 4092-6.

Escudero, LM, Wei, S-Y, Chiu, W-H, Modolell, J, Hsu, J-C (2003) Echinoid synergizes with the Notch signaling pathway in *Drosophila* mesothorax bristle patterning. *Development* **130**, 6305-16.

Esser, AF, Kolb, WP, Podack, ER, Muller-Eberhard, HJ (1979) Molecular reorganization of lipid bilayers by complement: a possible mechanism for membranolysis. *Proceedings of the National Academy of Sciences of the USA* **76**, 1410-4.

Evavold, CL, Ruan, J, Tan, Y, Xia, S, Wu, H, Kagan, JC (2018) The pore-forming protein gasdermin D regulates interleukin-1 secretion from living macrophages. *Immunity* **48**, 35-44 e6.

Faust, JE, Verma, A, Peng, C, McNew, JA (2012) An inventory of peroxisomal proteins and pathways in *Drosophila melanogaster*. *Traffic* **13**, 1378-92.

Feldmann, J, Callebaut, I, Raposo, G, Certain, S, Bacq, D, Dumont, C, Lambert, N, Ouachee-Chardin, M, Chedeville, G, Tamary, H, Minard-Colin, V, Vilmer, E, Blanche, S, Le Deist, F, Fischer, A, de Saint Basile, G (2003) Munc13-4 is essential for cytolytic granules fusion and is mutated in a form of familial hemophagocytic lymphohistiocytosis (FHL3). *Cell* **115**, 461-73.

Fields, KA, McCormack, R, de Armas, LR, Podack, ER (2013) Perforin-2 restricts growth of *Chlamydia trachomatis* in macrophages. *Infection and Immunity* **81**, 3045-54.

Fluiter, K, Opperhuizen, AL, Morgan, BP, Baas, F, Ramaglia, V (2014) Inhibition of the membrane attack complex of the complement system reduces secondary neuroaxonal loss and promotes neurologic recovery after traumatic brain injury in mice. *Journal of Immunology* **192**, 2339-48.

Forbes-Beadle, L, Crossman, T, Johnson, TK, Burke, R, Warr, CG, Whisstock, JC (2016) Development of the cellular immune system of *Drosophila* requires the membrane attack complex/perforin-like protein Torso-Like. *Genetics* **204**, 675-681.

Fosbrink, M, Niculescu, F, Rus, V, Shin, ML, Rus, H (2006) C5b-9-induced endothelial cell proliferation and migration are dependent on Akt inactivation of forkhead transcription factor FOXO1. *Journal of Biological Chemistry* **281**, 19009-18.

Freedman, RB (1979) How many distinct enzymes are responsible for the several cellular processes involving thiol-protein-disulfide interchange. *FEBS Letters* **97**, 201-210.

Freedman, RB (1989) Protein disulfide isomerase: multiple roles in the modification of nascent secretory proteins. *Cell* **57**, 1069-1072.

Freitag, CM, Lempp, T, Nguyen, TT, Jacob, CP, Weissflog, L, Romanos, M, Renner, TJ, Walitza, S, Warnke, A, Rujescu, D, Lesch, K-P, Reif, A (2016) The role of ASTN2 variants in childhood and adult ADHD, comorbid disorders and associated personality traits. *Journal of Neural Transmission (Vienna)* **123**, 849-58.

Froelich, CJ, Orth, K, Turbov, J, Seth, P, Gottlieb, R, Babior, B, Shah, GM, Bleackley, RC, Dixit, VM, Hanna, W (1996) New paradigm for lymphocyte granule-mediated cytotoxicity. Target cells bind and internalize granzyme B, but an endosomolytic agent is

necessary for cytosolic delivery and subsequent apoptosis. *Journal of Biological Chemistry* **271**, 29073-9.

Furriols, M, Casali, A, Casanova, J (1998) Dissecting the mechanism of torso receptor activation. *Mechanisms of Development* **70**, 111-8.

Gáliková, M, Diesner, M, Klepsatel, P, Hehlert, P, Xu, Y, Bickmeyer, I, Predel, R, Kühnlein, RP (2015) Energy homeostasis control in *Drosophila* adipokinetic hormone mutants. *Genetics* **201**, 665-83.

Gáliková, M, Klepsatel, P, Xu, Y, Kühnlein, RP (2017) The obesity-related Adipokinetic hormone controls feeding and expression of neuropeptide regulators of *Drosophila* metabolism. *European Journal of Lipid Science and Technology* **119**, 1600138.

Geffers, I, Serth, K, Chapman, G, Jaekel, R, Schuster-Gossler, K, Cordes, R, Sparrow, DB, Kremmer, E, Dunwoodie, SL, Klein, T, Gossler, A (2007) Divergent functions and distinct localization of the Notch ligands DLL1 and DLL3 *in vivo*. *Journal of Cell Biology* **178**, 465-76.

Gibbens, YY, Warren, JT, Gilbert, LI, O'Connor, MB (2011) Neuroendocrine regulation of *Drosophila* metamorphosis requires TGFβ/Activin signaling. *Development* **138**, 2693-703.

Gilbert, LI, Rybczynski, R, Warren, JT (2002) Control and biochemical nature of the ecdysteroidogenic pathway. *Annual Review of Entomology* **47**, 883-916.

Glessner, JT, Wang, K, Cai, G, Korvatska, O, Kim, CE, Wood, S, Zhang, H, Estes, A, Brune, CW, Bradfield, JP, Imielinski, M, Frackelton, EC, Reichert, J, Crawford, EL, Munson, J, Sleiman, PM, Chiavacci, R, Annaiah, K, Thomas, K, Hou, C, Glaberson, W, Flory, J, Otieno, F, Garris, M, Soorya, L, Klei, L, Piven, J, Meyer, KJ, Anagnostou, E, Sakurai, T, Game, RM, Rudd, DS, Zurawiecki, D, McDougle, CJ, Davis, LK, Miller, J, Posey, DJ, Michaels, S, Kolevzon, A, Silverman, JM, Bernier, R, Levy, SE, Schultz, RT, Dawson, G, Owley, T, McMahon, WM, Wassink, TH, Sweeney, JA, Nurnberger, JI, Coon, H, Sutcliffe, JS, Minshew, NJ, Grant, SF, Bucan, M, Cook, EH, Buxbaum, JD, Devlin, B, Schellenberg, GD, Hakonarson, H (2009) Autism genome-wide copy number variation reveals ubiquitin and neuronal genes. *Nature* **459**, 569-73.

Glise, B, Jones, DL, Ingham, PW (2002) Notch and Wingless modulate the response of cells to Hedgehog signalling in the *Drosophila* wing. *Developmental Biology* **248**, 93-106.

Gough, NR (2016) Focus Issue: New insights in GPCR to G protein signaling. *Science Signaling* **9**, eg6.

Gramates, LS, Marygold, SJ, Santos, GD, Urbano, J-M, Antonazzo, G, Matthews, BB, Rey, AJ, Tabone, CJ, Crosby, MA, Emmert, DB, Falls, K, Goodman, JL, Hu, Y, Ponting, L, Schroeder, AJ, Strelets, VB, Thurmond, J, Zhou, P, Consortium, TF (2017) FlyBase at 25: looking to the future. *Nucleic Acids Research* **45**, D663-D671.

Green, EW, Fedele, G, Giorgini, F, Kyriacou, CP (2014) A *Drosophila* RNAi collection is subject to dominant phenotypic effects. *Nature Methods* **11**, 222-3.

Grillo, M, Furriols, M, de Miguel, C, Franch-Marro, X, Casanova, J (2012) Conserved and divergent elements in Torso RTK activation in *Drosophila* development. *Scientific Reports* **2**, 762.

Grimm, O, Sanchez Zini, V, Kim, Y, Casanova, J, Shvartsman, SY, Wieschaus, E (2012) Torso RTK controls Capicua degradation by changing its subcellular localization. *Development* **139**, 3962-8.

Grönke, S, Müller, G, Hirsch, J, Fellert, S, Andreou, A, Haase, T, Jäckle, H, Kühnlein, RP (2007) Dual lipolytic control of body fat storage and mobilization in *Drosophila*. *PLoS Biology* **5**, e137.

Gupta-Rossi, N, Six, E, LeBail, O, Logeat, F, Chastagner, P, Olry, A, Israël, A, Brou, C (2004) Monoubiquitination and endocytosis direct γ-secretase cleavage of activated Notch receptor. *Journal of Cell Biology* **166**, 73-83.

Haag, ES, Raff, RA (1998) Isolation and characterization of three mRNAs enriched in embryos of the direct-developing sea urchin *Heliocidaris erythrogramma*: evolution of larval ectoderm. *Development Genes and Evolution* **208**, 188-204.

Haag, ES, Sly, BJ, Andrews, ME, Raff, RA (1999) Apextrin, a novel extracellular protein associated with larval ectoderm evolution in *Heliocidaris erythrogramma*. *Developmental Biology* **211**, 77-87.

Hadders, MA, Beringer, DX, Gros, P (2007) Structure of C8α-MACPF reveals mechanism of membrane attack in complement immune defense. *Science* **317**, 1552-4.

Hansch, GM, Seitz, M, Betz, M (1987) Effect of the late complement components C5b-9 on human monocytes: release of prostanoids, oxygen radicals and of a factor inducing cell proliferation. *International Archives of Allergy and Applied Immunology* **82**, 317-20.

Hartenstein, V, Posakony, JW (1990) A dual function of the *Notch* gene in *Drosophila* sensillum development. *Developmental Biology* **142**, 13-30.

He, C, Imai, M, Song, H, Quigg, RJ, Tomlinson, S (2005) Complement inhibitors targeted to the proximal tubule prevent injury in experimental nephrotic syndrome and demonstrate a key role for C5b-9. *Journal of Immunology* **174**, 5750-7.

He, W-t, Wan, H, Hu, L, Chen, P, Wang, X, Huang, Z, Yang, Z-H, Zhong, C-Q, Han, J (2015) Gasdermin D is an executor of pyroptosis and required for interleukin-1β secretion. *Cell Research* **25**, 1285-98.

Heino, TI, Karpanen, T, Wahlstrom, G, Pulkkinen, M, Eriksson, U, Alitalo, K, Roos, C (2001) The *Drosophila* VEGF receptor homolog is expressed in hemocytes. *Mechanisms of Development* **109**, 69-77.

Heinzen, EL, Need, AC, Hayden, KM, Chiba-Falek, O, Roses, AD, Strittmatter, WJ, Burke, JR, Hulette, CM, Welsh-Bohmer, KA, Goldstein, DB (2010) Genome-wide scan of copy number variation in late-onset Alzheimer's disease. *Journal of Alzheimer's Disease* **19**, 69-77.

Heitzler, P, Haenlin, M, Ramain, P, Calleja, M, Simpson, P (1996) A genetic analysis of *pannier*, a gene necessary for viability of dorsal tissues and bristle positioning in *Drosophila*. *Genetics* **143**, 1271-86.

Helfrich-Förster, C (1995) The period clock gene is expressed in central nervous system neurons which also produce a neuropeptide that reveals the projections of circadian pacemaker cells within the brain of *Drosophila melanogaster*. *Proceedings of the National Academy of Sciences of the USA* **92**, 612-6.

Henstridge, MA, Aulsebrook, L, Koyama, T, Johnson, TK, Whisstock, JC, Tiganis, T, Mirth, CK, Warr, CG (2018) Torso-Like Is a component of the hemolymph and regulates the insulin signaling pathway in *Drosophila*. *Genetics* **208**, 1523-1533.

Henstridge, MA, Johnson, TK, Warr, CG, Whisstock, JC (2014) Trunk cleavage is essential for *Drosophila* terminal patterning and can occur independently of Torso-like. *Nature Communications* **5**, 3419.

Hilger, D, Masureel, M, Kobilka, BK (2018) Structure and dynamics of GPCR signaling complexes. *Nature Structural & Molecular Biology* **25**, 4-12.

Hill, SY, Weeks, DE, Jones, BL, Zezza, N, Stiffler, S (2012) ASTN1 and alcohol dependence: family-based association analysis in multiplex alcohol dependence families. *American Journal of Medical Genetics Part B: Neuropsychiatric Genetics* **159B**, 445-55.

Hori, K, Sen, A, Kirchhausen, T, Artavanis-Tsakonas, S (2011) Synergy between the ESCRT-III complex and Deltex defines a ligand-independent Notch signal. *Journal of Cell Biology* **195**, 1005-15.

Hrdlicka, L, Gibson, M, Kiger, A, Micchelli, CA, Schober, M, Schöck, F, Perrimon, N (2002) Analysis of twenty-four Gal4 lines in *Drosophila melanogaster*. *Genesis* **34**, 51-7.

Huang, G, Huang, S, Yan, X, Yang, P, Li, J, Xu, W, Zhang, L, Wang, R, Yu, Y, Yuan, S, Chen, S, Luo, G, Xu, A (2014) Two apextrin-like proteins mediate extracellular and intracellular bacterial recognition in amphioxus. *Proceedings of the National Academy of Sciences of the USA* **111**, 13469-74.

Huang, G, Liu, H, Han, Y, Fan, L, Zhang, Q, Liu, J, Yu, X, Zhang, L, Chen, S, Dong, M, Wang, L, Xu, A (2007) Profile of acute immune response in Chinese amphioxus upon *Staphylococcus aureus* and *Vibrio parahaemolyticus* infection. *Developmental & Comparative Immunology* **31**, 1013-23.

Hyun, S, Lee, Y, Hong, S-T, Bang, S, Paik, D, Kang, J, Shin, J, Lee, J, Jeon, K, Hwang, S, Bae, E, Kim, J (2005) *Drosophila* GPCR Han is a receptor for the circadian clock neuropeptide PDF. *Neuron* **48**, 267-78.

Idone, V, Tam, C, Andrews, NW (2008) Two-way traffic on the road to plasma membrane repair. *Trends in Cell Biology* **18**, 552-9.

Iga, M, Nakaoka, T, Suzuki, Y, Kataoka, H (2014) Pigment dispersing factor regulates ecdysone biosynthesis via *Bombyx* neuropeptide G protein coupled receptor-B2 in the prothoracic glands of *Bombyx mori*. *PLoS One* **9**, e103239.

Ikeya, T, Galic, M, Belawat, P, Nairz, K, Hafen, E (2002) Nutrient-dependent expression of insulin-like peptides from neuroendocrine cells in the CNS contributes to growth regulation in *Drosophila*. *Current Biology* **12**, 1293-300.

Ishino, T, Chinzei, Y, Yuda, M (2005) A *Plasmodium* sporozoite protein with a membrane attack complex domain is required for breaching the liver sinusoidal cell layer prior to hepatocyte infection. *Cellular Microbiology* **7**, 199-208.

Ishino, T, Yano, K, Chinzei, Y, Yuda, M (2004) Cell-passage activity is required for the malarial parasite to cross the liver sinusoidal cell layer. *PLoS Biology* **2**, E4.

Ito, K, Awano, W, Suzuki, K, Hiromi, Y, Yamamoto, D (1997) The *Drosophila* mushroom body is a quadruple structure of clonal units each of which contains a virtually identical set of neurones and glial cells. *Development* **124**, 761-71.

Jack, J, DeLotto, Y (1992) Effect of wing scalloping mutations on *cut* expression and sense organ differentiation in the *Drosophila* wing margin. *Genetics* **131**, 353-63.

Jaekel, R, Klein, T (2006) The *Drosophila* Notch inhibitor and tumor suppressor gene l*ethal (2) giant discs* encodes a conserved regulator of endosomal trafficking. *Developmental Cell* **11**, 655-69.

Jane-wit, D, Surovtseva, YV, Qin, L, Li, G, Liu, R, Clark, P, Manes, TD, Wang, C, Kashgarian, M, Kirkiles-Smith, NC, Tellides, G, Pober, JS (2015) Complement membrane attack complexes activate noncanonical NF-κB by forming an Akt[+] NIK[+] signalosome on Rab5^{+} endosomes. *Proceedings of the National Academy of Sciences of the USA* **112**, 9686-91.

Janka, G, zur Stadt, U (2005) Familial and acquired hemophagocytic lymphohistiocytosis. *Hematology American Society of Hematology Education Program* 82-8.

Jiménez, G, González-Reyes, A, Casanova, J (2002) Cell surface proteins Nasrat and Polehole stabilize the Torso-like extracellular determinant in *Drosophila* oogenesis. *Genes & Development* **16**, 913-8.

Johns, AR, Henstridge, MA, Saligari, MJ, Moore, KA, Whisstock, JC, Warr, CG, Johnson, TK (2018) Genome-wide screen for new components of the *Drosophila melanogaster* Torso receptor tyrosine kinase pathway. *G3 (Bethesda)*

Johnson, TK, Crossman, T, Foote, KA, Henstridge, MA, Saligari, MJ, Forbes Beadle, L, Herr, A, Whisstock, JC, Warr, CG (2013) Torso-like functions independently of Torso to regulate *Drosophila* growth and developmental timing. *Proceedings of the National Academy of Sciences of the USA*

Johnson, TK, Henstridge, MA, Herr, A, Moore, KA, Whisstock, JC, Warr, CG (2015) Torso-like mediates extracellular accumulation of Furin-cleaved Trunk to pattern the Drosophila embryo termini. *Nature Communications* **6**, 8759.

Johnson, TK, Henstridge, MA, Warr, CG (2017a) MACPF/CDC proteins in development: Insights from *Drosophila* torso-like. *Seminars in Cell & Developmental Biology*

Johnson, TK, Moore, KA, Whisstock, JC, Warr, CG (2017b) Maternal Torso-Like coordinates tissue folding during *Drosophila* gastrulation. *Genetics* **206**, 1459-1468.

Jutras, I, Laplante, A, Boulais, J, Brunet, S, Thinakaran, G, Desjardins, M (2005) γ-secretase is a functional component of phagosomes. *Journal of Biological Chemistry* **280**, 36310-7.

Kadota, K, Ishino, T, Matsuyama, T, Chinzei, Y, Yuda, M (2004) Essential role of membrane-attack protein in malarial transmission to mosquito host. *Proceedings of the National Academy of Sciences of the USA* **101**, 16310-5.

Kägi, D, Ledermann, B, Bürki, K, Seiler, P, Odermatt, B, Olsen, KJ, Podack, ER, Zinkernagel, RM, Hengartner, H (1994) Cytotoxicity mediated by T cells and natural killer cells is greatly impaired in perforin-deficient mice. *Nature* **369**, 31-7.

Kaiserman, D, Bird, CH, Sun, J, Matthews, A, Ung, K, Whisstock, JC, Thompson, PE, Trapani, JA, Bird, PI (2006) The major human and mouse granzymes are structurally and functionally divergent. *Journal of Cell Biology* **175**, 619-30.

Kato, H, Sakai, T, Tamura, K, Minoguchi, S, Shirayoshi, Y, Hamada, Y, Tsujimoto, Y, Honjo, T (1996) Functional conservation of mouse Notch receptor family members. *FEBS Letters* **395**, 221-4.

Kaufmann, SH (2008) Immunology's foundation: the 100-year anniversary of the Nobel Prize to Paul Ehrlich and Elie Metchnikoff. *Nature Immunology* **9**, 705-12.

Kawano, H, Nakatani, T, Mori, T, Ueno, S, Fukaya, M, Abe, A, Kobayashi, M, Toda, F, Watanabe, M, Matsuoka, I (2004) Identification and characterization of novel developmentally regulated neural-specific proteins, BRINP family. *Molecular Brain Research* **125**, 60-75.

Kim, J, Neufeld, TP (2015) Dietary sugar promotes systemic TOR activation in *Drosophila* through AKH-dependent selective secretion of Dilp3. *Nature Communications* **6**, 6846.

Kim, SK, Rulifson, EJ (2004) Conserved mechanisms of glucose sensing and regulation by *Drosophila* corpora cardiaca cells. *Nature* **431**, 316-20.

Kim, WJ, Jan, LY, Jan, YN (2013) A PDF/NPF neuropeptide signaling circuitry of male *Drosophila melanogaster* controls rival-induced prolonged mating. *Neuron* **80**, 1190-205.

Klingler, M, Erdélyi, M, Szabad, J, Nüsslein-Volhard, C (1988) Function of *torso* in determining the terminal anlagen of the *Drosophila* embryo. *Nature* **335**, 275-7.

Kobayashi, M, Nakatani, T, Koda, T, Matsumoto, K-i, Ozaki, R, Mochida, N, Takao, K, Miyakawa, T, Matsuoka, I (2014) Absence of BRINP1 in mice causes increase of hippocampal neurogenesis and behavioral alterations relevant to human psychiatric disorders. *Molecular Brain* **7**, 12.

Kondos, SC, Hatfaludi, T, Voskoboinik, I, Trapani, JA, Law, RH, Whisstock, JC, Dunstone, MA (2010) The structure and function of mammalian membrane-attack complex/perforin-like proteins. *Tissue Antigens* **76**, 341-51.

Kopacek, J, Sakaguchi, S, Shigematsu, K, Nishida, N, Atarashi, R, Nakaoke, R, Moriuchi, R, Niwa, M, Katamine, S (2000) Upregulation of the genes encoding lysosomal hydrolases, a perforin-like protein, and peroxidases in the brains of mice affected with an experimental prion disease. *Journal of Virology* **74**, 411-7.

Koski, CL, Ramm, LE, Hammer, CH, Mayer, MM, Shin, ML (1983) Cytolysis of nucleated cells by complement: cell death displays multi-hit characteristics. *Proceedings of the National Academy of Sciences of the USA* **80**, 3816-20.

Koyama, T, Mirth, CK (2016) Growth-Blocking Peptides As Nutrition-Sensitive Signals for Insulin Secretion and Body Size Regulation. *PLoS Biology* **14**, e1002392.

Koyama, T, Rodrigues, MA, Athanasiadis, A, Shingleton, AW, Mirth, CK (2014) Nutritional control of body size through FoxO-Ultraspiracle mediated ecdysone biosynthesis. *eLife* **3**, e03091.

Krupp, JJ, Billeter, J-C, Wong, A, Choi, C, Nitabach, MN, Levine, JD (2013) Pigment-dispersing factor modulates pheromone production in clock cells that influence mating in *Drosophila*. *Neuron* **79**, 54-68.

Kunchithapautham, K, Rohrer, B (2011) Sublytic membrane-attack-complex (MAC) activation alters regulated rather than constitutive vascular endothelial growth factor (VEGF) secretion in retinal pigment epithelium monolayers. *Journal of Biological Chemistry* **286**, 23717-24.

Lantz, V, Ambrosio, L, Schedl, P (1992) The *Drosophila orb* gene is predicted to encode sex-specific germline RNA-binding proteins and has localized transcripts in ovaries and early embryos. *Development* **115**, 75-88.

Lantz, V, Schedl, P (1994) Multiple *cis*-acting targeting sequences are required for *orb* mRNA localization during *Drosophila* oogenesis. *Molecular and Cellular Biology* **14**, 2235-42.

Law, RH, Lukoyanova, N, Voskoboinik, I, Caradoc-Davies, TT, Baran, K, Dunstone, MA, D'Angelo, ME, Orlova, EV, Coulibaly, F, Verschoor, S, Browne, KA, Ciccone, A, Kuiper, MJ, Bird, PI, Trapani, JA, Saibil, HR, Whisstock, JC (2010) The structural basis for membrane binding and pore formation by lymphocyte perforin. *Nature* **468**, 447-51.

Layalle, S, Arquier, N, Léopold, P (2008) The TOR pathway couples nutrition and developmental timing in *Drosophila*. *Developmental Cell* **15**, 568-77.

Lear, BC, Merrill, CE, Lin, J-M, Schroeder, A, Zhang, L, Allada, R (2005) A G protein-coupled receptor, *groom-of-PDF*, is required for PDF neuron action in circadian behavior. *Neuron* **48**, 221-7.

Lee, M, Guo, J-P, Schwab, C, McGeer, EG, McGeer, PL (2012) Selective inhibition of the membrane attack complex of complement by low molecular weight components of the aurin tricarboxylic acid synthetic complex. *Neurobiology of Aging* **33**, 2237-46.

Lee, S-K, Thomas, GH (2011) Rac1 modulation of the apical domain is negatively regulated by β (Heavy)-spectrin. *Mechanisms of Development* **128**, 116-28.

Lee, T, Luo, L (1999) Mosaic analysis with a repressible cell marker for studies of gene function in neuronal morphogenesis. *Neuron* **22**, 451-61.

Lehmann, R, Jiménez, F, Dietrich, U, Campos-Ortega, JA (1983) On the phenotype and development of mutants of early neurogenesis in *Drosophila melanogaster. Wilehm Roux's Archives of Developmental Biology* **192**, 62-74.

Leslie, JD, Mayor, R (2013) Complement in animal development: Unexpected roles of a highly conserved pathway. *Seminars in Immunology* **25**, 39-46.

Letunic, I, Bork, P (2017) 20 years of the SMART protein domain annotation resource. *Nucleic Acids Research*

Li, Y, Guo, F, Shen, J, Rosbash, M (2014) PDF and cAMP enhance PER stability in *Drosophila* clock neurons. *Proceedings of the National Academy of Sciences of the USA* **111**, E1284-90.

Lichtenheld, MG, Olsen, KJ, Lu, P, Lowrey, DM, Hameed, A, Hengartner, H, Podack, ER (1988) Structure and function of human perforin. *Nature* **335**, 448-51.

Ligoxygakis, P, Bray, SJ, Apidianakis, Y, Delidakis, C (1999) Ectopic expression of individual *E(spl)* genes has differential effects on different cell fate decisions and underscores the biphasic requirement for Notch activity in wing margin establishment in *Drosophila. Development* **126**, 2205-14.

Lin, DM, Goodman, CS (1994) Ectopic and increased expression of Fasciclin II alters motoneuron growth cone guidance. *Neuron* **13**, 507-23.

Lin, Y, Stormo, GD, Taghert, PH (2004) The neuropeptide pigment-dispersing factor coordinates pacemaker interactions in the *Drosophila* circadian system. *Journal of Neuroscience* **24**, 7951-7.

Linneweber, GA, Jacobson, J, Busch, KE, Hudry, B, Christov, CP, Dormann, D, Yuan, M, Otani, T, Knust, E, de Bono, M, Miguel-Aliaga, I (2014) Neuronal control of metabolism through nutrient-dependent modulation of tracheal branching. *Cell* **156**, 69-83.

Lionel, AC, Tammimies, K, Vaags, AK, Rosenfeld, JA, Ahn, JW, Merico, D, Noor, A, Runke, CK, Pillalamarri, VK, Carter, MT, Gazzellone, MJ, Thiruvahindrapuram, B, Fagerberg, C, Laulund, LW, Pellecchia, G, Lamoureux, S, Deshpande, C, Clayton-Smith, J, White, AC, Leather, S, Trounce, J, Melanie Bedford, H, Hatchwell, E, Eis, PS, Yuen, RK, Walker, S, Uddin, M, Geraghty, MT, Nikkel, SM, Tomiak, EM, Fernandez, BA, Soreni, N, Crosbie, J, Arnold, PD, Schachar, RJ, Roberts, W, Paterson, AD, So, J, Szatmari, P, Chrysler, C, Woodbury-Smith, M, Brian Lowry, R, Zwaigenbaum, L, Mandyam, D, Wei, J, Macdonald, JR, Howe, JL, Nalpathamkalam, T, Wang, Z, Tolson, D, Cobb, DS, Wilks, TM, Sorensen, MJ, Bader, PI, An, Y, Wu, BL, Musumeci, SA, Romano, C, Postorivo, D,

Nardone, AM, Monica, MD, Scarano, G, Zoccante, L, Novara, F, Zuffardi, O, Ciccone, R, Antona, V, Carella, M, Zelante, L, Cavalli, P, Poggiani, C, Cavallari, U, Argiropoulos, B, Chernos, J, Brasch-Andersen, C, Speevak, M, Fichera, M, Ogilvie, CM, Shen, Y, Hodge, JC, Talkowski, ME, Stavropoulos, DJ, Marshall, CR, Scherer, SW (2014) Disruption of the *ASTN2/TRIM32* locus at 9q33.1 is a risk factor in males for autism spectrum disorders, ADHD and other neurodevelopmental phenotypes. *Human Molecular Genetics* **23**, 2752-68.

Lopez, JA, Susanto, O, Jenkins, MR, Lukoyanova, N, Sutton, VR, Law, RH, Johnston, A, Bird, CH, Bird, PI, Whisstock, JC, Trapani, JA, Saibil, HR, Voskoboinik, I (2013) Perforin forms transient pores on the target cell plasma membrane to facilitate rapid access of granzymes during killer cell attack. *Blood* **121**, 2659-68.

Lovelace, LL, Cooper, CL, Sodetz, JM, Lebioda, L (2011) Structure of human C8 protein provides mechanistic insight into membrane pore formation by complement. *Journal of Biological Chemistry* **286**, 17585-92.

Lukoyanova, N, Hoogenboom, BW, Saibil, HR (2016) The membrane attack complex, perforin and cholesterol-dependent cytolysin superfamily of pore-forming proteins. *Journal of Cell Science* **129**, 2125-33.

Lukoyanova, N, Kondos, SC, Farabella, I, Law, RH, Reboul, CF, Caradoc-Davies, TT, Spicer, BA, Kleifeld, O, Traore, DAK, Ekkel, SM, Voskoboinik, I, Trapani, JA, Hatfaludi, T, Oliver, K, Hotze, EM, Tweten, RK, Whisstock, JC, Topf, M, Saibil, HR, Dunstone, MA (2015) Conformational changes during pore formation by the perforin-related protein pleurotolysin. *PLoS Biology* **13**, e1002049.

Lukoyanova, N, Saibil, HR (2008) Friend or foe: the same fold for attack and defense. *Trends in Immunology* **29**, 51-3.

Manning, AJ, Peters, KA, Peifer, M, Rogers, SL (2013) Regulation of epithelial morphogenesis by the G protein-coupled receptor Mist and its ligand Fog. *Science Signaling* **6**, ra98.

Manseau, L, Baradaran, A, Brower, D, Budhu, A, Elefant, F, Phan, H, Philp, AV, Yang, M, Glover, D, Kaiser, K, Palter, K, Selleck, S (1997) GAL4 enhancer traps expressed in the embryo, larval brain, imaginal discs, and ovary of *Drosophila*. *Developmental Dynamics* **209**, 310-22.

Martin, J-R, Raibaud, A, Ollo, R (1994) Terminal pattern elements in *Drosophila* embryo induced by the torso-like protein. *Nature* **367**, 741-5.

Mast, FD, Li, J, Virk, MK, Hughes, SC, Simmonds, AJ, Rachubinski, RA (2011) A *Drosophila* model for the Zellweger spectrum of peroxisome biogenesis disorders. *Disease Models & Mechanisms* **4**, 659-72.

Mast, FD, Rachubinski, RA, Aitchison, JD (2015) Signaling dynamics and peroxisomes. *Current Opinion in Cell Biology* **35**, 131-6.

Masuho, I, Ostrovskaya, O, Kramer, GM, Jones, CD, Xie, K, Martemyanov, KA (2015) Distinct profiles of functional discrimination among G proteins determine the actions of G protein-coupled receptors. *Science Signaling* **8**, ra123.

McBrayer, Z, Ono, H, Shimell, M, Parvy, J-P, Beckstead, RB, Warren, JT, Thummel, CS, Dauphin-Villemant, C, Gilbert, LI, O'Connor, MB (2007) Prothoracicotropic hormone regulates developmental timing and body size in *Drosophila*. *Developmental Cell* **13**, 857-71.

McCormack, R, Bahnan, W, Shrestha, N, Boucher, J, Barreto, M, Barrera, CM, Dauer, EA, Freitag, NE, Khan, WN, Podack, ER, Schesser, K (2016) Perforin-2 protects host cells and mice by restricting the vacuole to cytosol transitioning of a bacterial pathogen. *Infection and Immunity* **84**, 1083-91.

McCormack, R, de Armas, LR, Shiratsuchi, M, Ramos, JE, Podack, ER (2013) Inhibition of intracellular bacterial replication in fibroblasts is dependent on the perforin-like protein (perforin-2) encoded by macrophage-expressed gene 1. *Journal of Innate Immunity* **5**, 185-94.

McCormack, RM, de Armas, LR, Shiratsuchi, M, Fiorentino, DG, Olsson, ML, Lichtenheld, MG, Morales, A, Lyapichev, K, Gonzalez, LE, Strbo, N, Sukumar, N, Stojadinovic, O, Plano, GV, Munson, GP, Tomic-Canic, M, Kirsner, RS, Russell, DG, Podack, ER (2015) Perforin-2 is essential for intracellular defense of parenchymal cells and phagocytes against pathogenic bacteria. *eLife* **4**, e06508.

McDowell, IC, Nikapitiya, C, Aguiar, D, Lane, CE, Istrail, S, Gomez-Chiarri, M (2014) Transcriptome of American oysters, *Crassostrea virginica*, in response to bacterial challenge: insights into potential mechanisms of disease resistance. *PLoS One* **9**, e105097.

McKay, RR, Zhu, L, Shortridge, RD (1995) A *Drosophila* gene that encodes a member of the protein disulfide isomerase/phospholipase C-α family. *Insect Biochemistry and Molecular Biology* **25**, 647-54.

Mertens, I, Vandingenen, A, Johnson, EC, Shafer, OT, Li, W, Trigg, JS, De Loof, A, Schoofs, L, Taghert, PH (2005) PDF receptor signaling in *Drosophila* contributes to both circadian and geotactic behaviors. *Neuron* **48**, 213-9.

Mezan, S, Feuz, JD, Deplancke, B, Kadener, S (2016) PDF signaling Is an integral part of the *Drosophila* circadian molecular oscillator. *Cell Reports* **17**, 708-719.

Micchelli, CA, Rulifson, EJ, Blair, SS (1997) The function and regulation of *cut* expression on the wing margin of *Drosophila*: Notch, Wingless and a dominant negative role for Delta and Serrate. *Development* **124**, 1485-95.

Miller, DJ, Hemmrich, G, Ball, EE, Hayward, DC, Khalturin, K, Funayama, N, Agata, K, Bosch, TC (2007) The innate immune repertoire in Cnidaria--ancestral complexity and stochastic gene loss. *Genome Biology* **8**, R59.

Mineo, A, Furriols, M, Casanova, J (2015) Accumulation of the *Drosophila* Torso-like protein at the blastoderm plasma membrane suggests that it translocates from the eggshell. *Development* **142**, 1299-304.

Mirth, CK, Riddiford, LM (2007) Size assessment and growth control: how adult size is determined in insects. *Bioessays* **29**, 344-55.

Mirth, CK, Shingleton, AW (2012) Integrating body and organ size in *Drosophila*: recent advances and outstanding problems. *Frontiers in Endocrinology (Lausanne)* **3**, 49.

Mirth, CK, Truman, JW, Riddiford, LM (2005) The role of the prothoracic gland in determining critical weight for metamorphosis in *Drosophila melanogaster*. *Current Biology* **15**, 1796-807.

Morgan, BP (1989) Complement membrane attack on nucleated cells: resistance, recovery and non-lethal effects. *Biochemical Journal* **264**, 1-14.

Morgan, BP (2016) The membrane attack complex as an inflammatory trigger. *Immunobiology* **221**, 747-51.

Morgan, BP, Boyd, C, Bubeck, D (2017) Molecular cell biology of complement membrane attack. *Seminars in Cell & Developmental Biology*

Morgan, BP, Dankert, JR, Esser, AF (1987) Recovery of human neutrophils from complement attack: removal of the membrane attack complex by endocytosis and exocytosis. *Journal of Immunology* **138**, 246-53.

Morgan, BP, Luzio, JP, Campbell, AK (1986) Intracellular Ca^{2+} and cell injury: a paradoxical role of Ca^{2+} in complement membrane attack. *Cell Calcium* **7**, 399-411.

Morioka, E, Matsumoto, A, Ikeda, M (2012) Neuronal influence on peripheral circadian oscillators in pupal *Drosophila* prothoracic glands. *Nature Communications* **3**, 909.

Motomiya, M, Kobayashi, M, Iwasaki, N, Minami, A, Matsuoka, I (2007) Activity-dependent regulation of BRINP family genes. *Biochemical and Biophysical Research Communications* **352**, 623-9.

Müller-Eberhard, HJ (1986) The membrane attack complex of complement. *Annual Review of Immunology* **4**, 503-28.

Munier, A-I, Doucet, D, Perrodou, E, Zachary, D, Meister, M, Hoffmann, JA, Janeway, CA, Jr., Lagueux, M (2002) PVF2, a PDGF/VEGF-like growth factor, induces hemocyte proliferation in *Drosophila* larvae. *EMBO Reports* **3**, 1195-200.

Myers, EM, Yu, J, Sehgal, A (2003) Circadian control of eclosion: Interaction between a central and peripheral clock in *Drosophila melanogaster*. *Current Biology* **13**, 526-33.

Nakaoka, T, Iga, M, Yamada, T, Koujima, I, Takeshima, M, Zhou, X, Suzuki, Y, Ogihara, MH, Kataoka, H (2017) Deep sequencing of the prothoracic gland transcriptome reveals new players in insect ecdysteroidogenesis. *PLoS One* **12**, e0172951.

Naor, Z (2009) Signaling by G-protein-coupled receptor (GPCR): studies on the GnRH receptor. *Frontiers in Neuroendocrinology* **30**, 10-29.

Nässel, DR, Winther, AM (2010) *Drosophila* neuropeptides in regulation of physiology and behavior. *Progress in Neurobiology* **92**, 42-104.

Neumann, CJ, Cohen, SM (1996) A hierarchy of cross-regulation involving *Notch*, *wingless*, *vestigial* and *cut* organizes the dorsal/ventral axis of the *Drosophila* wing. *Development* **122**, 3477-3485.

Ni, T, Gilbert, RJC (2017) Repurposing a pore: highly conserved perforin-like proteins with alternative mechanisms. *Philosophical Transactions of the Royal Society of London B: Biological Sciences* **372**,

Ni, T, Harlos, K, Gilbert, R (2016) Structure of astrotactin-2: a conserved vertebrate-specific and perforin-like membrane protein involved in neuronal development. *Open Biology* **6**,

Niculescu, F, Badea, T, Rus, H (1999) Sublytic C5b-9 induces proliferation of human aortic smooth muscle cells: role of mitogen activated protein kinase and phosphatidylinositol 3-kinase. *Atherosclerosis* **142**, 47-56.

Niculescu, F, Rus, H (2001) Mechanisms of signal transduction activated by sublytic assembly of terminal complement complexes on nucleated cells. *Immunologic Research* **24**, 191-9.

Niculescu, F, Rus, H, Shin, ML (1994) Receptor-independent activation of guanine nucleotide-binding regulatory proteins by terminal complement complexes. *Journal of Biological Chemistry* **269**, 4417-23.

Nijhout, HF, Riddiford, LM, Mirth, CK, Shingleton, AW, Suzuki, Y, Callier, V (2014) The developmental control of size in insects. *Wiley Interdisciplinary Reviews Developmental Biology* **3**, 113-34.

Nishiyama, H, Gill, JH, Pitt, E, Kennedy, W, Knowles, MA (2001) Negative regulation of G_1/S transition by the candidate bladder tumour suppressor gene *DBCCR1*. *Oncogene* **20**, 2956-64.

Niwa, R, Niwa, YS (2014a) Enzymes for ecdysteroid biosynthesis: their biological functions in insects and beyond. *Bioscience, Biotechnology, and Biochemistry* **78**, 1283-92.

Niwa, YS, Niwa, R (2014b) Neural control of steroid hormone biosynthesis during development in the fruit fly *Drosophila melanogaster*. *Genes & Genetic Systems* **89**, 27-34.

Noiva, R, Lennarz, WJ (1992) Protein disulfide isomerase. A multifunctional protein resident in the lumen of the endoplasmic reticulum. *Journal of Biological Chemistry* **267**, 3553-6.

Nolo, R, Abbott, LA, Bellen, HJ (2000) Senseless, a Zn finger transcription factor, is necessary and sufficient for sensory organ development in *Drosophila*. *Cell* **102**, 349-62.

Nüsslein-Volhard, C, Frohnhöfer, HG, Lehmann, R (1987) Determination of anteroposterior polarity in *Drosophila*. *Science* **238**, 1675-1681.

Oda, H, Tsukita, S (2001) Real-time imaging of cell-cell adherens junctions reveals that *Drosophila* mesoderm invagination begins with two phases of apical constriction of cells. *Journal of Cell Science* **114**, 493-501.

Ohhara, Y, Shimada-Niwa, Y, Niwa, R, Kayashima, Y, Hayashi, Y, Akagi, K, Ueda, H, Yamakawa-Kobayashi, K, Kobayashi, S (2015) Autocrine regulation of ecdysone synthesis by β3-octopamine receptor in the prothoracic gland is essential for *Drosophila* metamorphosis. *Proceedings of the National Academy of Sciences of the USA* **112**, 1452-7.

Orgogozo, V, Schweisguth, F, Bellaiche, Y (2002) Binary cell death decision regulated by unequal partitioning of Numb at mitosis. *Development* **129**, 4677-84.

Ota, K, Leonardi, A, Mikelj, M, Skocaj, M, Wohlschlager, T, Kunzler, M, Aebi, M, Narat, M, Krizaj, I, Anderluh, G, Sepcic, K, Macek, P (2013) Membrane cholesterol and sphingomyelin, and ostreolysin A are obligatory for pore-formation by a MACPF/CDC-like pore-forming protein, pleurotolysin B. *Biochimie* **95**, 1855-64.

Ou, Q, Zeng, J, Yamanaka, N, Brakken-Thal, C, O'Connor, MB, King-Jones, K (2016) The insect prothoracic gland as a model for steroid hormone biosynthesis and regulation. *Cell Reports* **16**, 247-62.

Palmer, WH, Deng, W-M (2015) Ligand-independent mechanisms of Notch activity. *Trends in Cell Biology* **25**, 697-707.

Pandey, UB, Nichols, CD (2011) Human disease models in *Drosophila melanogaster* and the role of the fly in therapeutic drug discovery. *Pharmacological Reviews* **63**, 411-36.

Papadimitriou, JC, Phelps, PC, Shin, ML, Smith, MW, Trump, BF (1994) Effects of Ca^{2+} deregulation on mitochondrial membrane potential and cell viability in nucleated cells following lytic complement attack. *Cell Calcium* **15**, 217-27.

Parisky, KM, Agosto, J, Pulver, SR, Shang, Y, Kuklin, E, Hodge, JJ, Kang, K, Liu, X, Garrity, PA, Rosbash, M, Griffith, LC (2008) PDF cells are a GABA-responsive wake-promoting component of the *Drosophila* sleep circuit. *Neuron* **60**, 672-82.

Paroush, Ze, Wainwright, SM, Ish-Horowicz, D (1997) Torso signalling regulates terminal patterning in *Drosophila* by antagonising Groucho-mediated repression. *Development* **124**, 3827-34.

Peitsch, MC, Amiguet, P, Guy, R, Brunner, J, Maizel, JV, Jr., Tschopp, J (1990) Localization and molecular modelling of the membrane-inserted domain of the ninth component of human complement and perforin. *Molecular Immunology* **27**, 589-602.

Peitsch, MC, Tschopp, J (1991) Assembly of macromolecular pores by immune defense systems. *Current Opinion in Cell Biology* **3**, 710-6.

Perrimon, N (1998) Creating mosaics in *Drosophila*. *International Journal of Developmental Biology* **42**, 243-7.

Podack, ER, Dennert, G (1983) Assembly of two types of tubules with putative cytolytic function by cloned natural killer cells. *Nature* **302**, 442-5.

Podack, ER, Konigsberg, PJ (1984) Cytolytic T cell granules. Isolation, structural, biochemical, and functional characterization. *Journal of Experimental Medicine* **160**, 695-710.

Podack, ER, Munson, GP (2016) Killing of Microbes and Cancer by the Immune System with Three Mammalian Pore-Forming Killer Proteins. *Frontiers in Immunology* **7**, 464.

Podack, ER, Young, JD-E, Cohn, ZA (1985) Isolation and biochemical and functional characterization of perforin 1 from cytolytic T-cell granules. *Proceedings of the National Academy of Sciences of the USA* **82**, 8629-33.

Poulson, DF (1937) Chromosomal deficiencies and the embryonic development of *Drosophila melanogaster*. *Proceedings of the National Academy of Sciences of the USA* **23**, 133-7.

Praper, T, Sonnen, A, Viero, G, Kladnik, A, Froelich, CJ, Anderluh, G, Dalla Serra, M, Gilbert, RJC (2011a) Human perforin employs different avenues to damage membranes. *Journal of Biological Chemistry* **286**, 2946-55.

Praper, T, Sonnen, AF-P, Kladnik, A, Andrighetti, AO, Viero, G, Morris, KJ, Volpi, E, Lunelli, L, Dalla Serra, M, Froelich, CJ, Gilbert, RJ, Anderluh, G (2011b) Perforin activity at membranes leads to invaginations and vesicle formation. *Proceedings of the National Academy of Sciences of the USA* **108**, 21016-21.

Qiu, W, Zhang, Y, Liu, X, Zhou, J, Li, Y, Zhou, Y, Shan, K, Xia, M, Che, N, Feng, X, Zhao, D, Wang, Y (2012) Sublytic C5b-9 complexes induce proliferative changes of glomerular mesangial cells in rat Thy-1 nephritis through TRAF6-mediated PI3K-dependent Akt1 activation. *Journal of Pathology* **226**, 619-32.

Ram, S, Lewis, LA, Rice, PA (2010) Infections of people with complement deficiencies and patients who have undergone splenectomy. *Clinical Microbiology Reviews* **23**, 740-80.

Reddy, A, Caler, EV, Andrews, NW (2001) Plasma membrane repair is mediated by Ca^{2+}-regulated exocytosis of lysosomes. *Cell* **106**, 157-69.

Renn, SC, Park, JH, Rosbash, M, Hall, JC, Taghert, PH (1999) A *pdf* neuropeptide gene mutation and ablation of PDF neurons each cause severe abnormalities of behavioral circadian rhythms in *Drosophila*. *Cell* **99**, 791-802.

Rewitz, KF, Yamanaka, N, Gilbert, LI, O'Connor, MB (2009) The insect neuropeptide PTTH activates receptor tyrosine kinase Torso to initiate metamorphosis. *Science* **326**, 1403-1405.

Rieger, D, Shafer, OT, Tomioka, K, Helfrich-Förster, C (2006) Functional analysis of circadian pacemaker neurons in *Drosophila melanogaster*. *Journal of Neuroscience* **26**, 2531-43.

Roden, LT, Miflin, BJ, Freedman, RB (1982) Protein disulfide isomerase is located in the endoplasmic reticulum of developing wheat endosperm. *FEBS Letters* **138**, 121-124.

Rosado, CJ, Buckle, AM, Law, RH, Butcher, RE, Kan, W-T, Bird, CH, Ung, K, Browne, KA, Baran, K, Bashtannyk-Puhalovich, TA, Faux, NG, Wong, W, Porter, CJ, Pike, RN, Ellisdon, AM, Pearce, MC, Bottomley, SP, Emsley, J, Smith, AI, Rossjohn, J, Hartland, EL, Voskoboinik, I, Trapani, JA, Bird, PI, Dunstone, MA, Whisstock, JC (2007) A common fold mediates vertebrate defense and bacterial attack. *Science* **317**, 1548-51.

Rosado, CJ, Kondos, S, Bull, TE, Kuiper, MJ, Law, RH, Buckle, AM, Voskoboinik, I, Bird, PI, Trapani, JA, Whisstock, JC, Dunstone, MA (2008) The MACPF/CDC family of pore-forming toxins. *Cellular Microbiology* **10**, 1765-74.

Rossjohn, J, Feil, SC, McKinstry, WJ, Tweten, RK, Parker, MW (1997) Structure of a cholesterol-binding, thiol-activated cytolysin and a model of its membrane form. *Cell* **89**, 685-92.

Rulifson, EJ, Kim, SK, Nusse, R (2002) Ablation of insulin-producing neurons in flies: growth and diabetic phenotypes. *Science* **296**, 1118-20.

Rus, H, Niculescu, F, Badea, T, Shin, ML (1997) Terminal complement complexes induce cell cycle entry in oligodendrocytes through mitogen activated protein kinase pathway. *Immunopharmacology* **38**, 177-87.

Sabado, V, Vienne, L, Nunes, JM, Rosbash, M, Nagoshi, E (2017) Fluorescence circadian imaging reveals a PDF-dependent transcriptional regulation of the *Drosophila* molecular clock. *Scientific Reports* **7**, 41560.

Sajwan, S, Sidorov, R, Staskova, T, Zaloudikova, A, Takasu, Y, Kodrik, D, Zurovec, M (2015) Targeted mutagenesis and functional analysis of adipokinetic hormone-encoding gene in *Drosophila*. *Insect Biochemistry and Molecular Biology* **61**, 79-86.

Sakata, T, Sakaguchi, H, Tsuda, L, Higashitani, A, Aigaki, T, Matsuno, K, Hayashi, S (2004) *Drosophila* Nedd4 regulates endocytosis of Notch and suppresses its ligand-independent activation. *Current Biology* **14**, 2228-36.

Sala, E, Ruggiero, L, Di Giacomo, G, Cremona, O (2012) Endocytosis in Notch signaling activation. In 'Molecular Regulation of Endocytosis.' (Ed. B Ceresa.) pp. 331-376. (InTech:

Sarma, JV, Ward, PA (2011) The complement system. *Cell and Tissue Research* **343**, 227-35.

Savant-Bhonsale, S, Montell, DJ (1993) *torso-like* encodes the localized determinant of *Drosophila* terminal pattern formation. *Genes & Development* **7**, 2548-55.

Schüpbach, T, Wieschaus, E (1986) Germline autonomy of maternal-effect mutations altering the embryonic body pattern of *Drosophila*. *Developmental Biology* **113**, 443-8.

Schüpbach, T, Wieschaus, E (1989) Female sterile mutations on the second chromosome of *Drosophila melanogaster*. I. Maternal effect mutations. *Genetics* **121**, 101-17.

Seluzicki, A, Flourakis, M, Kula-Eversole, E, Zhang, L, Kilman, V, Allada, R (2014) Dual PDF signaling pathways reset clocks via TIMELESS and acutely excite target neurons to control circadian behavior. *PLoS Biology* **12**, e1001810.

Selva, EM, Stronach, BE (2007) Germline clone analysis for maternally acting *Drosophila* Hedgehog components. In 'Hedgehog signaling protocols.' (Ed. JI Horabin.) (Humana Press: New Jersey)

Sen, J, Goltz, JS, Stevens, LM, Stein, D (1998) Spatially restricted expression of *pipe* in the *Drosophila* egg chamber defines embryonic dorsal-ventral polarity. *Cell* **95**, 471-81.

Serna, M, Giles, JL, Morgan, BP, Bubeck, D (2016) Structural basis of complement membrane attack complex formation. *Nature Communications* **7**, 10587.

Shafer, OT, Kim, DJ, Dunbar-Yaffe, R, Nikolaev, VO, Lohse, MJ, Taghert, PH (2008) Widespread receptivity to neuropeptide PDF throughout the neuronal circadian clock network of *Drosophila* revealed by real-time cyclic AMP imaging. *Neuron* **58**, 223-37.

Shafer, OT, Yao, Z (2014) Pigment-dispersing factor signaling and circadian rhythms in insect locomotor activity. *Current Opinion in Insect Science* **1**, 73-80.

Shang, Y, Griffith, LC, Rosbash, M (2008) Light-arousal and circadian photoreception circuits intersect at the large PDF cells of the *Drosophila* brain. *Proceedings of the National Academy of Sciences of the USA* **105**, 19587-94.

Sharp, TH, Koster, AJ, Gros, P (2016) Heterogeneous MAC initiator and pore structures in a lipid bilayer by phase-plate cryo-electron tomography. *Cell Reports* **15**, 1-8.

Sheeba, V, Fogle, KJ, Kaneko, M, Rashid, S, Chou, Y-T, Sharma, VK, Holmes, TC (2008) Large ventral lateral neurons modulate arousal and sleep in *Drosophila*. *Current Biology* **18**, 1537-45.

Shellenbarger, DL, Mohler, JD (1978) Temperature-sensitive periods and autonomy of pleiotropic effects of *l(1)Nts1*, a conditional Notch lethal in *Drosophila*. *Developmental Biology* **62**, 432-46.

Sherwood, DR, McClay, DR (1997) Identification and localization of a sea urchin Notch homologue: insights into vegetal plate regionalization and Notch receptor regulation. *Development* **124**, 3363-74.

Shi, L, Mai, S, Israels, S, Browne, K, Trapani, JA, Greenberg, AH (1997) Granzyme B (GraB) autonomously crosses the cell membrane and perforin initiates apoptosis and GraB nuclear localization. *Journal of Experimental Medicine* **185**, 855-66.

Shimell, M, Pan, X, Martin, FA, Ghosh, AC, Leopold, P, O'Connor, MB, Romero, NM (2018) Prothoracicotropic hormone modulates environmental adaptive plasticity through the control of developmental timing. *Development*

Shorts-Cary, L, Xu, M, Ertel, J, Kleinschmidt-Demasters, BK, Lillehei, K, Matsuoka, I, Nielsen-Preiss, S, Wierman, ME (2007) Bone morphogenetic protein and retinoic acid-inducible neural specific protein-3 is expressed in gonadotrope cell pituitary

adenomas and induces proliferation, migration, and invasion. *Endocrinology* **148**, 967-75.

Siegmund, T, Korge, G (2001) Innervation of the ring gland of *Drosophila melanogaster*. *Journal of Comparative Neurology* **431**, 481-91.

Sims, PJ, Wiedmer, T (1984) Kinetics of polymerization of a fluoresceinated derivative of complement protein C9 by the membrane-bound complex of complement proteins C5b-8. *Biochemistry* **23**, 3260-7.

Slack, C, Giannakou, ME, Foley, A, Goss, M, Partridge, L (2011) dFOXO-independent effects of reduced insulin-like signaling in *Drosophila*. *Aging Cell* **10**, 735-48.

Smyth, MJ, Dunn, GP, Schreiber, RD (2006) Cancer immunosurveillance and immunoediting: the roles of immunity in suppressing tumor development and shaping tumor immunogenicity. *Advances in Immunology* **90**, 1-50.

Solecki, DJ (2012) Sticky situations: recent advances in control of cell adhesion during neuronal migration. *Current Opinion in Neurobiology* **22**, 791-8.

Spicer, BA, Conroy, PJ, Law, RHP, Voskoboinik, I, Whisstock, JC (2017) Perforin – A key (shaped) weapon in the immunological arsenal. *Seminars in Cell & Developmental Biology*

Spilsbury, K, O'Mara, M-A, Wu, WM, Rowe, PB, Symonds, G, Takayama, Y (1995) Isolation of a novel macrophage-specific gene by differential cDNA analysis. *Blood* **85**, 1620-9.

Sprenger, F, Nüsslein-Volhard, C (1992) Torso receptor activity is regulated by a diffusible ligand produced at the extracellular terminal regions of the *Drosophila* egg. *Cell* **71**, 987-1001.

Sprenger, F, Stevens, LM, Nüsslein-Volhard, C (1989) The *Drosophila* gene *torso* encodes a putative receptor tyrosine kinase. *Nature* **338**, 478-83.

Sprenger, F, Trosclair, MM, Morrison, DK (1993) Biochemical analysis of Torso and D-Raf during *Drosophila* embryogenesis: implications for terminal signal transduction. *Molecular and Cellular Biology* **13**, 1163-72.

Stepp, SE, Dufourcq-Lagelouse, R, Le Deist, F, Bhawan, S, Certain, S, Mathew, PA, Henter, J-I, Bennett, M, Fischer, A, de Saint Basile, G, Kumar, V (1999) Perforin gene defects in familial hemophagocytic lymphohistiocytosis. *Science* **286**, 1957-9.

Stevens, LM, Beuchle, D, Jurcsak, J, Tong, X, Stein, DS (2003) The *Drosophila* embryonic patterning determinant Torsolike is a component of the eggshell. *Current Biology* **13**, 1058-63.

Stevens, LM, Frohnhöfer, HG, Klingler, M, Nüsslein-Volhard, C (1990) Localized requirement for *torso-like* expression in follicle cells for development of terminal anlagen of the *Drosophila* embryo. *Nature* **346**, 660-3.

Stewart, SE, D'Angelo, ME, Bird, PI (2012) Intercellular communication via the endo-lysosomal system: translocation of granzymes through membrane barriers. *Biochimica et Biophysica Acta: Proteins and Proteomics* **1824**, 59-67.

Stewart, SE, Kondos, S, Matthews, AY, D'Angelo, ME, Dunstone, MA, Whisstock, JC, Trapani, JA, Bird, PI (2014) The perforin pore facilitates the delivery of cationic cargos. *Journal of Biological Chemistry* **289**, 9172-81.

Stitt, TN, Gasser, UE, Hatten, ME (1991) Molecular mechanisms of glial-guided neuronal migration. *Annals of the New York Academy of Sciences* **633**, 113-21.

Sun, X, Artavanis-Tsakonas, S (1997) Secreted forms of DELTA and SERRATE define antagonists of Notch signaling in *Drosophila*. *Development* **124**, 3439-48.

Sutton, VR, Davis, JE, Cancilla, M, Johnstone, RW, Ruefli, AA, Sedelies, K, Browne, KA, Trapani, JA (2000) Initiation of apoptosis by granzyme B requires direct cleavage of Bid, but not direct granzyme B-mediated caspase activation. *Journal of Experimental Medicine* **192**, 1403-14.

Sutton, VR, Wowk, ME, Cancilla, M, Trapani, JA (2003) Caspase activation by granzyme B is indirect, and caspase autoprocessing requires the release of proapoptotic mitochondrial factors. *Immunity* **18**, 319-29.

Talsma, AD, Christov, CP, Terriente-Felix, A, Linneweber, GA, Perea, D, Wayland, M, Shafer, OT, Miguel-Aliaga, I (2012) Remote control of renal physiology by the intestinal neuropeptide pigment-dispersing factor in *Drosophila*. *Proceedings of the National Academy of Sciences of the USA* **109**, 12177-82.

Tamang, DL, Alves, BN, Elliott, V, Redelman, D, Wadhwa, R, Fraser, SA, Hudig, D (2009) Regulation of perforin lysis: implications for protein disulfide isomerase proteins. *Cell Immunology* **255**, 82-92.

Tan, LX, Toops, KA, Lakkaraju, A (2016) Protective responses to sublytic complement in the retinal pigment epithelium. *Proceedings of the National Academy of Sciences of the USA* **113**, 8789-94.

Tanaka, Y (2011) Recent topics on the regulatory mechanism of ecdysteroidogenesis by the prothoracic glands in insects. *Frontiers in Endocrinology (Lausanne)* **2**, 107.

Terashima, M, Kobayashi, M, Motomiya, M, Inoue, N, Yoshida, T, Okano, H, Iwasaki, N, Minami, A, Matsuoka, I (2010) Analysis of the expression and function of BRINP family genes during neuronal differentiation in mouse embryonic stem cell-derived neural stem cells. *Journal of Neuroscience Research* **88**, 1387-93.

Tettweiler, G, Miron, M, Jenkins, M, Sonenberg, N, Lasko, PF (2005) Starvation and oxidative stress resistance in *Drosophila* are mediated through the eIF4E-binding protein, d4E-BP. *Genes & Development* **19**, 1840-3.

Thiery, J, Keefe, D, Boulant, S, Boucrot, E, Walch, M, Martinvalet, D, Goping, IS, Bleackley, RC, Kirchhausen, T, Lieberman, J (2011) Perforin pores in the endosomal membrane trigger the release of endocytosed granzyme B into the cytosol of target cells. *Nature Immunology* **12**, 770-7.

Thiery, J, Keefe, D, Saffarian, S, Martinvalet, D, Walch, M, Boucrot, E, Kirchhausen, T, Lieberman, J (2010) Perforin activates clathrin- and dynamin-dependent

endocytosis, which is required for plasma membrane repair and delivery of granzyme B for granzyme-mediated apoptosis. *Blood* **115**, 1582-93.

Thurman, JM, Renner, B, Kunchithapautham, K, Ferreira, VP, Pangburn, MK, Ablonczy, Z, Tomlinson, S, Holers, VM, Rohrer, B (2009) Oxidative stress renders retinal pigment epithelial cells susceptible to complement-mediated injury. *Journal of Biological Chemistry* **284**, 16939-47.

Toma, DP, White, KP, Hirsch, J, Greenspan, RJ (2002) Identification of genes involved in *Drosophila melanogaster* geotaxis, a complex behavioral trait. *Nature Genetics* **31**, 349-53.

Tomancak, P, Beaton, A, Weiszmann, R, Kwan, E, Shu, S, Lewis, SE, Richards, S, Ashburner, M, Hartenstein, V, Celniker, SE, Rubin, GM (2002) Systematic determination of patterns of gene expression during *Drosophila* embryogenesis. *Genome Biology* **3**, RESEARCH0088.

Tomita, T, Noguchi, K, Mimuro, H, Ukaji, F, Ito, K, Sugawara-Tomita, N, Hashimoto, Y (2004) Pleurotolysin, a novel sphingomyelin-specific two-component cytolysin from the edible mushroom *Pleurotus ostreatus*, assembles into a transmembrane pore complex. *Journal of Biological Chemistry* **279**, 26975-82.

Triantafilou, K, Hughes, TR, Triantafilou, M, Morgan, BP (2013) The complement membrane attack complex triggers intracellular Ca^{2+} fluxes leading to NLRP3 inflammasome activation. *Journal of Cell Science* **126**, 2903-13.

Troost, T, Jaeckel, S, Ohlenhard, N, Klein, T (2012) The tumour suppressor Lethal (2) giant discs is required for the function of the ESCRT-III component Shrub/CHMP4. *Journal of Cell Science* **125**, 763-76.

Tschopp, J, Masson, D, Stanley, KK (1986) Structural/functional similarity between proteins involved in complement- and cytotoxic T-lymphocyte-mediated cytolysis. *Nature* **322**, 831-4.

Turano, C, Coppari, S, Altieri, F, Ferraro, A (2002) Proteins of the PDI family: unpredicted non-ER locations and functions. *Journal of Cellular Physiology* **193**, 154-63.

Tweten, RK (2005) Cholesterol-dependent cytolysins, a family of versatile pore-forming toxins. *Infection and Immunity* **73**, 6199-209.

van de Water, JA, Lamb, JB, van Oppen, MJ, Willis, BL, Bourne, DG (2015) Comparative immune responses of corals to stressors associated with offshore reef-based tourist platforms. *Conservation Physiology* **3**, cov032.

Van der Meer, JM (1977) Optical clean and permanent whole mount preparation for phase-constrast microscopy of cuticular structures of insect larvae. *Drosophila Informational Service* **52**, 160.

Ventura, G, Furriols, M, Martín, N, Barbosa, V, Casanova, J (2010) *closca*, a new gene required for both Torso RTK activation and vitelline membrane integrity. Germline proteins contribute to *Drosophila* eggshell composition. *Developmental Biology* **344**, 224-32.

Voskoboinik, I, Thia, M-C, Fletcher, J, Ciccone, A, Browne, KA, Smyth, MJ, Trapani, JA (2005) Calcium-dependent plasma membrane binding and cell lysis by perforin are mediated through its C2 domain: A critical role for aspartate residues 429, 435, 483, and 485 but not 491. *Journal of Biological Chemistry* **280**, 8426-34.

Voskoboinik, I, Trapani, JA (2013) Perforinopathy: a spectrum of human immune disease caused by defective perforin delivery or function. *Frontiers in Immunology* **4**, 441.

Voskoboinik, I, Whisstock, JC, Trapani, JA (2015) Perforin and granzymes: function, dysfunction and human pathology. *Nature Reviews Immunology* **15**, 388-400.

Vrijenhoek, T, Buizer-Voskamp, JE, van der Stelt, I, Strengman, E, Consortium, GRaOiPG, Sabatti, C, Geurts van Kessel, A, Brunner, HG, Ophoff, RA, Veltman, JA (2008) Recurrent CNVs disrupt three candidate genes in schizophrenia patients. *American Journal of Human Genetics* **83**, 504-10.

Waldhauer, I, Steinle, A (2008) NK cells and cancer immunosurveillance. *Oncogene* **27**, 5932-43.

Walsh, CM, Matloubian, M, Liu, CC, Ueda, R, Kurahara, CG, Christensen, JL, Huang, MT, Young, JD, Ahmed, R, Clark, WR (1994) Immune function in mice lacking the *perforin* gene. *Proceedings of the National Academy of Sciences of the USA* **91**, 10854-8.

Wang, K-S, Tonarelli, S, Luo, X, Wang, L, Su, B, Zuo, L, Mao, C, Rubin, L, Briones, D, Xu, C (2015) Polymorphisms within ASTN2 gene are associated with age at onset of Alzheimer's disease. *Journal of Neural Transmission (Vienna)* **122**, 701-8.

Wilson, PM, Fryer, RH, Fang, Y, Hatten, ME (2010) *Astn2*, a novel member of the astrotactin gene family, regulates the trafficking of ASTN1 during glial-guided neuronal migration. *Journal of Neuroscience* **30**, 8529-40.

Wright, KO, Messing, EM, Reeder, JE (2004) DBCCR1 mediates death in cultured bladder tumor cells. *Oncogene* **23**, 82-90.

Xie, G, Zhang, H, Du, G, Huang, Q, Liang, X, Ma, J, Jiao, R (2012) Uif, a large transmembrane protein with EGF-like repeats, can antagonize Notch signaling in *Drosophila*. *PLoS One* **7**, e36362.

Xiong, P, Shiratsuchi, M, Matsushima, T, Liao, J, Tanaka, E, Nakashima, Y, Takayanagi, R, Ogawa, Y (2017) Regulation of expression and trafficking of perforin-2 by LPS and TNF-α. *Cellular Immunology* **320**, 1-10.

Yagi, H, Conroy, PJ, Leung, EW, Law, RH, Trapani, JA, Voskoboinik, I, Whisstock, JC, Norton, RS (2015) Structural Basis for Ca^{2+}-mediated Interaction of the Perforin C2 Domain with Lipid Membranes. *Journal of Biological Chemistry* **290**, 25213-26.

Yamamoto, S, Jaiswal, M, Charng, W-L, Gambin, T, Karaca, E, Mirzaa, G, Wiszniewski, W, Sandoval, H, Haelterman, NA, Xiong, B, Zhang, K, Bayat, V, David, G, Li, T, Chen, K, Gala, U, Harel, T, Pehlivan, D, Penney, S, Vissers, LE, de Ligt, J, Jhangiani, SN, Xie, Y, Tsang, SH, Parman, Y, Sivaci, M, Battaloglu, E, Muzny, D, Wan, Y-W, Liu, Z, Lin-Moore, AT, Clark, RD, Curry, CJ, Link, N, Schulze, KL, Boerwinkle, E, Dobyns, WB,

Allikmets, R, Gibbs, RA, Chen, R, Lupski, JR, Wangler, MF, Bellen, HJ (2014) A *Drosophila* genetic resource of mutants to study mechanisms underlying human genetic diseases. *Cell* **159**, 200-14.

Yamanaka, N, Hua, Y-J, Roller, L, Spalovská-Valachová, I, Mizoguchi, A, Kataoka, H, Tanaka, Y (2010) *Bombyx* prothoracicostatic peptides activate the sex peptide receptor to regulate ecdysteroid biosynthesis. *Proceedings of the National Academy of Sciences of the USA* **107**, 2060-5.

Yamanaka, N, Marques, G, O'Connor, MB (2015) Vesicle-mediated steroid hormone secretion in *Drosophila melanogaster*. *Cell* **163**, 907-19.

Yamanaka, N, Rewitz, KF, O'Connor, MB (2013) Ecdysone control of developmental transitions: lessons from *Drosophila* research. *Annual Review of Entomology* **58**, 497-516.

Yao, Z, Shafer, OT (2014) The *Drosophila* circadian clock is a variably coupled network of multiple peptidergic units. *Science* **343**, 1516-20.

Yoshii, T, Wulbeck, C, Sehadova, H, Veleri, S, Bichler, D, Stanewsky, R, Helfrich-Forster, C (2009) The neuropeptide pigment-dispersing factor adjusts period and phase of *Drosophila*'s clock. *Journal of Neuroscience* **29**, 2597-610.

Young, JD-E, Cohn, ZA, Podack, ER (1986) The ninth component of complement and the pore-forming protein (perforin 1) from cytotoxic T cells: structural, immunological, and functional similarities. *Science* **233**, 184-90.

Zhang, H, Stallock, JP, Ng, JC, Reinhard, C, Neufeld, TP (2000) Regulation of cellular growth by the *Drosophila* target of rapamycin dTOR. *Genes & Development* **14**, 2712-24.

Zhang, Y, Emery, P (2013) GW182 controls *Drosophila* circadian behavior and PDF-receptor signaling. *Neuron* **78**, 152-65.

Zheng, C, Heintz, N, Hatten, ME (1996) CNS gene encoding astrotactin, which supports neuronal migration along glial fibers. *Science* **272**, 417-9.

Ziporen, L, Donin, N, Shmushkovich, T, Gross, A, Fishelson, Z (2009) Programmed necrotic cell death induced by complement involves a Bid-dependent pathway. *Journal of Immunology* **182**, 515-21.

zur Stadt, U, Rohr, J, Seifert, W, Koch, F, Grieve, S, Pagel, J, Strauß, J, Kasper, B, Nürnberg, G, Becker, C, Maul-Pavicic, A, Beutel, K, Janka, G, Griffiths, G, Ehl, S, Hennies, HC (2009) Familial hemophagocytic lymphohistiocytosis type 5 (FHL-5) is caused by mutations in Munc18-2 and impaired binding to syntaxin 11. *American Journal of Human Genetics* **85**, 482-92.

zur Stadt, U, Schmidt, S, Kasper, B, Beutel, K, Diler, AS, Henter, JI, Kabisch, H, Schneppenheim, R, Nürnberg, P, Janka, G, Hennies, HC (2005) Linkage of familial hemophagocytic lymphohistiocytosis (FHL) type-4 to chromosome 6q24 and identification of mutations in syntaxin 11. *Human Molecular Genetics* **14**, 827-34.

Appendices

Appendix 1 – Media, solutions and reagents

AP buffer
50μL 20% Tween-20 (Sigma)
9.95mL BM3

Apple juice agar (for embryo collection)
203mL Apple juice (Berri)
26.1g Dextrose (Merck)
13.03g Sucrose (Merck)
29.7g Agar (Merck)
1.5mL 10M NaOH (BDH)
dH_2O to 500mL
Autoclave before pouring.

Blocking solution
5% normal goat serum (NGS) in PTx

BM3
20mL 1M Tris-HCl pH 9.5
20mL 1M NaCl (Amresco)
10mL 1M $MgCl_2$ (BDH)
DEPC H_2O to 200mL

Fly food media
For 300 vials:
3450mL dH_2O
36g Potassium tartrate (Merck)
2.3g Calcium chloride (Merck)
24g Agar (Oxoid)
54g Yeast (Borregaard)
240g Glucose (Amresco)
120g Sugar (Bundberg)
Combine above ingredients and bring to the boil.
900mL dH_2O
300g Semolina (Weston Milling)
Add semolina and dH_2O, mix and bring to the boil while stirring; remove from heat.

18mL Propionic acid (Merck)

36mL Nipagen (Methyl-p-hydroxylbenzoate in 100% Ethanol)

Add Propionic acid and Nipagen, stir well and dispense; set aside to cool.

DEPC H$_2$O

1mL DEPC

milliQ dH$_2$O to 1L, leave at 37°C overnight, autoclave

Genomic DNA extraction buffer (Grind buffer)

68g 0.2M Sucrose (Merck)

1.21g 0.1M Tris-base, pH 9.2 (Promega)

1.86g 50mM EDTA

0.5g SDS (Promega)

dH$_2$O to 100mL

Hoyer's Mountant

30g Gum Arabic (Sigma)

200g Chloral hydrate (Sigma)

16mL Glycerol (Merck)

50mL dH$_2$O

10x PBS

80g NaCl (Amresco)

2g KCl (BDH)

14.4g Na$_2$HPO$_4$ (Merck)

2.4g KH$_2$PO$_4$ (Merck)

dH$_2$O to 1L, pH to 7.4

PBS + 0.1% Triton X (PTx)

50mL 10x PBS

0.5mL Triton X-100 (Sigma)

dH$_2$O to 500mL

Pre-hybridisation buffer (or Hybridisation buffer – store at -20°C)

100mL 20 x SSC

250mL Formamide (Merck)

0.5mL Tween-20 (Sigma)

0.5mL 50mg/mL Heparin (Sigma)

dH$_2$O to 500mL

146

20x SSC

175.3g NaCl

88.2g Sodium citrate

DEPC H_2O to 1L, pH 7.0 (with HCl)

5x TBE buffer

54g Tris base (Promega)

27.5g Boric acid (Merck)

20mL 0.5M EDTA, pH 8.0 (Merck)

dH_2O to 1L

Appendix 2 – ANOVA data table for Figure 2.9B

To investigate the effects of time, genotype and the interaction between time and genotype for the ecdysone titre experiment, the means, curves and interactions were all tested for statistical significance using an ANOVA. All three of these factors were significantly different to varying degrees. Only the statistical significance of the curves, representing the effects of genotype, were reported in the main text. The full ANOVA table has also been included below.

Table S1: ANOVA statistics for Figure 2.9B

ANOVA Table (Type II tests)					
	Sum Sq.	Df	F value	Pf (>F)	Sig.
poly(Time, 2)	399948	2	5.7887	0.005186	** p<0.01
Genotype	1534818	2	22.2145	7.892e-8	*** p<0.001
poly(Time, 2): Genotype	730410	4	5.2859	0.001104	** p<0.01
Residuals	1934541	56			

Appendix 3 – DNA and protein sequences for MACPF constructs

>musMPEG1

```
atgaacagcttcatggccttggtcctcatctggatgataatagcgtgtgctgaagcagacaagcctcttg
gagaaacgggcaccactggatttcaaatatgcaagaatgccctgaaactacctgtcttggaggtcctacc
aggaggaggctgggataatctgagaaatgtagacatgggacgggtgatggacttgacatacaccaactgt
aagaccacagaagatgggcagtacatcatccccgatgaagtgtatactattcctcagaaagagagcaacc
tggagatgaactcagaagtcctggagtcctggatgaattaccagagtaccacctcactttctatcaacac
agaactcgcccttttctccagagtcaacggcaagttctctactgagttccaaaggatgaagacccttcaa
gtaaaggaccaagctgtgactaccagggttcaggtaagaaaccggatctacacagtgaaaaccaccccaa
cttcagagctcagcttggggtttacgaaggcacttatggacatctgtgaccaactagagaaaaaccagac
gaagatggccacctacctggcagagctcttgatcctcaactatggcacacgtaatcactagtgtggat
gctggggctgcactggttcaggaggatcacgtaaggtcctccttccttctggacaaccagaatagccaga
acaccgtgaccgcttctgcagggattgccttcttaaacattgtgaacttcaaagttgaaacagactacat
ttctcagaccagtttgacgaaggactacctgtcgaacaggaccaactccaggtgcagagttttggaggg
gttcccttctatccaggcatcaccttagaaacctggcagaagggcatcactaaccacctagtggcaatag
accgtgctggcttgcctctgcatttcttcattaaacctgacaagctacctggcttgccaggtcccttggt
gaagaagctgtcgaagacagtggaaactgctgtgagacactattacacttttaacactcacccaggatgc
acaaatgttgattcccccaactttaattttcaagccaatatggatgatgattcctgtgatgcgaaagtca
ccaacttcacctttggtggagtttatcaggaatgcactgaactgtcaggtgatgttctttgccaaaacct
ggagcagaagaacctgctcacaggtgatttctcttgtccccctggctacacccctgtccatctgctctcc
cagacccatgaagagggttacagtcgtctggaatgtaaaaagaaatgcaccctcaagattttctgcaaga
cagtgtgtgaagatgtgttcagagtggccaaggctgaatttagggcttattggtgtgtggctgctggcca
agtacctgacaactcaggacttctctttggaggagtcttcactgacaagaccatcaacccatgacaaat
gcacagtcatgcccagcaggctacatcccactgaacctgtttgaaagcctcaaggtatgtgtgtccctgg
attatgagttggggttcaagttttcagtccccttggtggttcttcagttgtataatggggaacccctt
ggttaattctgatacagctaaagacgtcagagcaccatctctgaaaaagtgtcccggggggcttcagccaa
cacctagctgttatcagtgatggatgccaagtgtcctactgtgtcaaggctggaatcttcacaggaggt
ccctgctccctgtcaggctcccaccttataccaaaccacctcttatgagccaggttgccaccaacactgt
catagtgaccaatagtgagactgccagatcctggattaaggatcctcagaccaaccagtggaagctggga
gaacctctggagcttcgtagggccatgacagtcatccatggggacagtaatggaatgtcaggagggaag
ctgctggaatcactttgggagtcaccatagcactaggagttgtcattaccttggccatctatggtacccg
gaagtacaagaagaaggaataccaggaaattgaggagcaggagagtttggttggaagcttagcaacagat
gcaacagtccttaatggagaagaggatccaagtccagctggtaccgattataaggatgacgatgacaagt
aa
```

==MNSFMALVLIWMIIACAEADKPLG==ETGTTGFQICKNALKLPVLEVLPGGGWDNLRNVDMGRVMDLTYTNC
KTTEDGQYIIPDEVYTIPQKESNLEMNSEVLESWMNYQSTTSLSINTELALFSRVNGKFSTEFQRMKTLQ
VKDQAVTTRVQVRNRIYTVKTTPTSELSLGFTKALMDICDQLEKNQTKMATYLAELLILNYGTHVITSVD
AGAALVQEDHVRSSFLLDNQNSQNTVTASAGIAFLNIVNFKVETDYISQTSLTKDYLSNRTNSRVQSFGG
VPFYPGITLETWQKGITNHLVAIDRAGLPLHFFIKPDKLPGLPGPLVKKLSKTVETAVRHYYTFNTHPGC
TNVDSPNFNFQANMDDDSCDAKVTNFTFGGVYQECTELSGDVLCQNLEQKNLLTGDFSCPPGYTPVHLLS
QTHEEGYSRLECKKKCTLKIFCKTVCEDVFRVAKAEFRAYWCVAAGQVPDNSGLLFGGVFTDKTINPMTN
AQSCPAGYIPLNLFESLKVCVSLDYELGFKFSVPFGGFFSCIMGNPLVNSDTAKDVRAPSLKKCPGGFSQ
HLAVISDGCQVSYCVKAGIFTGGSLLPVRLPPYTKPPLMSQVATNTVIVTNSETARSWIKDPQTNQWKLG
EPLELRRAMTVIHGDSNGMSGGEA==AGITLGVTIALGVVITLAIY==GTRKYKKKEYQEIEEQESLVGSLATD
ATVLNGEEDPSPAGT==DYKDDDDK==

==Signal peptide==
==Trans-membrane domain==
==Flag tag==

>HeApx (full length)

```
gcggccgcATGGTGGGCCCACGTACAGCATGTGGCGGATTGCTCATCCTCTTCTCACTATTGCCCGTGAT
ATCACTCGGCGCTTCGACCTTGCCGATCCCGAATCCGATGAAATACATCGGCATTGGGTACAACATCATC
GACGGTAATCCCGAGGGTGATAACAGGGTTGCTGGCGGCGTCGATCCTGGTCTCCTGGTCTCTCGCCGTA
TCTTCGAACTCACCTACGATAACGGGAAAACGACGAATGACAACGAGTATAGAGTGCCTGATGAGGTGGA
ATTCCAGCAGCGCAGCAGCTCCTTTACCTCGAAGGAGACGGATACCTTCTACGGAACAAAGAGCTACGCA
AAGAAACTTTCACATCAGGTGCAGGCTGACGCTAGCGTTGAAGCGGTCTTTGCTTCAGTGAAGTTTTCTG
CCAGCCACCGGTACGAGTCCATTTCTAATGATGCCAGCACAAAAGGCTACGTTACTCCTCGGAGCAAAC
GATTCAGAACTTCGGCCACATGCGCTACTTGACCAGTCTTGCTGAACATGATGGATTCGAGATTGCAAGG
GAATTCCGTATTGACGTCTGTGACCTGCCTACGACATACGCCACCAATACATACATGGAGTTCCTTTCAA
AATGGGGAACGAGCGTTGTGACGGAGGCTGATGTCGGAGTCCGTACTGGTATAAACTCCCGTGAAGACCG
ATCTTCTTTCGTCAAAGATGCTTCAACAGATATGTCGAATAGCGTGAGTGTTGAAGGGAACTACAAAATC
TTCTCCGCTTCGTTGTCTGTAGACATGGACAGGTTCTCTCAAAGCGCATCATCGGAGAAAAAAATGGGGA
CGGAATATACCAGGTACACAATTGGCAGCGAAGAGTTTAATGAACCCATCACTATTAGTCTCATCGGCTT
AGAGGAAGCTTTGAATGACGAATACTGGAGCAGGCAATCGGAATATGAAAGCAGCGGAGAATGCCCAAGC
AATTGGGCAAGGTCAACCATCGCTACCAACATCTTGACCGGCCTCAAGGAATACGCCAACTACAGAGGAG
TTGTTCCTAGTTCAGACCCTGATGTGACCGTGCCTCTGACCTGGCCCGATGGAAAGTACGCTCTTCCCGA
GGCAGTGACACTCGGTGATAATACCTGCCCTAATACAGACTACATGACATGGAGCTTCGGTTTGTTCTAC
CAATTCACGGACGATGGTGGAGTAAATACCTGTTCCGAGAACAACCATCTGACCAACTACTGTGAACGTA
CCCACATGAGGACCTACTACTGCGTGAAGACCACTCCCAAGGCGACGGATTCCTCGTGGTCTTGGATGCC
CGGCGTCTACTGTATCTTCAAGAATGGTGACACTTGCCTGACGGGTTCACCGATGGTTTCATCAAGTGGA
ACGACGCTAGCGAGCAAAAGGGCATTGACACGGAATATAACACAATGCCTGCAGGAATTATTACCCTGGA
GCTACAGAAATTGActcgag
```

MVGPRTACGGLLILFSLLPVISLGASTLPIPNPMKYIGIGYNIIDGNPEGDNRVAGGVDPGLLVSRRIFE
LTYDNGKTTNDNEYRVPDEVEFQQRSSSFTSKETDTFYGTKSYAKKLSHQVQADASEAVFASVKFSASHR
YESISNDASTKGYVYSSEQTIQNFGHMRYLTSLAEHDGFEIAREFRIDVCDLPTTYATNTYMEFLSKWGT
SVVTEADVGVRTGINSREDRSSFVKDASTDMSNSVSVEGNYKIFSASLSVDMDRFSQSASSEKKMGTEYT
RYTIGSEEFNEPITISLIGLEEALNDEYWSRQSEYESSGECPSNWARSTIATNILTGLKEYANYRGVVPS
SDPDVTVPLTWPDGKYALPEAVTLGDNTCPNTDYMTWSFGLFYQFTDDGGVNTCSENNHLTNYCERTHMR
TYYCVKTTPKATDSSWSWMPGVYCIFKNGDTCLTGSPMVSSSGTTLASKRALTRNITQCLQELLPWSYRN

Signal peptide

150

>Apx^{MACPF}

>Apx^{MACPF}

>Apx[MACPF]

gcggccgcATGGTGGGCCCACGTACAGCATGTGGCGGATTGCTCATCCTCTTCTCACTATTGCCCGTGAT
ATCACTCGGCGCTTCGACCTTGCCGATCCCGAATCCGATGAAATACATCGGCATTGGGTACAACATCATC
GACGGTAATCCCGAGGGTGATAACAGGGTTGCTGGCGGCGTCGATCCTGGTCTCCTGGTCTCTCGCCGTA
TCTTCGAACTCACCTACGATAACGGGAAAACGACGAATGACAACGAGTATAGAGTGCCTGATGAGGTGGA
ATTCCAGCAGCGCAGCAGCTCCTTTACCTCGAAGGAGACGGATACCTTCTACGGAACAAAGAGCTACGCA
AAGAAACTTTCACATCAGGTGCAGGCTGACGCTAGCGTTGAAGCGGTCTTTGCTTCAGTGAAGTTTTCTG
CCAGCCACCGGTACGAGTCCATTTCTAATGATGCCAGCACAAAAGGCTACGTTTACTCCTCGGAGCAAAC
GATTCAGAACTTCGGCCACATGCGCTACTTGACCAGTCTTGCTGAACATGATGGATTCGAGATTGCAAGG
GAATTCCGTATTGACGTCTGTGACCTGCCTACGACATACGCCACCAATACATACATGGAGTTCCTTTCAA
AATGGGGAACGAGCGTTGTGACGGAGGCTGATGTCGGAGTCCGTACTGGTATAAACTCCCGTGAAGACCG
ATCTTCTTTCGTCAAAGATGCTTCAACAGATATGTCGAATAGCGTGAGTGTTGAAGGGAACTACAAATC
TTCTCCGCTTCGTTGTCTGTAGACATGGACAGGTTCTCTCAAAGCGCATCATCGGAGAAAAAAATGGGGA
CGGAATATACCAGGTACACAATTGGCAGCGAAGAGTTTAATGAACCCATCACTATTAGTCTCATCGGCTT
AGAGGAAGCTTTGAATGACGAATACTGGAGCAGGCAATCGGAATATGAAAGCAGCGGAGAATGCCCAAGC
AATTGGGCAAGGTCAACCATCGCTACCAACATCTTGACCGGCCTCAAGGAATACGCCAACTACAGAGGAG
TTGTTCCTAGTTCAGACCCTGATGTGACCGTGCCTCTGACCTGGCCCGATGGAAAGTACGCTCTTCCCGA
GGCAGTGACACTCGGTGATAATACCTGCCCTAATACAGACTACATGACATGGAGCTTCGGTTTGTTCTAC
CAATGActcgag

MVGPRTACGGLLILFSLLPVISLGASTLPIPNPMKYIGIGYNIIDGNPEGDNRVAGGVDPGLLVSRRIFE
LTYDNGKTTNDNEYRVPDEVEFQQRSSSFTSKETDTFYGTKSYAKKLSHQVQADASVEAVFASVKFSASH
RYESISNDASTKGYVYSSEQTIQNFGHMRYLTSLAEHDGFEIAREFRIDVCDLPTTYATNTYMEFLSKWG
TSVVTEADVGVRTGINSREDRSSFVKDASTDMSNSVSVEGNYKIFSASLSVDMDRFSQSASSEKKMGTEY
TRYTIGSEEFNEPITISLIGLEEALNDEYWSRQSEYESSGECPSNWARSTIATNILTGLKEYANYRGVVP
SSDPDVTVPLTWPDGKYALPEAVTLGDNTCPNTDYMTWSFGLFYQ

Signal peptide

>Apx^C

```
gcggccgcATGGTGGGCCCACGTACAGCATGTGGCGGATTGCTCATCCTCTTCTCACTATTGCCCGTGAT
ATCACTCGGCGCTTCGACCTTGCCGAATACCTGCCCTAATACAGACTACATGACATGGAGCTTCGGTTTG
TTCTACCAATTCACGGACGATGGTGGAGTAAATACCTGTTCCGAGAACAACCATCTGACCAACTACTGTG
AACGTACCCACATGAGGACCTACTACTGCGTGAAGACCACTCCCAAGGCGACGGATTCCTCGTGGTCTTG
GATGCCCGGCGTCTACTGTATCTTCAAGAATGGTGACACTTGCCTGACGGGTTCACCGATGGTTTCATCA
AGTGGAACGACGCTAGCGAGCAAAAGGGCATTGACACGGAATATAACACAATGCCTGCAGGAATTATTAC
CCTGGAGCTACAGAAATTGActcgag
```

MVGPRTACGGLLILFSLLPVISLGASTLPNTCPNTDYMTWSFGLFYQFTDDGGVNTCSENNHLTNYCERT
HMRTYYCVKTTPKATDSSWSWMPGVYCIFKNGDTCLTGSPMVSSSGTTLASKRALTRNITQCLQELLPWS
YRN

Signal peptide

Table S1: Human clones for generation of *UAS-MACPF* constructs (Methods 3.2.1)

Human gene	Clone ID#
C6	HsCD00505887
C7	HsCD00505812
C8α	HsCD00513576
C8β	HsCD00513570
C9	HsCD00512508
ASTN2	HsCD00511419
BRINP1 (DCB1)	HsCD00509835
BRINP2 (FAM5B)	HsCD00505760
BRINP3 (FAM5C)	HsCD00516254